UNIVERSITY OF
BIRMINGHAM

Hydrology of paraglacial catchments in a changing climate: impacts on biodiversity hotspots

---

Michael Grocott

A thesis submitted to the University of Birmingham for the degree of DOCTOR OF PHILOSOPHY

School of Geography, Earth & Environmental Studies (GEES)
College of Life and Environmental Studies (LES)
University of Birmingham
October 2016

Abstract

Groundwater (GW) –fed streams are ubiquitous in paraglacial floodplains and have been termed 'biodiversity hotspots'. These streams and associated ecosystems are important aquatic and terrestrial habitats that provide favourable environmental conditions in paraglacial systems. GW-fed stream occurrence on floodplains has been linked to preferential flow paths (PFPs), which are important conduits of subsurface flow across paraglacial floodplains. However, the hydrological dynamics which support PFPs and related streams remain largely unknown. Consequently the implications of anthropogenic climate change upon these valuable habitats are a significant research gap. To address this, a study of GW-fed streams within Denali National Park & Preserve (DNPP), Alaska was conducted during 2013 and 2014. Three interrelated sub-themes were considered. Firstly the hydrogeomorphic controls that influence PFPs were examined and applied to a site-specific water balance analysis, which estimated key water sources that supported GW-stream recharge. Secondly the importance of hillslope-floodplain connectivity to GW-stream recharge was established; and the role of PFPs in lateral hydrologic exchange with valley sides determined. Thirdly the first-order controls upon GW-fed streams were established at an intra-catchment scale; and the sensitivity of these controls to the effects of climate change considered. Key research outcomes are: (1) PFPs are important to the occurrence of GW-fed streams; (2) Hillslope runoff from adjacent valley sides to GW-fed streams provides a significant contribution to their water balance; (3) Colluvial deposits are important aquifers on valley sides that delay, store, and sustain the release of hillslope runoff to GW-fed streams; (4) PFPs are a significant first-order control upon GW-fed streams; and (5) Long-term declines in sediment export within paraglacial catchments will impact PFP stability, but in the short- to medium- term changing hydrological dynamics are most detrimental to GW-fed stream occurrence.

For my grandparents,

Thomas & Joan,

Tom & Nancy,

"It's always good to remember where you come from and celebrate it. To remember where you come from is part of where you're going" – Anthony Burgess

Acknowledgements

I would foremost like to thank my supervisors: Dr Nick Kettridge, Dr Chris Bradley, and Professor Sandy Milner for their support, guidance, and encouragement throughout the last three and a half years, and in the completion of this thesis. Their support included invaluable advice, assistance, and enthusiasm in the field; epitomised by an excursion in freezing snow to Gorge Creek with Nick that will live long in the memory.

I am indebted to the National Park Service for kind permission to conduct research within Denali National Park & Preserve. I extend individual thanks to Denny Capps and Lucy Tyrrell of the National Park Service in particular, whose continued support for the research and logistical assistance made the fieldwork possible. I would also like to thank the residents of the Toklat Road Camp who made working in the remoteness of Denali possible, enjoyable, and memorable. Particular thanks to Bob James whose regular trips to Fairbanks and generosity kept me well stocked on the fieldwork essentials of food and beer. Also I thank the 'Toklat Dorm Mom's'; Monica Magari and Jakara Hubbard for creating a home from home.

For their efforts in the field, and for tolerating my company, I express my immense gratitude to Stefanie Aumayr, Holly Mills, Lawrence Bird, Dani Dagan, Stephannie Dotson, Jake McCommons, and Alina Pontynen. For assisting in organising field equipment I thank Richard Johnson. I am grateful to Gillian Kingston, Eimear Orgill, and Maria Thompson for their support in water chemistry analysis, and to Ian Boomer for stable isotope analysis. To NERC I am grateful for the provision of a studentship which made this research possible. I am also thankful to the Denali Education Center and the Arctic Institute of North America for the provision of funding which assisted with fieldwork costs and the acquisition of equipment.

For their advice, the pleasure of their company, and maintaining my sanity over the past three and a half years I thank James O'Neill, Ellis Stacey, Grace Garner, Kieran Khamis and countless others from Geography or who frequented Staff House. I extend deep personal gratitude to Harriet Joy who provided immeasurable support, and tolerated my occasional moodiness, during the writing of this thesis.

I am most grateful of all to my parents, Nigel and Carole, for their unreserved support in this venture and who I assure my student days are now over. Finally I express thanks to my sister, Sarah, whose continued academic, professional, and personal success in life has driven my competitive nature and led me to achievements beyond what I ever envisaged I was capable of.

Table of Contents

Abstract i

Acknowledgements iii

CHAPTER 1: INTRODUCTION 1

1.1 PARAGLACIAL, PERIGLACIAL, OR PROGLACIAL: DEFINING THE PARAGLACIAL ENVIRONMENT 2

1.2 PARAGLACIAL ENVIRONMENTS IN THE 21ST CENTURY 6

1.3 BIODIVERSITY HOTSPOTS WITHIN PARAGLACIAL ENVIRONMENTS 8

1.3.1 Hydrological dynamics of biodiversity hotspots: outlining the research gap 10

1.4 AIMS & OBJECTIVES 14

1.5 OUTLINE OF THESIS 15

CHAPTER 2: METHODOLOGY 17

2.1 FIELD SITES 18

2.1.1 MF Toklat 23

2.1.2 East Fork Toklat 30

2.1.3 Teklanika 33

2.1.4 Gorge Creek 35

2.2 METEORLOGICAL DATA 38

2.3 FIELD METHODS & LABORATORY ANALYSIS 40

2.3.1 Lithofacies and hydrofacies identification 40

2.3.2 Hydraulic conductivity measurements 43

2.3.3 Hydrometric monitoring 45

2.3.4 Hydrochemistry and stable isotope sampling 47

2.4 DATA & STATISTICAL ANALYSIS 50

2.4.1 Terrace water balance 50

2.4.2 Two-component hydrograph separations 54

2.4.3 Mean residence times 55

2.4.4 Principal component analysis 56

CHAPTER 3: PREFERENTIAL FLOW PATHWAYS WITHIN PARAGLACIAL FLOODPLAINS: HYDROGEOMORPHIC CONTROLS UPON THE OCCURRENCE AND STABILITY OF BIODIVERSITY HOTSPOTS 57

3.1 SCOPE OF CHAPTER 58

3.2 INTRODUCTION 59

3.3 STUDY SITE 61
3.4 METHODOLOGY 61
3.5 RESULTS 62
3.5.1 Lithofacies and hydrofacies characterisation 62
3.5.2 Vertical variation in hydrofacies 63
3.5.3 Lateral spatial distribution in hydraulic conductivity 65
3.5.4 Groundwater Storage 67
3.5.5 Vertical hydraulic gradient 71
3.5.6 Water balance 74
3.6 DISCUSSION 75
3.6.1 Preferential flow pathways and groundwater recharge 75
3.6.2 Valley side water sources 76
3.6.3 Conceptualising understanding 77
3.6.4 Implications of conceptual understanding 81
3.7 SUMMARY 82
CHAPTER 4: HILLSLOPE-FLOODPLAIN CONNECTIVITY IN PARAGLACIAL CATCHMENTS: COLLUVIAL DEPOSITS REGULATING FLOODPLAIN HYDROLOGICAL DYNAMICS 84
4.1 SCOPE OF CHAPTER 85
4.2 INTRODUCTION 86
4.3 STUDY SITE 88
4.4 METHODOLOGY 88
4.5 RESULTS 88
4.5.1 Stream discharge 88
4.5.2 Groundwater behaviour 91
4.5.3 Geochemical composition of waters 93
4.5.4 Stable isotope composition of water 99
4.5.5 Hydrograph separations 101
4.5.6 Mean residence times 104
4.6 DISCUSSION 105
4.6.1 Hillslope-floodplain connectivity and the role of preferential flow paths 105
4.6.2 Characterising the hydrological behaviour of colluvial deposits 107
4.6.3 Quantifying streamflow contribution from colluvial deposits 109

4.6.4 Colluvial deposit influence on GW-fed streams: implications of shifting hydrological dynamics 109
4.7 SUMMARY 110
CHAPTER 5: FIRST-ORDER CONTROLS ON GROUNDWATER-FED STREAMS AND THEIR LONG-TERM STABILITY IN PARAGLACIAL CATCHMENTS 112
5.1 SCOPE OF CHAPTER 113
5.2 INTRODUCTION 114
5.3 FIELD SITES 116
5.4 METHODOLOGY 116
5.5 RESULTS 117
5.5.1 Groundwater behaviour 117
5.5.2 Geochemical and isotopic signatures of terrace waters 119
5.5.3 Principal component analysis 125
5.5.4 Valley side flow contribution 130
5.6 DISCUSSION 133
5.6.1 Preferential flow pathway prevalence at the intra-catchment scale 133
5.6.2 Hillslope runoff influence on groundwater-fed stream recharge 134
5.6.3 Establishing first-order controls on groundwater-fed streams 137
5.6.4 Implications of climate change for first-order controls and the long-term stability of groundwater-fed streams 138
5.7 SUMMARY 140
CHAPTER 6: SYNTHESIS, IMPLICATIONS AND FUTURE DIRECTIONS 142
6.1 Introduction 143
6.2 Key research findings 144
6.3 Conceptualising hydrological dynamics of groundwater-fed streams 145
6.4 Implications for biodiversity hotspots 148
6.4.1 Shifting hydrological dynamics 148
6.4.2 Changing geomorphic processes 151
6.5 Future work 153
6.6 Final remarks 155
REFERENCES 156
APPENDICES i
APPENDIX A: HYDRAULIC CONDUCTIVITY DATA FOR UPPER TRANSECT ii

6.6.1 Appendix Ai: Hydraulic conductivity (K) measurements at MF Toklat along the upper transect (UT) for; (a) surface K ($K_{0.0}$); and (b) K at 1.0 m depth ($K_{1.0}$). X-axis indicates distance from the hillslope ii

List of Figures

Figure 1.1: (a) Church & Ryder, (1972) sediment yield rate relative to time after deglaciation; and (b) Church & Slaymaker (1989) sediment wave model. Figure taken from Slaymaker (2009) 4

Figure 1.2: Groundwater-fed streams on a floodplain terrace, Middle Fork (MF) Toklat River (a paraglacial catchment), Denali National Park & Preserve (DNPP). Associated riparian vegetation is supported by shallow groundwater levels across the terrace. 8

Figure 1.3: Base of a colluvial deposit within the MF Toklat catchment, DNPP, extending onto the active floodplain. These valley side colluvial structures are both valuable storage and conduits of flow for hillslope runoff in paraglacial environments 11

Figure 2.1: (a) location of DNPP within Alaska and relative to the Arctic Circle; (b) location of study sites within DNPP..... 19

Figure 2.2: Geological map for sites. Key geologic units for the catchments are labelled on the map with unit description provided in the legend 20

Figure 2.3: Field site location and glacial coverage within respective watersheds. Only the Gorge Creek site was located within a non-glaciated catchment. Image obtained from Google. 24

Figure 2.4: (a) MF Toklat terrace, landscape units, and location of active river channels on the floodplain. Four colluvial deposits extend down the valley side adjacent to the terrace. Alpine meadows are also present alongside fractured bedrock on valley sides. Sample site locations are also shown for surface water (SW), glacial river (GR), snowpack (SP), debris fan (DF), and hillslope flow (HF); (b) DEM of terrace base showing GW-fed stream distribution and stream cluster (SC) groupings. Location of piezometer nests along lower (LT), middle (MT), and upper (UT) transects are also shown. Image for (a) obtained from Google. 25

Figure 2.5: (a) surface air temperature data from automated weather station ~5 Km NW of MF Toklat site; (b) stream temperature data for SW1 (SC1), SW2 (SC2), and SW3 (SC3). Data obtained using TinyTag Aquatic 2 (TG-4100) temperature loggers..... 27

Figure 2.6: EM survey data collected during May 2014. Resistivity values >451 on the valley sides are due to the occurrence of discontinuous permafrost. Image obtained from Google…28

Figure 2.7: Frozen soil on the hillslopes adjacent to the MF Toklat terrace, identified in areas with higher resistivity values. 29

Figure 2.8: EF Toklat terrace and surrounding landscape units. Alpine meadows were present on lower reaches of slopes adjacent to the terrace. Colluvial deposits occurred on steeper slopes at higher elevation. The park road can is also clearly identifiable traversing the adjacent hillslope from north to south. Sample sites included surface water (SW) on the terrace; piezometers (LT & MT); upstream groundwater (GW); hillslope seepage (HS) from the base of the hillslope; hillslope flow (HF) from one of the alpine meadow areas above the terrace; and the main glacial East Fork River (EF). Image obtained from Google. 31

Figure 2.9: Photograph of East Fork (EF) Toklat field site, looking downstream from the adjacent valley-side. The vegetated base is clearly identifiable along with GW-fed stream channels. Alpine meadow areas can also be recognised at the base of the adjacent hillslope. 32

Figure 2.10: Tek terrace and surrounding landscape units. GW-fed streams only flowed close to the hillslope on the terrace margins Sample sites included surface water (SW), piezometers (MT), the main glacial river channel (Tek), and hillslope seepage (HS) from the valley side. Image sources from Google. 34

Figure 2.11: Image looking upstream of the Tek field site, the terrace can be seen to the right of the Teklanika River. A GW-fed stream can be seen flowing at the margin of the terrace. Spruce forests are present either side of the floodplain due to the lower elevation of the field site. 35

Figure 2.12: Gorge Creek (GC) terrace and surrounding landscape units. To the NE of the terrace a stream flows through a ravine and across the field site. Three colluvial deposits extend onto the terrace from the adjacent valley side. Sample sites include surface water (SW), piezometers (T), a debris fan (DF), and hillslope flow (HF). Image obtained from Google. 36

Figure 2.13: Gorge Creek (GC) terrace from the south face valley side. In contrast to the other field sites vegetation cover was mature and dense across the entire terrace 37

Figure 2.14: Location of outcrops (P1 – P4) selected for detailed sedimentary descriptions and profiles. Outcrops were selected to represent the range of sedimentary environments observed. This included exposures with overlying soil layers (Profile 2 – P2) and those near GW-fed streams (Profile 3 – P3). Satellite image from Google. 42

Figure 2.15: Conceptual model for fluxes included as part of water balance estimates for the terrace and adjacent hillslope. Grey coloured arrows indicate inputs into the system and black arrows are representative of outputs 51

Figure 3.1: Digitised hydrofacies layers placed onto sedimentary profiles of exposed terrace carried out on the MF Toklat terrace. Higher *K* units were observed in upper layers at terrace base in Profiles 1 and 2. Low *K* units were present near GW-fed streams (Profile 3). 64

Figure 3.2: (a) $K_{0.0}$; and (b) $K_{1.0}$ hydraulic conductivity values for individual middle transect (MT) sites. Grey shaded areas for (a) separate groupings of low and high *K* sediments, and soil layers. X-axis shows increasing distance across the transect from the hillslope 66

Figure 3.3: Precipitation and GW levels for selected middle transect (MT) sites during (a) 2013 and (b) 2014. Data presented for all MT sites from piezometers installed at 1.0 m depth. GW across the terrace did not exhibit a flashy response to storm events in either year 68

Figure 3.4: GW responses for upper transect (UT) sites during (a) 2014 and (b) a comparison of responses at site UT4 during 2013 and 2014. GW levels rose earlier and at a faster rate during 2014 70

Figure 3.5: Vertical hydraulic gradients (dH/dL) across; (a) the middle transect (MT); and (b) the upper transect (UT) during 2014. Positive values are indicative of upward water movement. 72

Figure 3.6: Vertical hydraulic gradients (dH/dL) for hydrofacies where gradients were available. Stronger gradients (positive and negative) are observed for hydrofacies with higher mean log *K* (values in brackets). 73

Figure 3.7: Total water balance estimate for terrace and adjacent valley side area during 2014. Horizontal subsurface flow ($Q_{subsurface}$) did not account for significant export of aquifer storage, and was several orders of magnitude lower than any other estimated flux 74

Figure 3.8: Conceptual summary of water balance analysis. Hydrological stores and fluxes presented are proportional relative to their calculated size. The conceptualisation demonstrates how hydrological fluxes from the adjacent valley side could equal or exceed groundwater recharge from upstream of the terrace unit. Colluvial deposits, alpine meadow, and fractured bedrock on valley sides could provide valuable aquifers, retaining groundwater on valley sides; with colluvial deposits then acting as important conduits of flow to sustain GW-fed streams. Given the combination of large catchment area, minimal glacial coverage, and prevalence colluvial deposits, alpine meadow, and fractured bedrock upstream of the terrace; hillslope runoff sources may provide a larger component of upstream input to GW-fed streams on the terrace than previously thought. Glacial meltwater may be a less influential component of these streams, which are instead predominantly ran-fed, or driven, from valley-side runoff sources. The minimal export of groundwater through horizontal subsurface flow reflects the channelization of groundwater across the terrace that leads to the emergence of GW-fed streams, and which account for almost all groundwater exported from the terrace. The lack of diffuse flow across the terrace combined with the presence of high *K* hydrofacies (associated with strong VHGs) highlights the important role of PFPs as concentrated conduits of flow through the terrace. Given the significance of valley side inputs and importance of PFPs to GW-fed stream occurrence identified in this chapter the potential role of PFPs in hillslope-floodplain connectivity should be further explored.....80

Figure 4.1: Precipitation for the MF Toklat and stream discharge at sites SW1, SW2, and SW3 during 2013 and 2014. Discrete responses to individual storm events were observed at SW1 and SW2 during 2014, caused by overland flow from adjacent hillslopes flowing across the terrace and into individual channels. Similar responses to storm events during 2013 were not observed as overall precipitation during summer months was 34.1% lower and so hillslopes were not sufficiently saturated to cause overland flow responses. Increases in discharge at SW3 between JD 192 – 215 in 2014 and after JD 215 in 2013 were caused by backwater from the main glacial river inundating the stream channel during these periods. ..89

Figure 4.2: Precipitation for the MF Toklat and groundwater levels at sites MT3, MT7, and MT14 during 2013 and 2014 92

Figure 4.3: (Ca^{2+} + Mg^{2+}) vs SO_4^{2-} ratios for end-members (GW and DF); (a) surface water; and (b) middle transect sites. Plots show combined 2013 and 2014 data. 95

Figure 4.4: Piper diagram for two identified end-members within the MF Toklat catchment. A debris fan (DF) on the valley side upstream of the GW-fed streams and groundwater (GW) from up-valley. 96

Figure 4.5: Boxplots for selected variables at SW and MT sites for 2013 and 2014, in addition to identified end-members DF and GW 98

Figure 4.6: Temporal plots for δ^2H at surface water (SW) and groundwater (MT) sites in 2013 and 2014. Sampling period in 2013 was 6th July to 1st September (JD 187 – 244) and in 2014 was 22nd May to 2nd September (JD 142 – 245). 100

Figure 4.7: Estimated mean percentage flow contribution from end-member DF for surface water (SW) sites in 2013 and associated confidence intervals (standard deviations) 102

Figure 4.8: Estimated mean flow contribution from DF to surface water (SW) sites in 2014. Confidence intervals based on standard deviations. 103

Figure 5.1: Total daily precipitation and groundwater levels at sites; Middle Fork (MF) Toklat, East Fork (EF), and Teklanika (Tek). GW levels inferred from pressure transducers at all locations with the exception of MT3 at MF Toklat, where manual spot measurement are presented. 118

Figure 5.2: Piper plots for groundwater (MT) and surface water (SW) locations at sites (a) Middle Fork (MF) Toklat, (b) East Fork (EF), and (c) Teklanika (Tek) 120

Figure 5.3: Spatial variation in silica (SiO_2) for (a) surface water (SW) and (b) groundwater (MT) locations at MF Toklat, East Fork, and Teklanika sites 122

Figure 5.4: Total daily precipitation and temporal response of δ^2H at surface water (SW) and nitrate (NO_3^-) at groundwater (MT) locations for MF Toklat, EF, and Tek. Linear trends in

seasonal response of δ^2H observed at MF Toklat for SW1 (R^2 = 0.61; p = 0.001), SW2 (R^2 = 0.50; p = 0.005), and SW3 (R^2 = 0.44; p = 0.013); and at EF for SW1 (R^2 = 0.90; p = 0.013). Linear trends in seasonal response of NO_3^- observed at MF Toklat for MT1 (R^2 = 0.28; p = 0.06) and MT7 (R^2 = 0.45; p = 0.01) and at Tek for MT1 (R^2 = 0.94; p = 0.03) 124

Figure 5.5: Variable plots for individual variables at sites; (a) Middle Fork (MF) Toklat; (b) East Fork (EF); (c) Teklanika (Tek);, and (d) Gorge Creek (GC). Principal Component (PC)1 (Dim1) and PC2 (Dim2) are presented with percentages indicated total variance explained by respective principal components 126

Figure 5.6: Individuals plots for sites (a) MF Toklat, (b) EF, (c) Tek, and (d) GC. Large symbols in bold are centroids for individual sample locations (e.g. SW1). Identified end members at sites included debris fans (DF), hillslope flow (HF), hillslope springs (HS), groundwater (GW). At (c) the main Teklanika River (Tek) was included and at (d) Gorge Creek (GC). Labelled arrows indicate temporal movement of individual locations over the season at sites where observed. 129

Figure 5.7: Two component hydrograph separations for surface water (SW) and groundwater (MT) locations at (a) MF Toklat, (b) EF, (c) Tek, and (d) GC. (a)/(d) separations show contribution from individual colluvial deposits. (b)/(c) provide a breakdown of flow from adjacent hillslope area, rather than from a single colluvial deposit..... 132

Figure 6.1: Conceptual summary outlining key controls on GW-fed stream presence on paraglacial floodplains. PFPs are the dominant first-order control on their occurrence whose effectiveness to act as channels of flow is dependent upon: (1) continual renewal and development; and (2) recharge of the floodplain water table during summer months. (1) is controlled by up-valley sediment export from glacial meltwaters, which maintains channel avulsion and alluviation, while restricting vegetation growth. Hillslope runoff processes provide an important contribution to (2), particularly colluvial deposits, which retain groundwater on valley sides and provide gradual, sustained flow to the floodplain..... 146

Figure 6.2: Revised conceptual model outlining implications of changes in short to medium-term controls (hydrological dynamics) and long-term controls (hydrogeomorphic processes) upon GW-fed stream occurrence on paraglacial floodplains. Positive, negative, and unknown

responses are considered. Positive responses (green) are those which will see an increase in their occurrence in response to changes (e.g. vegetation growth on terraces). Negative responses (red) will see a decline (e.g. smaller snowpack). In the short- to medium-term shrinking winter snowpack, declining permafrost thaw, and subsequent smaller groundwater stores on valley sides may lead to reduced recharge of the floodplain water table. In addition declining permafrost coverage will open up deeper flow paths on valleys-sides which will increase residence times. Long-term consequences of glacial retreat will lead to a decline in up-valley sediment export that will restrict channel avulsion and alluviation processes. Subsequent declines in PFP formation and renewal and increased vegetation growth will have a negative impact on PFP effectiveness and may lead to ephemeral GW-fed streams. Overall, shifts in controls on GW-fed streams may have a detrimental impact on their role as biodiversity hotspots..... 149

List of Tables

Table 2.1: Summary of key characteristics for all field sites utilised as part of this research..22

Table 2.2: Temperature (°C) and precipitation (mm) data for 2013 and 2014 from an automated weather station 5 Km NW of the MF Toklat field site. High mean temperatures in 2013 contrasted with much higher summer precipitation in 2014. 39

Table 2.3: Summer temperature and precipitation data for an automated weather station located at DNPP HQ. Data presented for 2013, 2014, and normal values for 1981-2010. For departure from normal, red indicates values above average and blue values below. 39

Table 2.4: Standardised code for lithofacies identification 41

Table 2.5: Sampling locations and identified end-members for all field sites. Three surface water (SW) and three groundwater (MT) locations were sampled at all sites except GC 48

Table 3.1: Identified hydrofacies on the MF Toklat terrace with associated sediment texture breakdown, log *K* values, and percentage porosity 63

Table 3.2: GW levels at the beginning and end of monitoring periods for middle transect (MT) sites during 2013 and 2014. Values in bold indicate where GW levels rose above the surface.....69

Table 4.1: Physicochemical properties of sampled surface water (SW), middle transect (MT), and identified end-members sites for 2013 and 2014 sampling periods. Combined mean values (**in bold**) and associated standard deviations (*in italics*) are presented. Debris fan (DF) and upstream groundwater (GW) flow were used for two-component hydrograph separations. Summer precipitation (Precip.), winter snowpack (SP), and glacial melt (GM) geochemical and isotopic signatures are also presented. Precip. samples were collected using a rain collector at a road camp ~5 km downstream (NE) of the site (within the same catchment), and isotopic composition was calculated as a weighted average using the method of McDonnell *et al.* (1990). 94

Table 4.2: Mean discharge (Q) and percentage flow contribution for surface water (SW) sites from end-members DF and GW in 2013 (*Standard deviations in italics*). Associated uncertainty values are also presented 102

Table 4.3: Two-component hydrograph separation results for 2014. See Table 3.2 caption for further details 103

Table 4.4: MRT estimates for SW sites, the main MF Toklat River (GR) and hillslope debris fan (DF). Table includes weighted mean annual measured δ^2H [‰] (C_0), annual amplitude for predicted δ^2H [‰] (A), phase lag [rad] (ψ), MRT estimate in days (D) and months (M), R^2, and *p*-values. 104

Table 5.1: Mean (in bold) and standard deviation (σ) values for selected geochemical and isotopic compositions for surface water (SW) and groundwater (MT) locations at sites MF Toklat, East Fork, and Teklanika 121

Table 5.2: Complete list of *P*-values and associated R^2 values at each site for individual variables along PC1 and PC2. Where *P-values* are listed as zero returned numbers were infinitesimally small. 127

Table 5.3: Mean, maximum, and minimum uncertainty values at 95% confidence level. Mean uncertainty for individual components is also listed. At MF Toklat and EF component 1 (C_1) was debris fan (DF) and hillslope flow (HF) respectively. Component 2 (C_2) was upstream groundwater (GW). At GC C_1 was DF and C_2 was HF; and at Tek C_1 was HF and C_2 was upstream flow from the Tek River. 131

CHAPTER 1: INTRODUCTION

1.1 PARAGLACIAL, PERIGLACIAL, OR PROGLACIAL: DEFINING THE PARAGLACIAL ENVIRONMENT

The term ‘paraglacial’ was first defined by Church and Ryder (1972) as ‘nonglacial processes that are directly conditioned by glaciation’. Consequently no specific landform or process can be uniquely attributed to paraglacial environments (Ballantyne, 2002b), as both periglacial and proglacial environments and the suite of landforms and processes associated with fluvial and mass movement influences are included in the paraglacial term (Slaymaker, 2009) as defined by Church and Ryder. In contrast to paraglacial environments the terms ‘periglacial’ and ‘proglacial’ have clear definitions (Ballantyne, 2002b).

Periglacial conditions do not necessarily require the presence of glacial conditions in a particular catchment (Church and Ryder, 1972). Instead periglacial environments are generally considered regions characterised regular freeze-thaw cycles and extensive seasonal freezing; or permafrost regions (Slaymaker, 2009). Characteristic features of periglacial conditions are associated with the effects of permafrost (e.g. tundra polygons, pingoes, and palsas) and thermokarst structures where thawing of permafrost persists (French, 2000). In addition intense frost activity generates rock debris and patterned ground, although sediments are not effectively removed for fluvial transport and deposition (Slaymaker, 2011). Periglacial settings are found in a range of environments extending from the polar deserts of the high arctic through to mid- and low latitude alpine areas.

Proglacial environments encompass the glacier foreland beyond the ice-margin zone, proximal to the glacier terminus (Bennett, 2011). Fluctuations in the extent of ice melt are a strong influence on the flow regimes of proglacial rivers which are typified by strong diurnal and seasonal variations, and often characterised by rapid changes in flow (Heckmann *et al.*,

2016). Sediment yields for proglacial rivers are typically high, comprising glacially-derived sediments as well as the surrounding hillslopes (colluvium) and forefield floodplain (glacial-fluvial) (Heckmann *et al.*, 2016). These conditions are collectively responsible for a highly dynamic environment in which fluvial sedimentary features evolve rapidly with both glaciofluvial erosional (e.g. drainage diversions and spillways) and depositional (e.g. moraines, sandar, and braided outwash) forms occurring (Embleton-Hamann, 2004; Slaymaker, 2011).

It has been proposed that a more appropriate conceptualisation of the paraglacial environment would be as a period of time and as 'landforms and landscapes that are transitional from glacial to non-glacial conditions' (Slaymaker, 2009). Paraglacial environments are thus neither defined by unique processes or specific locations, but are rather dynamic systems defined by a rate of change and trajectory from a glacial to non-glacial environment (Slaymaker, 2009; Slaymaker, 2011) Glacial retreat associated with paraglacial landscapes creates a highly dynamic and active environment where the increased abundance of mobile sediments and greater fluvioglacial activity influence geomorphic activity (Klaar *et al.*, 2015).

The sources of elevated sediment loads within paraglacial environments are both glacial landforms (e.g. moraines, tills, and outwash) and the alteration of both proglacial and non-glacierised areas by processes including mass movement, freeze-thaw cycles, fluvial reworking, and slope activity (e.g. rockfall and debris fans) (Klaar *et al.*, 2015). Landform alteration is then driven by the modification and movement of these sediments (Ballantyne, 2002a) and, ultimately, the transitional period of time over which these physical processes occur, regarded as the 'paraglacial adjustment period' (Benn and Evans, 2010), is considered to have ended when glacially conditioned sediment yields have been expended or achieved stability (Ballantyne, 2002b; Klaar *et al.*, 2015; Schumm and Rea, 1995).

For a number of reasons there can be difficulties in distinguishing between proglacial and paraglacial environments due to the significant crossover in the landforms and processes associated with each one. Church and Ryder (1972) considered proglacial settings as the foremost stages of paraglaciation (Figure 1.1a). Some regard the inclusion of paraglacial to cover proglacial processes as unnecessary given proglacial is a unique geologic condition (Eyles and Kocsis, 1988). However, it has also been argued the inclusion recognises the context within which local-scale proglacial processes sit, but at a larger scale (Slaymaker, 2009). Eyles and Kocsis (1988) also highlighted that Church and Ryder (1972) did not clarify the timescale for the paraglacial period. Although the definition by Ballantyne (2002b), outlined above, does provide clarity to this ambiguous issue.

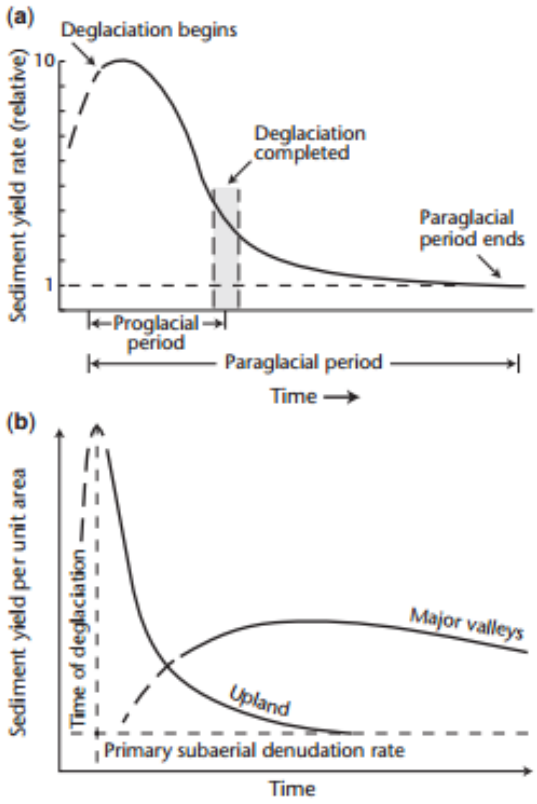

Figure 1.1: (a) Church & Ryder, (1972) sediment yield rate relative to time after deglaciation; and (b) Church & Slaymaker (1989) sediment wave model. Figure taken from Slaymaker (2009)

Given that the period of paraglacial conditions is dependent on the supply of glacially derived sediment (Ballantyne, 2002b; Slaymaker, 2011) it is important to understand how sediment is released from storage in these environments (Slaymaker, 2009). This has been summarised by the Church and Slaymaker (1989) sediment wave model, outlined in Figure 1.1b. In smaller, headwater catchments steeper topography, greater precipitation, and elevated erosion rates result in greater sediment yields that decline monotonically after deglaciation relative to catchment area (Slaymaker, 2009). However, in larger catchments (10 to 30,000 Km^2) Church and Slaymaker (1989) found sediment yields increased initially after deglaction, before declining. It has been suggested this behaviour is caused by a 'wave' of primary, or secondary, glacially-sourced sediment reworked from headwater catchments and transported to larger, downstream trunk valleys (Harbor and Warburton, 1993). Subsequently larger basins show a lag in peak sediment yields, and whose amplitude also declines with increasing catchment area (Harbor and Warburton, 1993).

The paraglacial environment then is a transitional landscape that is defined by the trajectory and rate of change (Figure 1.1), and which is not characterised by spatial proximity to glaciers (Proglacial) or specific processes and landforms (i.e. Proglacial & Periglacial) (Slaymaker, 2009). Instead the paraglacial adjustment period is dependent on glacigenic sediment availability and length of time until the supply is exhausted or stabilises (Church and Ryder (1972); Figure 1.1a). In addition spatial scale of paraglacial environments (catchment area) will exert significant influence on the duration of paraglaciation (Church and Slaymaker (1989); Figure 1.1b). In summary paraglacial (as used in this thesis) is defined as 'non-glacial earth surface processes, sediment accumulations, landforms, land systems, and landscapes that are directly conditioned by glaciation and deglaciation' (Ballantyne, 2002b).

1.2 PARAGLACIAL ENVIRONMENTS IN THE 21ST CENTURY

Paraglacial environments are a prevalent part of catchment headwaters across arctic, sub-arctic, and alpine regions globally (Knight and Harrison, 2014). These glacierised systems are particularly sensitive to the impacts of anthropogenic climate change (Barnett *et al.,* 2005; Immerzeel *et al.,* 2010), and have been subjected to unprecedented glacial retreat throughout the second half of the 20th Century (Zemp *et al.,* 2015). The rate of retreat is forecast to increase throughout the 21st Century (Huss and Hock, 2015), and major alterations in the hydrologic regimes of paraglacial catchments are anticipated as a consequence (Finger *et al.,* 2012; Immerzeel *et al.,* 2012). Declining glacial meltwater contribution will be compounded by shrinking winter snowpack's, projected earlier spring melt, and shifting summer precipitation patterns (Milner *et al.,* 2009; Singh and Bengtsson, 2005; Stewart, 2009). Such shifts in the hydrological dynamics of paraglacial catchments will result in the increasing relative contribution of precipitation and groundwater fluxes (Tague and Grant, 2009) to the water balance of these systems, and subsequent uncertainty in runoff response (Baraer *et al.,* 2012; Juen *et al.,* 2007).

The substantial and radical alterations expected in the hydrologic regimes of paraglacial environments will have serious implications for water resource management, ecosystems, and water quality (Vorosmarty *et al.,* 2010). Declining meltwater runoff will lead to increased pressure on water resources (Baraer *et al.,* 2012; Finger *et al.,* 2012; Immerzeel *et al.,* 2010). Currently glaciers account for 75% of the world's freshwater store and over 1 billion people are reliant upon glacial meltwater as part of their freshwater supply (Milner *et al.,* 2009). Changes to hydrologic regimes will also impact hydroelectric power generation, notably in regions such as the Alps and Andes (Finger *et al.,* 2012; Vergara *et al.,* 2007).

Changes in the hydrological dynamics of paraglacial environments as a consequence of climate change will exert significant stresses on aquatic habitats (Woodward *et al.*, 2010). Within glacial rivers this includes declining species richness and loss of specialised species amongst macroinvertebrate assemblages (Brown *et al.*, 2007; Jacobsen *et al.*, 2012). Glacial runoff generates challenging environmental conditions (Milner and Petts, 1994) that subsequently result in unique macroinvertebrate assemblages (Muhlfeld *et al.*, 2011; Snook and Milner, 2001). Declining glacial runoff and resultant shifts in environmental conditions may lead to declining beta diversity in glacial-fed rivers within paraglacial catchments (Finn *et al.*, 2013). Beta diversity is the ratio between regional (gamma) and local (alpha) diversities and therefore quantifies the amount of unique biological communities in a region (Whittaker, 1960). Increased variability in runoff and associated uncertainty in the thermal regime of glacial rivers will also have negative implications for fish populations, such as salmon (Padilla *et al.*, 2015).

Glacial retreat will expose large volumes of sediment, altering weathering dynamics in paraglacial catchments, subsequently influencing solute fluxes (Anderson, 2007; Moore *et al.*, 2009; Tranter, 2003a). Deglaciation will also have significant impacts on suspended sediment loads (Brown *et al.*, 2007; Moore *et al.*, 2009), causing short-term increases in yields, before subsequent long-term declines (Gurnell *et al.*, 2000). Furthermore, in catchments where permafrost coverage is shrinking deeper hydrological flow pathways may develop (Carey *et al.*, 2013; Douglas *et al.*, 2013), which it is anticipated will lead to changes in dissolved organic carbon (DOC) and solute fluxes from headwater catchments (Carey *et al.*, 2013; Striegl *et al.*, 2007). Shifts in water quality within paraglacial catchments will have implications for the global carbon cycle, aquatic habitats, and heavy metal mobility (Brown *et al.*, 2006; Douglas *et al.*, 2013; Petrone *et al.*, 2006; Walvoord and Striegl, 2007).

1.3 BIODIVERSITY HOTSPOTS WITHIN PARAGLACIAL ENVIRONMENTS

Groundwater (GW) –fed streams are prominent features within paraglacial floodplains (Figure 1.2), whose occurrence is attributed to extensive, widespread groundwater-surface water (GW-SW) interactions that occur within fluvioglacial floodplain deposits (Levy *et al.*, 2015; Poole *et al.*, 2006; Stanford and Ward, 1993).

Across paraglacial floodplains GW-fed streams provide valuable aquatic habitats (Levy *et al.*, 2015; Robinson *et al.*, 2008). Perennial streamflow, stable temperature regimes, low suspended sediment levels, and elevated nutrient and solute loads (Caldwell *et al.*, 2015; Crossman *et al.*, 2011; Fureder *et al.*, 2001; Malard *et al.*, 2000; Tockner *et al.*, 2002) result in GW-fed streams supporting greater taxonomic abundance and richness amongst macroinvertebrate assemblages, compared to main river channels (Arscott *et al.*, 2005; Brown *et al.*, 2003; Death and Winterbourn, 1995; Robinson and Doering, 2012). For this reason

Figure 1.2: Groundwater-fed streams on a floodplain terrace, Middle Fork (MF) Toklat River (a paraglacial catchment), Denali National Park & Preserve (DNPP). Associated riparian vegetation is supported by shallow groundwater levels across the terrace.

GW-fed streams have been regarded by others as valuable biodiversity hotspots (Crossman *et al.*, 2011). Furthermore, areas where GW-fed stream networks exist on paraglacial floodplains are considered valuable riverine habitat patches (Arscott *et al.*, 2002). Shallow groundwater levels support riparian vegetation (Caldwell *et al.*, 2015; Ward *et al.*, 2002) that form a critical part of the terrestrial ecosystem in paraglacial catchments (Paetzold *et al.*, 2005; Tabacchi *et al.*, 1998). Consequently GW-fed streams and associated riparian vegetation are integral aquatic-terrestrial transition zones (Whited *et al.*, 2007).

GW-fed streams are ultimately a function of the fluvial geomorphic processes that shape the riverscape (Lorang and Hauer, 2007). Within paraglacial catchments it is cut-and-fill alluviation and channel avulsion processes that dictate the geomorphic landforms (e.g. bars and braided channels) which characterise these environments (Lorang and Hauer, 2007; Poole *et al.*, 2002). GW-fed streams occur on paraglacial floodplains where abandoned channels (paleochannels) are intersected by the water table (Caldwell *et al.*, 2015; Lorang and Hauer, 2007; Poole *et al.*, 2002). Paleochannels intertwine both the surface and subsurface of fluvioglacial floodplains and can be described as preferential flow pathways (PFPs) (Poole *et al.*, 2002). The coarser sedimentary textures of PFPs (Miall, 1978) results in them having a higher hydraulic conductivity (*K*) and makes them conduits of subsurface flow (Anderson *et al.*, 1999; Heinz and Aigner, 2003b; Klingbeil *et al.*, 1999; Poole *et al.*, 2002). Subsequently PFPs exert a significant influence upon floodplain hydrological connectivity (Bracken and Croke, 2007) and are regarded as an important hydrofacies (Anderson, 1989) within fluvioglacial aquifers (Bayer *et al.*, 2011; Heinz and Aigner, 2003a).

1.3.1 Hydrological dynamics of biodiversity hotspots: outlining the research gap

Given the ecological importance of GW-fed streams in paraglacial catchments, substantial uncertainty remains regarding the hydrological dynamics and hydrogeomorphic controls that support them (Caldwell *et al.*, 2015; Levy *et al.*, 2015; Poole, 2010). With the exception of the established link between GW-fed stream occurrence and the presence of PFPs (Poole *et al.*, 2002) the hydrological connectivity of PFPs and water sources which support them within paraglacial catchments remain a significant unknown (Larned, 2012). With anticipated changes in the water balance of paraglacial catchment throughout the 21st Century (Baraer *et al.*, 2012; Milner *et al.*, 2009) there could be serious implications for the perennial nature of GW-fed streams (Fureder *et al.*, 2001) and there is a need to address this major research gap.

Consideration of the contribution of PFPs to hydrological connectivity across paraglacial floodplains is also required, in part, due to the growing body of scientific literature that recognises the significance of groundwater in headwater catchments (Baraer *et al.*, 2015; Blaen *et al.*, 2014; Gordon *et al.*, 2015; Hood and Hayashi, 2015; Hood *et al.*, 2006; Malard *et al.*, 1999; Mast *et al.*, 1995; Weekes *et al.*, 2015). In some small alpine headwater basins groundwater has been estimated to contribute as much as 75% (Clow *et al.*, 2003) and 60% of streamflow (Liu *et al.*, 2004). Current understanding of groundwater dynamics in headwater catchments has identified colluvial deposits (e.g. talus cones and debris fans; Figure 1.3) as critical stores (Clow *et al.*, 2003; Langston *et al.*, 2011), and conduits, of groundwater flow from valley sides in these systems (Caballero *et al.*, 2002; Muir *et al.*, 2011). Colluvial deposits, which are widespread in paraglacial environments (Ballantyne, 2002b), retain groundwater on valley sides and act as small, but valuable, aquifers in paraglacial catchments (Weekes *et al.*, 2015).

Figure 1.3: Base of a colluvial deposit within the MF Toklat catchment, DNPP, extending onto the active floodplain. These valley side colluvial structures are both valuable storage and conduits of flow for hillslope runoff in paraglacial environments

The relative importance of groundwater within paraglacial catchments is anticipated to increase further throughout the 21st Century (Baraer *et al.*, 2012), as a consequence of the effects of anthropogenic climate change (Barnett *et al.*, 2005). Yet how important valley side groundwater stores, such as colluvial deposits, are to GW-fed streams or how they are connected to the floodplain remains a significant unknown (Gordon *et al.*, 2015). The concept of hillslope-floodplain connectivity (Poole, 2010) has not been appropriately considered in paraglacial catchments, or the potential role for connectivity provided by PFPs.

Hillslope-floodplain connectivity (commonly referred to as hillslope-stream connectivity) is the hydrological connection of hillslopes to streams through surface and subsurface channels (Bracken and Croke, 2007). The use of the term hillslope-floodplain connectivity reflects the

interest in hydrological connectivity to the floodplain (and associated GW-fed streams), and not just the main river channels in catchments. Existing understanding of subsurface hillslope-stream connectivity has established that flow can be diffuse (Jencso *et al.*, 2009), channelized along bedrock topography (Freer *et al.*, 1997), or concentrated within macropores (PFPs) (Holden and Burt, 2002; Uchida *et al.*, 2001). In addition physical structures (e.g. PFP networks), antecedent conditions, and driving forces (e.g. precipitation patterns) have all been recognised as important controls on the occurrence of hillslope-floodplain connectivity (Blume and van Meerveld, 2015).

Currently though there are few studies which consider explicitly subsurface hillslope-floodplain connectivity, with the majority focusing on surface (overland flow) connectivity (Blume and van Meerveld, 2015). Continued improvement of our understanding of catchment runoff responses (including predictions) and stream water quality in catchments is dependent upon further increasing understanding of subsurface hillslope-floodplain connectivity (Blume and van Meerveld, 2015). Furthermore, studies of subsurface hillslope-floodplain connectivity which have been presented are almost exclusively for catchments in temperate regions of the world, and therefore do not necessarily reflect the physical structures (e.g. talus slopes), antecedent conditions (permafrost), and driving forces (e.g. spring melt) that occur in paraglacial environments.

Subsequently understanding of hillslope-floodplain connectivity in paraglacial settings remains a major research gap. Yet as a consequence of glacial retreat paraglacial hillslope areas are increasing (Heckmann *et al.*, 2016). Paraglaciation has been identified as the single most significant process influencing sediment supply and landscape change in arctic, sub-arctic, and alpine environments over the next century (Knight and Harrison, 2014) with subsequent increases in the number of colluvial deposits and hillslope runoff within these

environments (Heckmann *et al.*, 2016). However, as discussed understanding of the hydrologic storage capacity and flow paths of physical structures on paraglacial hillslopes remain uncertain (Gordon *et al.*, 2015). Given the growing recognition of the significance of GW-flow in paraglacial catchments (Hood and Hayashi, 2015), and potential role of colluvial aquifers on valley sides (Weekes *et al.*, 2015), establishing hillslope-floodplain connectivity and defining the contribution of hillslope runoff to GW-fed streams on paraglacial floodplains should be urgently addressed.

The first-order controls (Buttle, 2006; Devito *et al.*, 2005) on GW-fed stream occurrence within paraglacial settings have not been established, although PFPs are associated with their presence (Caldwell *et al.*, 2015). The concept of first-order controls considers a hierarchal approach to determine fundamental controls on runoff (i.e. climate, geology, geomorphology, soil, and topography) (Devito *et al.*, 2005), which for GW-fed streams on paraglacial floodplain is considered at a subcatchment scale (Gleeson and Paszkowski, 2014). Without an understanding of first-order controls it is difficult to consider the sensitivity of GW-fed streams to climate change. For example, glacial retreat in paraglacial environments could have significant implications for the long-term stability of PFPs (Poole *et al.*, 2002). Long-term declines in sediment loads as a consequence of glacial retreat (Church and Ryder, 1972; Gurnell *et al.*, 2000; Orwin and Smart, 2004) could be detrimental PFPs (Poole *et al.*, 2002). Less frequent channel avulsion (Levy *et al.*, 2015; Poole *et al.*, 2002), topographic forcing (Marren and Toomath, 2014), and development of mature-stage vegetation succession (Caldwell *et al.*, 2015; Klaar *et al.*, 2015; Lorang and Hauer, 2007) could all impact the formation of new PFPs and effectiveness of existing channels as conduits of flow (Poole *et al.*, 2002). Establishing if PFPs are a critical first-order control is then a major research gap given concerns over their long-term stability and potential importance to GW-fed streams.

Addressing the fundamental research gaps outlined, this thesis summaries site specific research conducted during 2013 and 2014 on GW-fed streams within Denali National Park & Preserve (DNPP), Alaska. Research encompassed the application of hydrometric, hydrogeomorphological, hydrochemical, and geophysical analysis in a site specific study to improve understanding of the hydrogeomorphic controls and hydrological dynamics that support GW-fed streams. Knowledge developed was then applied at an intra-catchment scale to establish fundament first order controls upon the occurrence of GW-fed streams on paraglacial floodplains.

1.4 AIMS & OBJECTIVES

The overall aim: of the research was to understand the **hydrological dynamics and geomorphic controls upon groundwater-fed streams within paraglacial floodplains**. To address this aim, three specific objectives for the research were identified:

1. Establish the key hydrogeomorphic controls on PFPs and GW-fed streams;
    - Determine the spatiotemporal nature of floodplain recharge during summer months
    - Quantify GW-fed stream recharge and hillslope runoff fluxes during summer months
    - Develop a conceptual model of the hydrological dynamics supporting floodplain recharge
2. Determine the significance of hillslope-floodplain connectivity in sustaining streamflow of biodiversity hotspots;
    - Determine the significance of PFPs to hillslope-floodplain connectivity

- Establish the role of colluvial deposits as groundwater aquifers and conduits of flow on hillslopes
- Quantify flow from colluvial deposits to individual GW-fed streams

3. Establish first-order controls upon GW-fed stream and consider their sensitivity to climate change;
    - Determine whether perennial GW-fed stream occurrence is consistently dependent on the presence of PFPs
    - Establish if hillslope runoff provides a significant contribution to GW-fed streams at an intra-catchment scale
    - Characterise climate change impacts upon first-order controls and subsequent consequences for the long-term stability of GW-fed streams

Site specific research was conducted within DNPP during the summer of 2013 and was expanded during summer 2014 to provide a broader, intra-catchment scale context to the research.

1.5 OUTLINE OF THESIS

This thesis consists of a methodology chapter, three empirical chapters, and synthesis. The structure is as follows:

A methodology chapter which provides detailed descriptions for all field sites, fieldwork methods used, laboratory analysis conducted, and data/statistical analysis applied.

Chapter three, entitled ‘Preferential flow pathways within paraglacial floodplains: hydrogeomorphic control upon the occurrence and stability of biodiversity hotspots’; aims to characterise the hydrogeomorphic controls upon the occurrence of GW-fed streams within paraglacial floodplains, and identifies their hydrological dynamics.

Chapter four, entitled ‘Hillslope-floodplain connectivity in paraglacial catchments: colluvial deposits regulating floodplain hydrological dynamics’; investigates the role of PFPs in hillslope-floodplain connectivity and establishes the importance of colluvial deposits as stores and conduits of valley side groundwater flow in paraglacial catchments.

Chapter five, entitled ‘First-order controls on groundwater-fed streams and their long-term stability in paraglacial catchments’; considers if the physicochemical properties of groundwater-fed streams indicate first-order controls upon their hydrological dynamics, and deliberates the potential consequences of climate change upon them.

The concluding chapter draws together key findings and synthesises research outcomes for the three chapters.

CHAPTER 2: METHODOLOGY

2.1 FIELD SITES

Research was conducted during 2013 and 2014 in Denali National Park and Preserve (DNPP), Alaska. DNPP is situated in interior Alaska (62° 50’ to 64° 00’N; 150° 00’ to 152° 50’W) and covers an area of ~26,000 km^2 (Figure 2.1a). The Alaska Range dominates DNPP with the three highest peaks in the range; Denali (6,190 m), Mount Foraker (5,304 m), and Mount Hunter (4,442 m), all located within the park. DNPP was selected as it provided an opportunity to conduct research in a pristine environment and natural catchments, uninhibited by local anthropogenic activity. Previous research had already established that GW-fed streams within DNPP acted as important biodiversity hotspots (Crossman *et al.*, 2011; Milner *et al.*, 2006). In addition GW-fed streams are a widespread feature of floodplains within DNPP. Riverine habitat patches (Malard *et al.*, 2002) where GW-fed streams persist may account for ~40% of floodplain areas within the park (Crossman *et al.*, 2012). Such extensive GW-fed stream occurrence within DNPP was advantageous for the intra-catchment scale approach taken to deliver on the outlined objectives.

The geology of the Alaska Range and its associated foothills is varied with siliceous metamorphic outcrops, siliclastic sandstone and limestone layers, and mafic and felsic volcanic deposits all present (Figure 2.2; Wilson *et al.*, 1998). Floodplains in these catchments are dominated by fluvioglacial outwash and related geomorphological structures, such as; braided channels, gravel bars, and terraces. Discontinuous permafrost is present on many valley sides (Yocum *et al.*, 2006), as are colluvial deposits such as talus cones, alluvial fans, and scree slopes that are typically widespread and prominent in paraglacial environments (Ballantyne, 2002b). At higher elevations within DNPP, above the treeline, alpine tundra and sporadic perched wetlands dominate the gentler slopes of valley sides. While at lower elevations Spruce woodlands are more prominent.

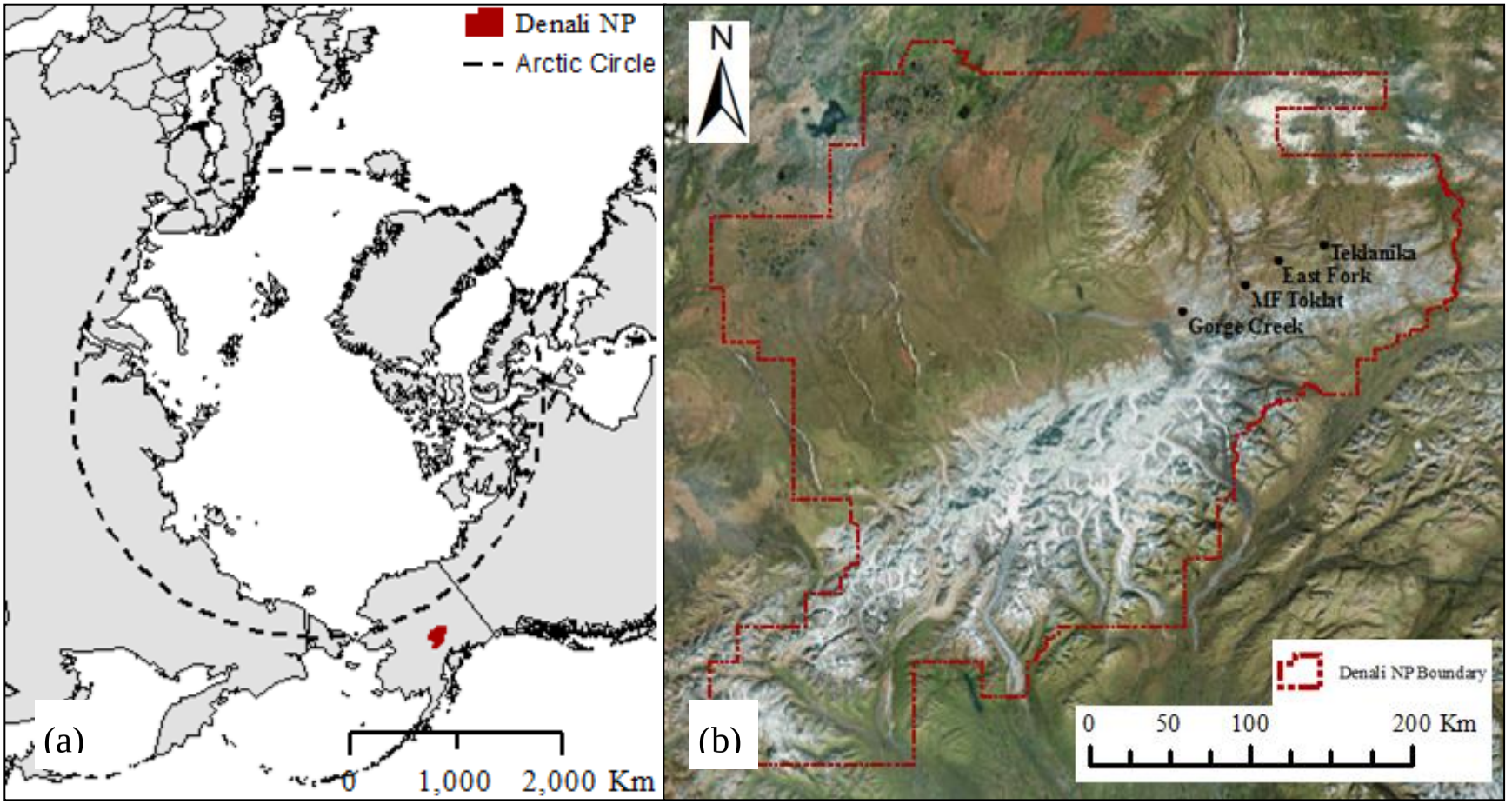

Figure 2.1: (a) location of DNPP within Alaska and relative to the Arctic Circle; (b) location of study sites within DNPP

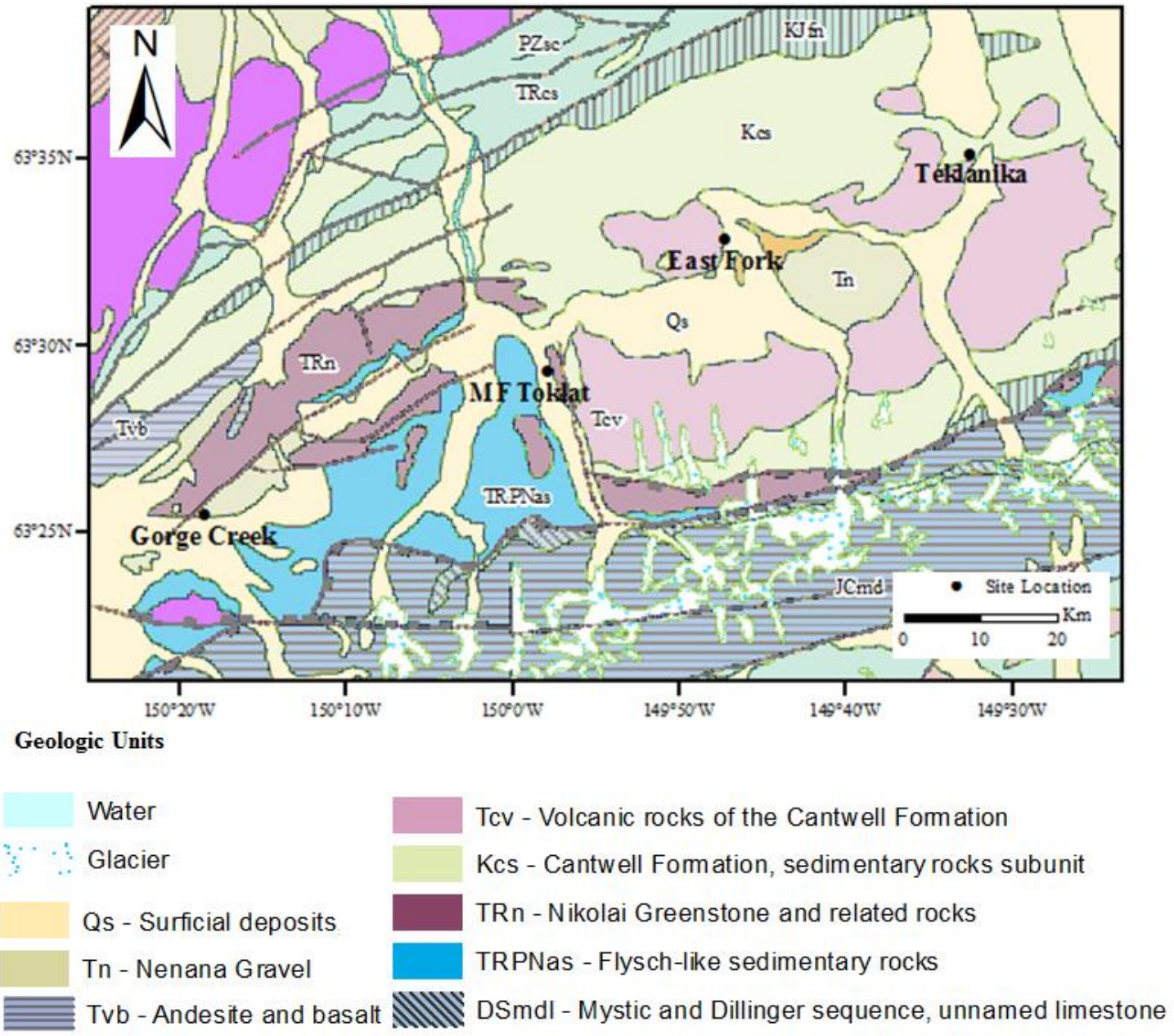

Figure 2.2: Geological map for sites. Key geologic units for the catchments are labelled on the map with unit description provided in the legend

The four sites selected for the study were located on the northern side of the Alaska Range, which is dominated by south to north flowing glacial-fed rivers that form the headwaters of the Yukon Basin, and which are separated by the foothills of the Alaska Range which extend in a series of east-west orientated ridges (Thornberry-Ehrlich, 2010). The site specific study (for objectives (1) and (2)) centred on a site on the east branch of the Middle Fork (MF) Toklat River, which had been the focus of previous research (Crossman *et al.*, 2011; Crossman *et al.*, 2013). For the intra-catchment study (objective (3)) an additional three sites were selected; on the East Fork (EF) River, Teklanika (Tek) River, and at Gorge Creek (GC).

A summary of important field site characteristics are provided in (Table 2.1). All sites were within paraglacial environments; evidenced by the geomorphic features present in each catchment (Table 2.1; see section 1.1). Deglaciation was occurring at all sites, with the exception of GC where it was already complete. Subsequently the elevated sediment yield rates associated with paraglacial adjustment periods were expected at all sites (Figure 1.1a) Furthermore, upstream catchment area for field sites varied between 18 and 176 km^2 and so based on the sediment wave model of Church and Slaymaker (1989) it might be anticipated that peak sediment yield rates have not yet been reached (Figure 1.1b).

Terrace areas ranged from 0.07 to 0.89 km^2, with the smallest terrace located on the Tek and largest on the MF Toklat. All terraces were located within the active orthofluvial zone. These are depositional environments lacking scouring flows, and are areas of the floodplain where flooding is infrequent and mature-stage vegetation succession is allowed to develop (Lorang and Hauer, 2007). They are typified by rapidly expanding areas of accretion with thin, well-drained soils, dearth of organic matter (Caldwell *et al.*, 2015).Terraces were elevated between 0.5 and 2.0 m above the active floodplain and characterised by perennial streams that emerged and flowed across them, with the exception of GC where streams were ephemeral.

	Middle Fork (MF) Toklat	East Fork (EF)	Teklanika (Tek)	Gorge Creek (GC)
Location (Degrees, Minutes, Seconds)	149° 57' 58.36"W / 63° 28 '22.14"N	149° 47' 16.87"W / 63° 32' 53.45"N	149° 32' 12.29"W / 63° 35' 15.38"N	150° 18' 31.15"W / 63° 25' 26.28"N
Terrace elevation (m)	1035	965	915	975
Terrace area (Km^2)	0.89	0.16	0.07	0.50
Upstream catchment area (Km^2)	114	176	161	18
Glacial coverage (%)	4.5	6.1	6.1	0
Catchment geology	Siliceous metamorphics; Siliclastic sandstones; Mafic & felsic volcanics; limestone	Siliceous metamorphics; Siliclastic sandstones; Mafic & felsic volcanics; limestone	Siliceous metamorphics; Siliclastic sandstones; Mafic & felsic volcanics; limestone	Siliceous metamorphics; Siliclastic sandstones; Mafic & felsic volcanics
Floodplain sediments	Clast-suppoted, fluvioglacial gravels, sands, and silts	Clast-suppoted, fluvioglacial gravels, sands, and silts	Clast-suppoted, fluvioglacial gravels, sands, and silts	Clast-suppoted, fluvioglacial gravels, sands, and silts
Geomorphic features	Glaciers; Alpine tundra; Colluvium; Fluvioglacial landforms; Discontinuous permafrost	Glaciers; Alpine tundra; Colluvium; Fluvioglacial landforms; Discontinuous permafrost	Glaciers; Alpine tundra; Colluvium; Fluvioglacial landforms; Discontinuous permafrost	Alpine tundra; Colluvium; Fluvioglacial landforms; Discontinuous permafrost
Catchment vegetation	Willow, Birch, and Dwarf Shrubs; Sedges; Grasses; Legumes	Willow, Birch, and Dwarf Shrubs; Grasses; Legumes; Alder; Stunted Spruce	Willow, Birch, and Dwarf Shrubs; Legumes; Grasses; Alder; Stunted Spruce; Spruce	Willow, Birch, and Dwarf Shrubs; Sedges; Legumes; Grasses; Alder

Table 2.1: Summary of key characteristics for all field sites utilised as part of this research

2.1.1 MF Toklat

A floodplain terrace in the east branch of the north flowing MF Toklat River, DNPP, Alaska (63° 29' 38.23"N, 149° 58' 5.99"W) was the focus of extensive hydrogeomorphic surveying and hydrometric monitoring in the summers of 2013 and 2014. The site has been the focus of previous research that had identified GW-fed streams on the terrace and established their importance as biodiversity hotspots (Crossman *et al.*, 2011; Crossman *et al.*, 2012; Crossman *et al.*, 2013). The MF Toklat is a braided, north flowing glacial-fed tributary of the Yukon River. In its headwaters, upstream of the floodplain terrace, the Toklat divides into an east (114 km^2) and west branch (152 km^2) (Podolak, 2013).

Three small glaciers remain at the head of the east branch with a total area of ~6 km^2 (Crossman *et al.*, 2013), equal to ~5.3% of the total catchment surface area upstream of the site (Figure 2.3). Between 1954 and 2012 glacial retreat within the catchment averaged ~25 m per year (Crossman *et al.*, 2013), while rates of thinning increased from 1.5 m yr^{-1} during 2001-2008 to 2.0 m yr^{-1} between 2008-2010 (DENA., 2012). The terrace extended for 2600 m along the eastern edge of the MF Toklat floodplain and was 600 m across at its widest extent (Figure 2.4). The base of the terrace was at 1015 m.a.s.l rising to 1070 m.a.s.l at its furthest extent upstream, and had a down-valley gradient of 2% (Crossman *et al.*, 2011)

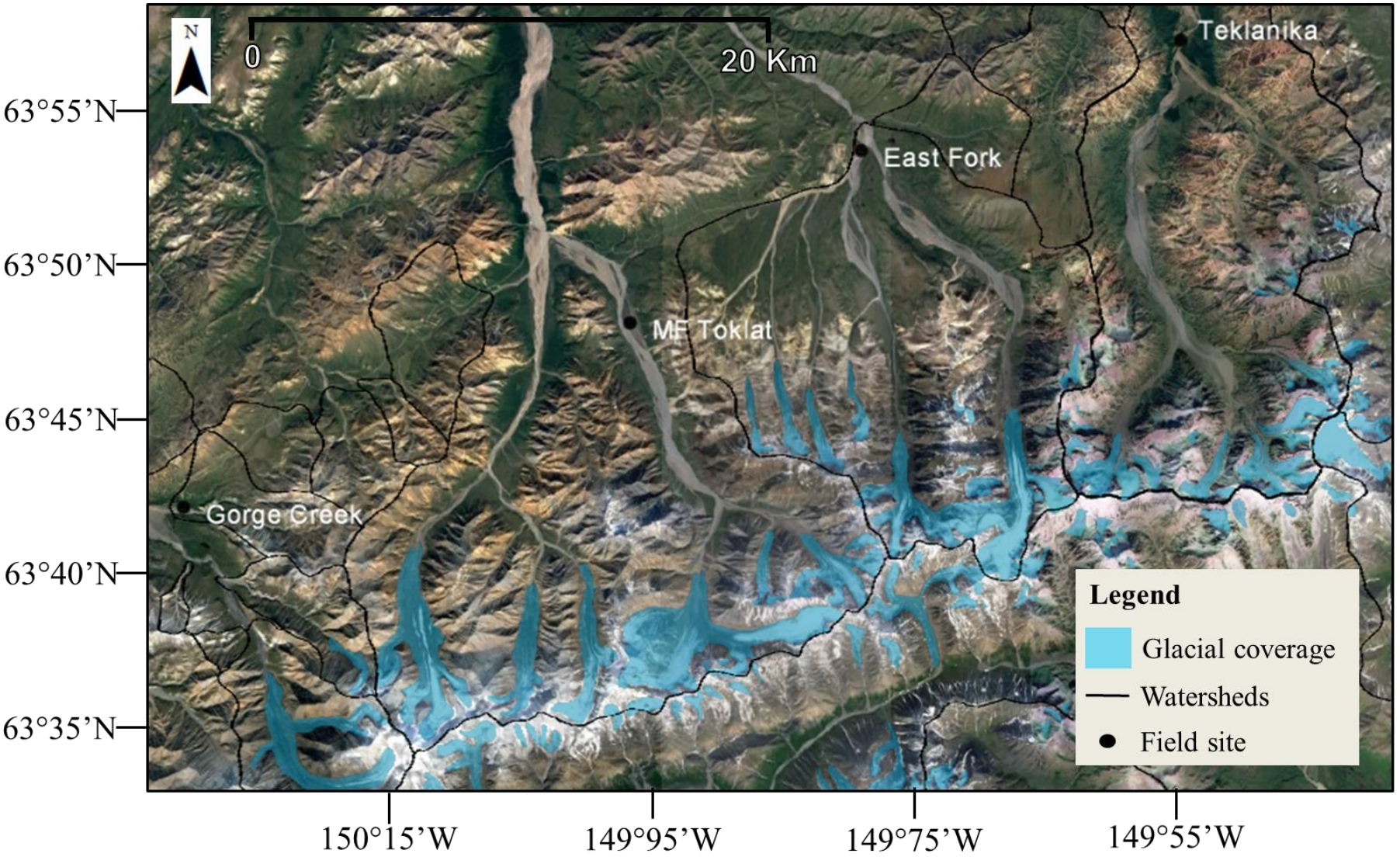

Figure 2.3: Field site location and glacial coverage within respective watersheds. Only the Gorge Creek site was located within a non-glaciated catchment. Image obtained from Google.

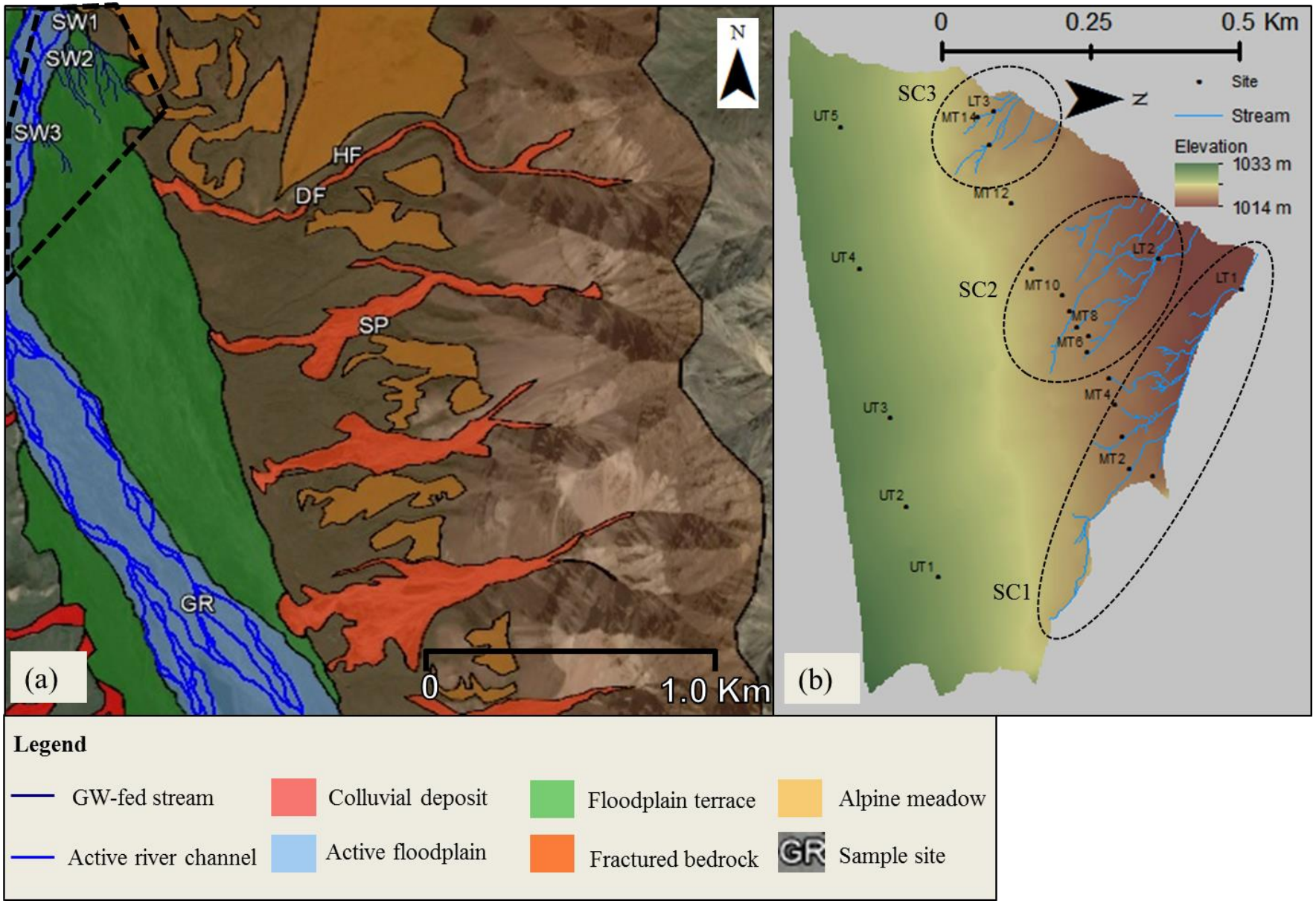

Figure 2.4: (a) MF Toklat terrace, landscape units, and location of active river channels on the floodplain. Four colluvial deposits extend down the valley side adjacent to the terrace. Alpine meadows are also present alongside fractured bedrock on valley sides. Sample site locations are also shown for surface water (SW), glacial river (GR), snowpack (SP), debris fan (DF), and hillslope flow (HF); (b) DEM of terrace base showing GW-fed stream distribution and stream cluster (SC) groupings. Location of piezometer nests along lower (LT), middle (MT), and upper (UT) transects are also shown. Image for (a) obtained from Google.

GW-fed stream networks at the base of the terrace (Figure 2.4; mapped June 2013) were clustered into three groups. Stream cluster 1 (SC1) was at the northeast point of the terrace, nearest the hill slope, and formed a dendritic drainage pattern that flowed from the terrace as a single, 10^{th} order stream at point SW1. SC2 was a group of six separate streams extending 30 to 140 m south-west of SC1. SC3 comprised five separate streams extending 85 to 190 m south-west of SC2. Stream head positions on the terrace were not static, with streams extending up-valley on the terrace through both summer 2013 and 2014. Between May and September 2014 some streams extended up to 912 m further up-valley. Extension of GW-fed streams in summer months was subsequently followed by retreat during winter months. This pattern of GW-fed stream behaviour was not accompanied by the formation of new streams flowing from the terrace.

Stream temperature data for SW1 (SC1), SW2 (SC2), and SW3 (SC3) between June 2013 and July 2015 pointed to streams within SC1 and SC2 being perennial in nature and those within SC3 being ephemeral (Figure 2.5). Stream temperatures at SW1 and SW2 remained stable, just above 0°C, throughout the monitoring period and at no point mirrored surface air temperatures. This would indicate the streams did not either freeze or run dry, suggestive of perennial flow. At SW3, by contrast, stream temperatures mirrored air temperature between March and May 2014. This is indicative that the channel ran dry and that the stream exhibited ephemeral behaviour. These are observations which align with those of Crossman *et al.* (2011).

(a)

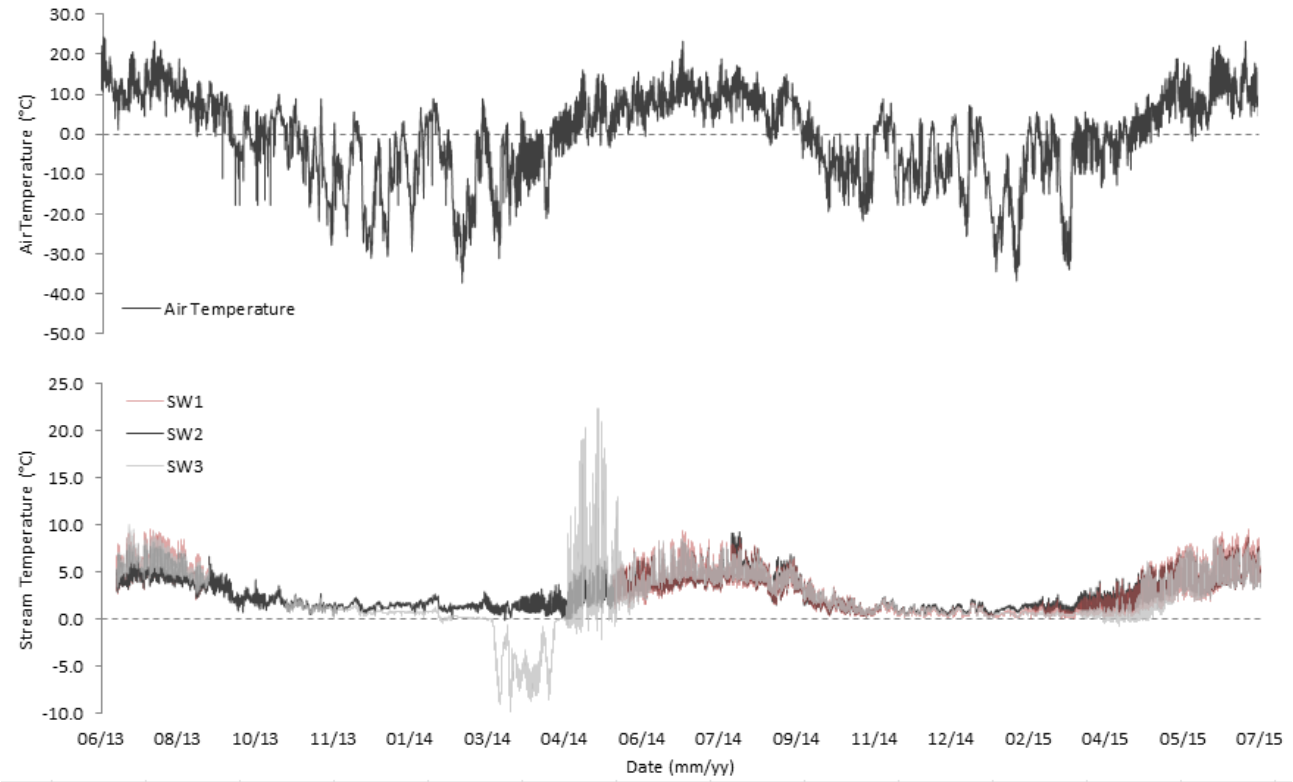

Figure 2.5: (a) surface air temperature data from automated weather station ~5 Km NW of MF Toklat site; (b) stream temperature data for SW1 (SC1), SW2 (SC2), and SW3 (SC3). Data obtained using TinyTag Aquatic 2 (TG-4100) temperature loggers.

Hillslopes adjacent to the terrace were predominantly vegetated with occasional, sporadic alpine meadows (Figure 2.4a). During May 2014 electromagnetic (EM) surveying, using a Geonics EM-31, of the floodplain and adjacent hillslopes was carried out (Figure 2.6). Resistivity values >451 on the hillslopes above the site suggest pockets of discontinuous permafrost within weathered and soil layers on valley sides (Palacky, 1988). Areas of higher resistivity on the hillslopes aligned with physical observations of frozen soil in the subsurface (Figure 2.7). These observations supported the findings of Yocum *et al.* (2006) who estimated discontinuous permafrost coverage in the catchment of between 20 - 80%, with thinning of the active layer in the summer months of 1.0 – 1.5 m. Low values on the terrace showed permafrost did not occur on the floodplain and was instead restricted to valley sides.

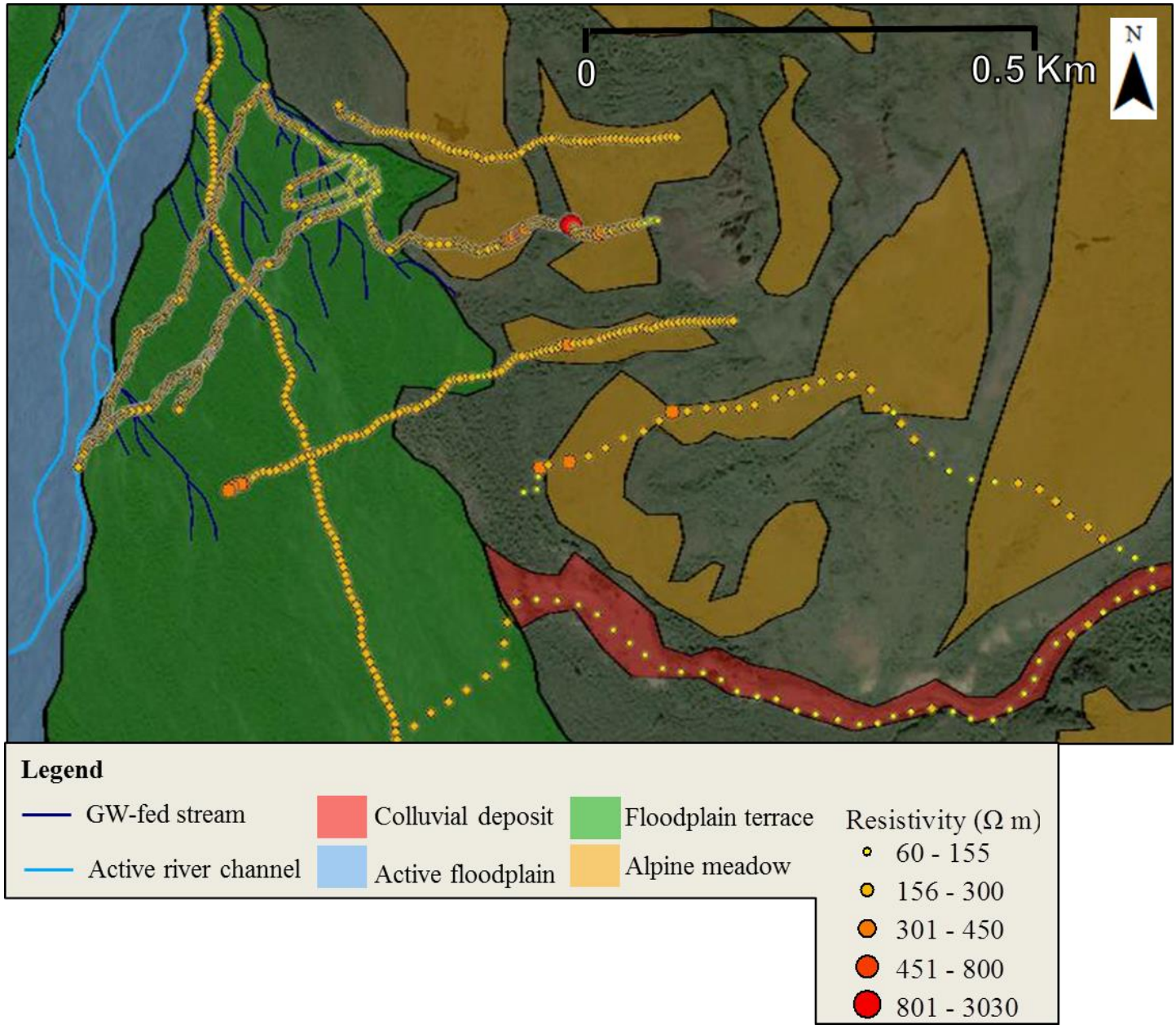

Figure 2.6: EM survey data collected during May 2014. Resistivity values >451 on the valley sides are due to the occurrence of discontinuous permafrost. Image obtained from Google.

Figure 2.7: Frozen soil on the hillslopes adjacent to the MF Toklat terrace, identified in areas with higher resistivity values.

Four separate colluvial deposits extended down the eastern valley side to the base of the hillslope, three of which protruded onto the terrace (Figure 2.4a). Across the valley floor fluvial-glacial outwash, of unknown thickness, overlaid basal glacial till deposits (Crossman *et al.*, 2011). At the base of the hillslope, adjacent to the terrace, the underlying geology was a subvolcanic formation (Figure 2.2), with volcanic units and sedimentary formations of the Cantwell Formation present further upslope (Wilson *et al.*, 1998). All units present on the valley side were a potential source of fractured bedrock (Figure 2.4a).

2.1.2 East Fork Toklat

A terrace on the East Fork (EF) Toklat River (149° 47’ 16.87”W / 63° 32’ 53.45”N) was one of three additional field sites included as part of an intra-catchment study for objective 3 (Chapter 5). The upstream catchment area, 176 Km^2, was the largest for any of the sites and glacial coverage was 6.1% (Table 2.1). The terrace was 500 m downstream of a confluence where flow from the four Polychrome Glaciers and associated hillslope areas converged (Figure 2.3). These glaciers have receded rapidly in the past 100 years (DENA., 2012) and consequently exposed colluvial deposits and fluvioglacial landforms (e.g. lateral moraines) are abundant within the deglaciated valleys. Downstream of the foothills an expansive area of fluvioglacial outwash (of unknown thickness) occurs (Figure 2.2), and is where the field site is located. The terrace is located on the floodplain margin (within the Orthofluvial zone), adjacent to steep valley sides formed from outcrops of volcanic rocks of the Cantwell Formation. On the hillslopes above the terrace alpine meadows are present at lower reaches, while on the steeper slopes colluvial deposits have formed (Figure 2.8).

The terrace itself had an area of ~0.16 Km, was 1080 m in length and 350 m across at its widest extent. Along its longitudinal profile the terrace rose from 940 to 962 m.a.s.l upstream, with a slope gradient of 2.04%. Towards the base of the terrace, where GW-fed streams formed, mature vegetation had developed (Figure 2.9). In particular Alaska willow (*Salix alaxensis*) was a dominant presence. Higher up the terrace vegetation cover became sparse leaving exposed terrace sediment. At its base the terrace backed onto the top of another terrace, discernible by a slight elevation drop (< 0.5 m). The GW-fed stream nearest the hillslope (SW1) flowed onto, and across the other terrace. All other GW-fed streams on the site flowed directly from the terrace and across the active floodplain (Figure 2.8).

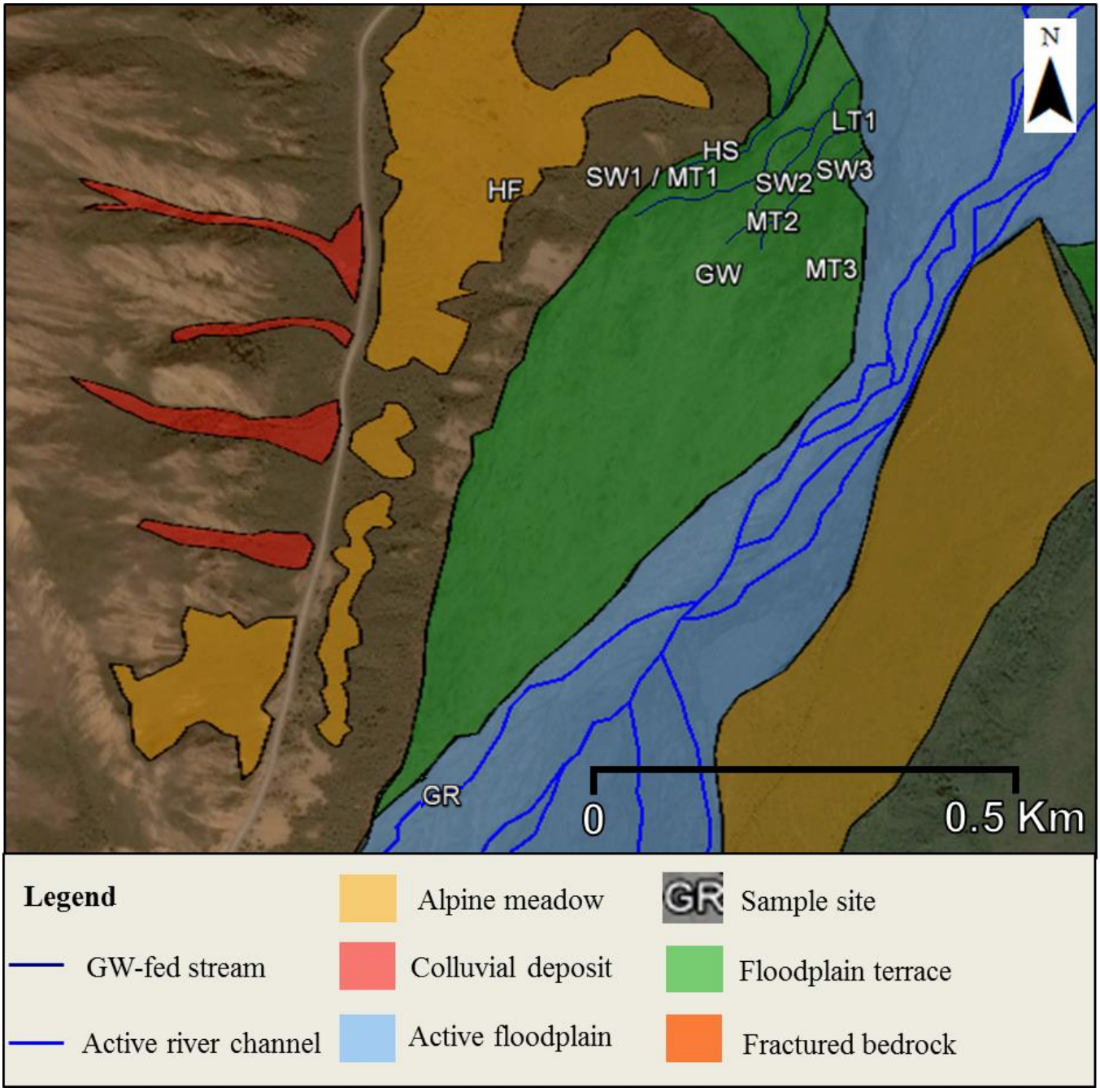

Figure 2.8: EF Toklat terrace and surrounding landscape units. Alpine meadows were present on lower reaches of slopes adjacent to the terrace. Colluvial deposits occurred on steeper slopes at higher elevation. The park road can is also clearly identifiable traversing the adjacent hillslope from north to south. Sample sites included surface water (SW) on the terrace; piezometers (LT & MT); upstream groundwater (GW); hillslope seepage (HS) from the base of the hillslope; hillslope flow (HF) from one of the alpine meadow areas above the terrace; and the main glacial East Fork River (EF). Image obtained from Google.

Figure 2.9: Photograph of East Fork (EF) Toklat field site, looking downstream from the adjacent valley-side. The vegetated base is clearly identifiable along with GW-fed stream channels. Alpine meadow areas can also be recognised at the base of the adjacent hillslope.

2.1.3 Teklanika

A terrace on the Teklanika (Tek) River (149° 32’ 12.29”W / 63° 35’ 15.38”N) was the smallest (0.07 Km^2) included as part of the intra-catchment study (Table 2.1). Upstream catchment area, at 161 Km^2, was the second largest of all the field sites. Glacial coverage equated to 6.1% of upstream catchment area. Geology in the catchment was dominated by volcanic and sedimentary rocks of the Cantwell Formation (Figure 2.2); both sources of fractured bedrock. The terrace was located within a large, glacial U-shaped valley at the base of the NE facing slopes of Cathedral Mountain (elevation = 1482 m); an outcrop of volcanic rock of the Cantwell Formation. The floodplain was composed of fluvioglacial outwash (unknown thickness). The active floodplain of the Tek River narrowed where the terrace was located (Figure 2.10) due to the presence of volcanic outcrops on either side of the river (Figure 2.2), which are not easily eroded (Thornberry-Ehrlich, 2010).

The terrace was at the lowest elevation for any of the field sites (Table 2.1). Due to its lower elevation this was the only site located below the tree line, and where spruce forests occupied surrounding hillslopes (Figure 2.10). On the hillslopes above the terrace areas of alpine meadow were also present, and at higher reaches on Cathedral Mountain colluvial deposits were identified and which extended down to the top of the terrace (Figure 2.11). The terrace was elevated between 0.5 and 1.0 m above the active floodplain and rose from 889 to 897 m.a.s.l along its 552 m length; a gradient of 1.45%. The terrace was 250 m across at its widest extent. Vegetation was denser and more mature both towards the base and hillslope margins of the terrace, similar to at both MF Tok and EF. Perennial GW-fed streams flowed at the margins of the terrace, near to the hillslopes. Flow was not observed in channels further across the terrace (towards the active floodplain), which were identifiable from satellite imagery (Figure 2.10).

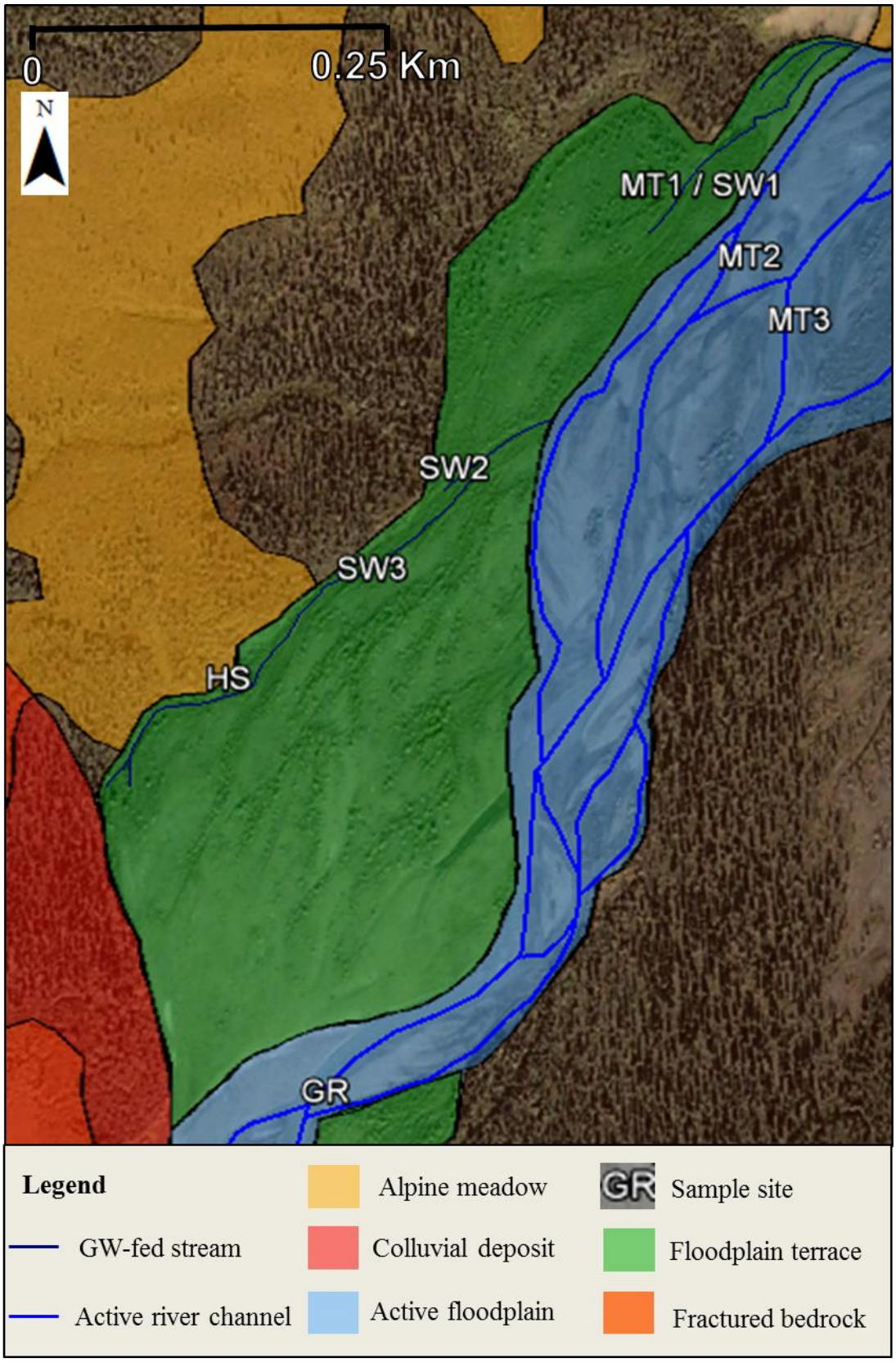

Figure 2.10: Tek terrace and surrounding landscape units. GW-fed streams only flowed close to the hillslope on the terrace margins Sample sites included surface water (SW), piezometers (MT), the main glacial river channel (Tek), and hillslope seepage (HS) from the valley side. Image sources from Google.

Figure 2.11: Image looking upstream of the Tek field site, the terrace can be seen to the right of the Teklanika River. A GW-fed stream can be seen flowing at the margin of the terrace. Spruce forests are present either side of the floodplain due to the lower elevation of the field site.

2.1.4 Gorge Creek

A terrace within the Gorge Creek (GC) watershed (150° 18' 31.15"W / 63° 25' 26.28"N) provided the only field site located in a deglaciated catchment (Figure 2.3). Upstream catchment area for the site was 18 Km^2, an order of magnitude less in size compared to the three other field sites (Table 2.1). A south facing steep valley side on the northern side of the terrace has formed from resistant outcrops of metamorphic greenstones and related rocks (Figure 2.2). These steep slopes have resulted in three colluvial deposits that extent onto the terrace (Figure 2.12). To the NE of the terrace a stream flow through a ravine, cut into Nenana Gravel deposits, and flows directly onto and across the terrace. Higher up the valley side to the north of the terrace lower gradient slopes have allowed some alpine meadow formation. The active floodplain and terrace were comprised of fluvioglacial outwash (unknown thickness).

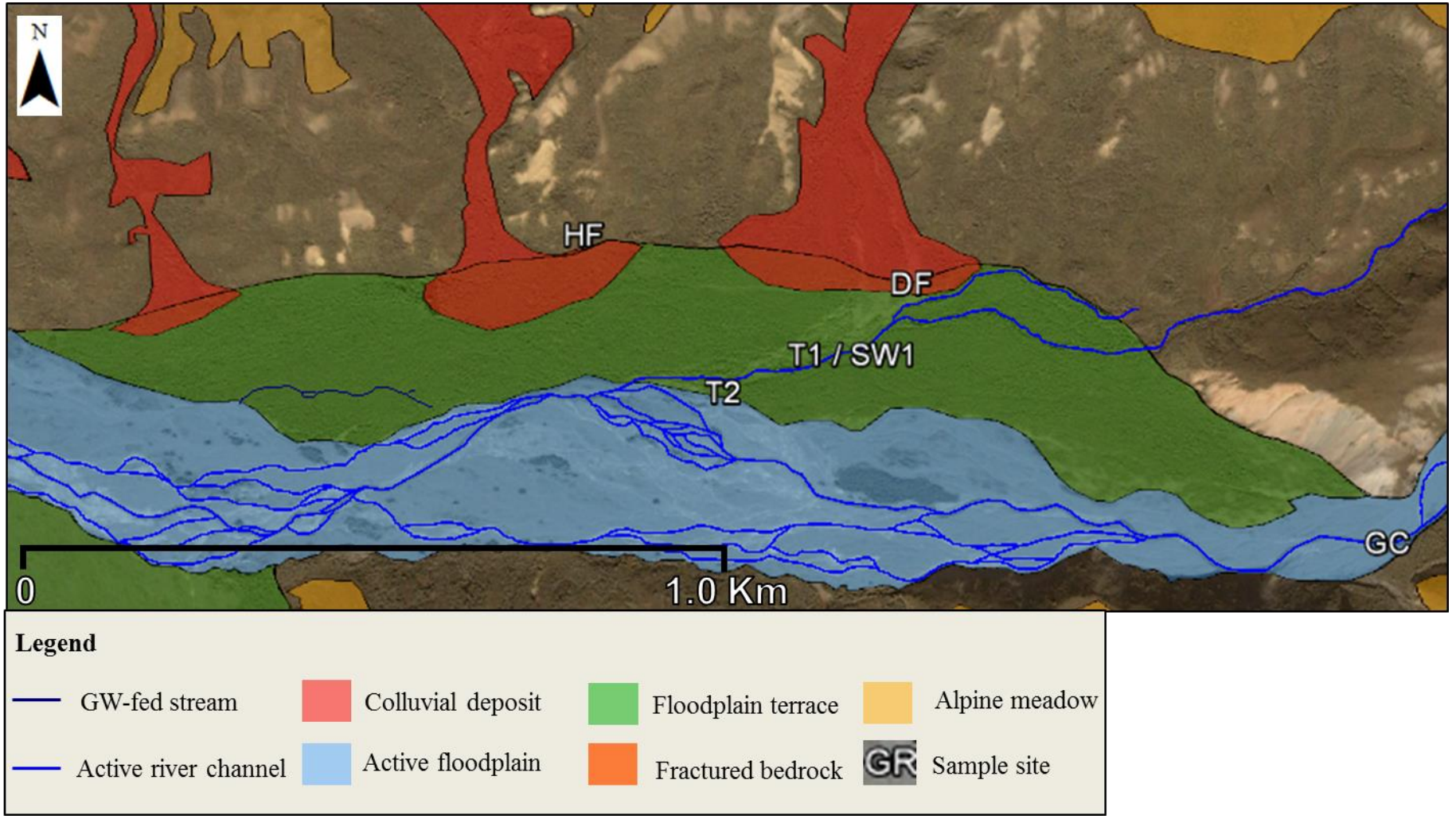

Figure 2.12: Gorge Creek (GC) terrace and surrounding landscape units. To the NE of the terrace a stream flows through a ravine and across the field site. Three colluvial deposits extend onto the terrace from the adjacent valley side. Sample sites include surface water (SW), piezometers (T), a debris fan (DF), and hillslope flow (HF). Image obtained from Google.

The terrace itself was the second largest of the field sites (0.5 Km^2). Elevation of the terrace above the active floodplain ranged between 0.5 and 1.5 m. At its widest extent the terrace was 230 m across. Along its longitudinal profile the terraces rose from 945 to 985 m.a.s.l across a distance of 1,550 m; the downstream gradient was 2.58%. There were no perennial GW-fed streams on the terrace, with all channels exhibiting ephemeral behaviour (personal observation). Vegetation cover on the terrace was the densest of any field site (Figure 2.13). Mature vegetation including Willow, Birch, and Dwarf Shrubs were more abundant in presence and the terrace was the only site where Alder was present (Table 2.1).

Figure 2.13: Gorge Creek (GC) terrace from the south face valley side. In contrast to the other field sites vegetation cover was mature and dense across the entire terrace

2.2 METEORLOGICAL DATA

Temperature (°C) and total precipitation (mm) data for both field seasons (2013 & 2014) during summer months (June, July, and August) is presented in Table 2.2. Data was obtained from an automated weather station located 5 Km NW of the MF Toklat field site (WRCC., 2014b), within the same catchment. Mean summer temperatures were markedly higher in 2013 compared to 2014, and in particular mean June temperatures were 4.8 °C higher. By contrast precipitation was higher during 2014 for all three months. Noticeably total precipitation was 101.3 mm higher in June 2014 compared to 2013.

Long term precipitation and temperature records are provided by the National Park Service (NPS) for DNPP Headquarters (148° 57' 48.85"W / 63° 43' 16.70"N; elevation = 625 m), located 33 Km ENW of the most easterly field site (Tek). Average temperature and total precipitation data for summer months during 2013 and 2014 at the Park HQ are presented alongside normal values for the period 1981-2010 in Table 2.3. The departure from normal shows that 2013 was both a warmer and drier year than normal, while 2014 was cooler and wetter. June 2013 was the second warmest June on record for DNPP. By contrast June 2014 was the 11th wettest and coolest June on record. In addition July 2014 was the 9th wettest on record.

2013				
	Precipitation (mm)	Temperature (°C)		
		Mean	*Max*	*Min*
June	28.4	13.0	24.4	2.2
July	99.5	11.8	23.3	1.1
August	101.6	9.8	21.1	-0.6

2014				
	Precipitation (mm)	Temperature (°C)		
		Mean	*Max*	*Min*
June	129.7	8.2	18.3	-0.6
July	105.9	10.4	23.3	1.7
August	112.7	9.5	17.2	-1.1

Table 2.2: Temperature (°C) and precipitation (mm) data for 2013 and 2014 from an automated weather station 5 Km NW of the MF Toklat field site. High mean temperatures in 2013 contrasted with much higher summer precipitation in 2014.

		2013		2014	
Temperature (°C)	**1981 - 2010 Normal**	**Monthly Average**	**Departure from normal**	**Monthly Average**	**Departure from normal**
June	11.56	14.33	**+2.78**	9.50	**-2.06**
July	13.11	13.45	**+0.33**	11.78	**-1.33**
August	10.33	11.89	**+1.56**	11.00	**+0.67**

Precipitation (mm)	**1981-2010 Normal**	**Total monthly**	**Departure from normal**	**Total monthly**	**Departure from normal**
June	54.61	20.07	**-34.54**	92.96	**+38.35**
July	81.79	48.51	**-33.27**	117.09	**+35.31**
August	68.83	65.28	**-3.56**	58.67	**-10.16**

Table 2.3: Summer temperature and precipitation data for an automated weather station located at DNPP HQ. Data presented for 2013, 2014, and normal values for 1981-2010. For departure from normal, red indicates values above average and blue values below.

2.3 FIELD METHODS & LABORATORY ANALYSIS

Detailed descriptions of field methods applied during 2013 and 2014 field seasons to deliver on the outlined aims and objectives are outlined below. In addition a thorough breakdown of lab analysis conducted is also provided.

2.3.1 Lithofacies and hydrofacies identification

Hydrofacies are regarded as lithofacies with a unique range of hydraulic conductivities (Anderson, 1989); a single lithofacies can be comprised of multiple hydrofacies. Therefore identifying the range of individual hydrofacies present on the MF Toklat was important to establishing the prevalence and significance of PFPs. Three transects (upper (UT), middle (MT), and lower (LT); Figure 2.4b) which ran perpendicular across the terrace were utilised for the analysis. Along the three transects 22 individual sites (LT1 to LT3; MT1 to MT14; and UT1 to UT5) were selected for lithofacies and hydrofacies identification. Grab samples of ~500 g of surface sediment were collected manually at each site using a scoop. Grain-size distribution analysis (GSDA) and sediment descriptions were determined for each site by sieving. Wet and dry sieving was conducted for sediment > 0.063 mm in size while grain-size fractions < 0.063 mm were determined using a Malvern Mastersizer 2000. Effective porosity was calculated and textural group classification and grain-size statistics were undertaken using the Gradistat software package (Blott and Pye, 2001).

This data was then applied to identify the lithofacies at each site using a modification of Miall's (1978) classification, grain-size-statistics, and textural descriptions from GSDA and field observations (Bayer *et al.*, 2011; Heinz and Aigner, 2003a; Klingbeil *et al.*, 1999). A standardised code was allocated to each lithofacies (Table 2.4) representing main grain size (I_1), minor matrix component (i_1), texture (i_2), stratification (i_3), and additional information

(i_4). Lithofacies classifications were then linked to surface hydraulic conductivities ($K_{0.0}$) calculated for each site (see section 2.3.2.1) to identify the range of hydrofacies present on the terrace.

Indicies/features	Abbreviation
i_1 grain-size	c, cobbles
	s, sand
I_1 grain-size	G, gravel
	P, soil
i_2 texture	c, clast-supported
i_3 stratification	m , massive (no bedding)
i_4 additional information	b, bimodal

Table 2.4: Standardised code for lithofacies identification

2.3.1.1 Outcrop-based hydrofacies characterisation and digitisation

Further to the extensive spatial survey of lateral variations in $K_{0.0}$, and associated particle size distribution on the terrace four outcrops were selected for more detailed sedimentary descriptions and profiles (Figure 2.14). Outcrops were selected to cover the range of sedimentary environments and lithofacies present on the terrace. This included areas with overlying soil layers and mature vegetation, as well as near to GW-fed streams. The profiles would help provide understanding of vertical variation in hydrofacies on the terrace. For each profile sediment texture including particle-size range, overall texture, sorting, clast size, and clast roundness were determined for identified layers. In addition samples were collected from each layer for GSDA, following the method outlined in section 2.3.1. 2D sedimentological outcrop mapping was then carried out on profile images using ArcGIS 10.2. Following the method of Klingbeil *et al.* (1999) digitised boundaries of individual layer were converted to polygons, classified by identified lithofacies code and linked to respective hydrofacies.

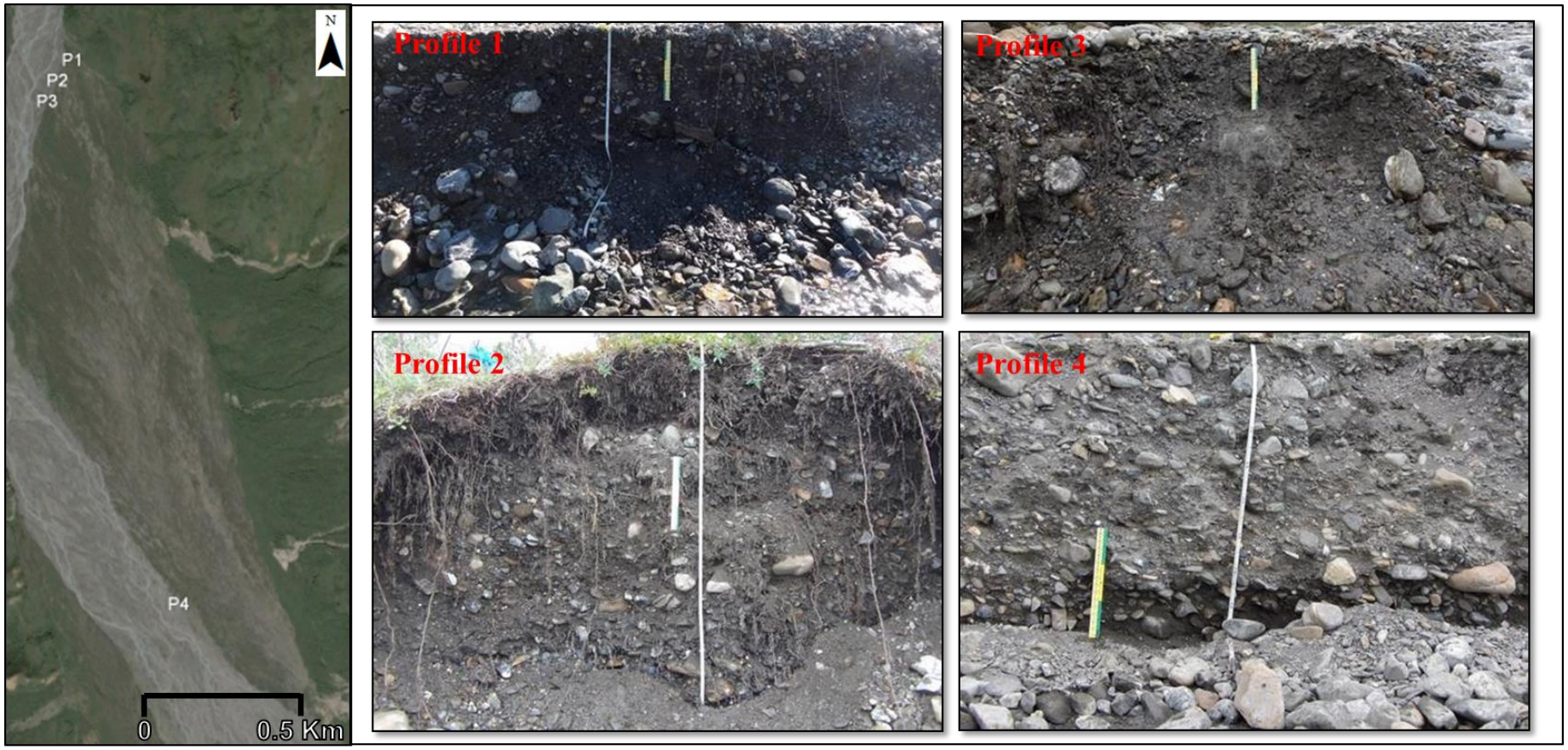

Figure 2.14: Location of outcrops (P1 – P4) selected for detailed sedimentary descriptions and profiles. Outcrops were selected to represent the range of sedimentary environments observed. This included exposures with overlying soil layers (Profile 2 – P2) and those near GW-fed streams (Profile 3 – P3). Satellite image from Google.

2.3.2 Hydraulic conductivity measurements

2.3.2.1 Surface measurements

As part of identifying hydrofacies on the MF Toklat terrace and their spatial variation surface infiltration tests were conducted at all 22 sites across the three transects (LT, MT, and UT; Figure 2.4b) to determine saturated near-surface hydraulic conductivity ($K_{0.0}$). Annular rings (internal diameter (ID) 0.11 m) were inserted to a depth of ~0.01 m and measured quantities of water (100 ml) were allowed to infiltrate under null pressure, until the infiltration rate reached steady-state (Lassabatère *et al.*, 2006). A minimum of three replicates were performed at each site. Grab samples of surface sediment (~500 g) were collected at each site to determine dry bulk density, volumetric water content, and porosity gravimetrically. Calculated $K_{0.0}$ and porosity values were linked to identify hydrofacies codes, according to the lithofacies classification outlined in section 2.3.1.

2.3.2.2 Subsurface measurements

Hydraulic conductivity at a depth of 1.0 m ($K_{1.0}$) was also measured at each of the 22 individual sites across all three transects by carrying out slug tests for piezometers installed at each site (Figure 2.4b). Piezometers were cylindrical open-ended chlorinated polyvinyl chloride (CPVC) tubing (ID 22 – 29 mm) perforated up to 0.1 m above the base. Piezometers were installed using an installation unit introduced by Baxter *et al.* (2003). This consisted of a stainless steel outer sleeve (1.5 m length) and solid stainless steel driving rod with hammer cap that was inserted inside the sleeve. The entire unit was driven to the required depth using a sledgehammer. Once in position the solid inner was removed and a CPVC piezometer inserted inside the sleeve. Finally the outer sleeve was removed, leaving the piezometer installed.

Site locations along the middle (MT) and upper (UT) transects were positioned to provide the most even spatial coverage possible. Lower (LT) sites were located next to stream gauges. A number of factors restricted installation location for MT and UT sites; such as vegetation cover, depth of the water table, and the heterogeneity of sediment. On some occasion's coarse sediment (e.g. boulders) in the subsurface restricted insertion of the installation unit to depth. Given the anticipated link between GW-fed stream occurrence and the presence of paleochannels a number of piezometers were installed at sites within channels (LT1-3, MT2, MT3, MT6, MT8, MT10, MT13, & MT14). Elevated $K_{1.0}$ above the rest of the terrace for these locations would be suggestive of these channels acting as PFPs and support the possibility of a link between GW-fed streams and paleochannels.

Slug tests were performed in accordance with the methods of Surridge *et al.* (2005). A minimum of three replicate measurements were carried out at each site. Piezometer water levels were inferred at 1 s intervals using pressure transducers (In-Situ® Inc. miniTROLL SSP-100). Following equilibration after insertion of the logger into the piezometer a slug extraction, or insertion, was carried out using a known volume of water (Surridge *et al.*, 2005). The volume of water withdrawn, or added, was dependent on anticipated *K* values for individual piezometers. $K_{1.0}$ was calculated by applying equation (1):

$$K = a\frac{A}{Ft} \cdot \log_e\left(\frac{h}{h_0}\right) \quad (1)$$

where K is hydraulic conductivity ($L\ T^{-1}$); A is cross-sectional area of the piezometer (L^2); F is a shape factor (L); h_0 is initial head difference (L); and h is the head difference at a given time since the slug withdrawal or insertion (Surridge *et al.*, 2005). F is a numerical constant for piezometer intake (L) and was calculated in accordance with Ratnam *et al.* (2001):

$$\frac{F}{d} = 3.1146 + 1.8726N + 2.4135 \cdot \sqrt{N} \quad (2)$$

where N is the ratio between the length (l) and diameter (d) of the porous section of the piezometer (Silvestri *et al.*, 2012).

2.3.3 Hydrometric monitoring

2.3.3.1 MF Toklat

Groundwater (GW) levels and stream discharge on the terrace were monitored between 6th July and 2nd September (Julian calendar day (JD) 187 to 245) during 2013 and between 22nd May and 6th September (JD 142 to 249) during 2014. Discharge was quantified at surface water (SW) sites SW1 (LT1), SW2 (LT2), and SW3 (LT3) using a locally determined stage-discharge relationship. Continuous stage measurements were made using pressure transducer loggers (Solinst® Model 3001 Levelogger Junior Edge) and discharge was measured a minimum of every 7 days throughout the monitoring period using a SENSA RC2 Water Velocity Meter and application of the mean-section method.

For GW monitoring nested piezometers were installed at each of the 22 sites along the three transects (Figure 2.4b). These allowed the spatiotemporal response in GW-levels during summer months to be monitored. Vertical (VHG) and horizontal (HHG) hydraulic gradients across the terrace could also be determined. LT and MT nests were installed in the summer of 2013 and UT nests during summer 2014. Each nest comprised a shallow (0.5 m) and deep (1.0 m) piezometer and individual piezometer location and elevation was logged using a DGPS. Detailed explanation of piezometer design and installation is provided in section 2.3.2.2. GW levels were measured manually on a minimum of weekly intervals using a dip meter. Pressure transducer s (In-Situ® Inc. miniTROLL SSP-100 and TruTrack WT-HR 500)

were installed at MT3, MT7, and MT13 to provide a continuous record of GW response across the terrace during summer months.

2.3.3.2 EF, Tek, & GC

For the three remaining sites networks of nested, shallow piezometers were installed during 2014 to monitor the seasonal response and behaviour of the shallow GW level. Details on piezometer design and installation are provided in section 2.3.2.2. At EF 5 piezometer nests were installed (LT1, MT1-3, & GW; Figure 2.8), forming a diamond shape across the terrace. A diamond pattern allowed GW levels, VHG, and HHG to be monitored across the full spatial extent of the terraces; while minimising the number of installations required at remote sites with challenging access. At Tek a transect of three nests were installed (MT1-3; Figure 2.10). Unlike at other field sites two nests (MT2 and MT3) were located on the active floodplain. For Tek this provided an insight into GW level and spatiotemporal response on the floodplain compared to the elevated terrace.

During 2014 continuous monitoring of GW level occurred from; 03rd June to 04th September (JD 154 to 247) at EF; and 23rd June to 04th September (JD 174 to 247) at Tek. At both EF field sites pressure transducers (Solinst® Model 3001 Levelogger Junior Edge, and Rugged TROLL® 100) were installed at sites MT1 and MT3 to provide a continuous measurement of GW levels and spatiotemporal behaviour. GW levels at GC were typically > 1.0 m below the surface, and so were difficult to monitor. Two nested piezometers were installed at GC (T1 and T2; Figure 2.12) to observe if GW levels rose to within 1.0 m of the surface in response to storm events during the monitoring period between 2nd June and 3rd September 2014 (JD 153 to 246).

2.3.4 Hydrochemistry and stable isotope sampling

At all field sites middle transect (MT), surface water (SW), and identified end-members were sampled throughout the monitoring periods during 2013 and 2014. A total of 263 samples during 2013 and 288 samples during 2014 were collected. For each field site three SW and MT locations were selected for sampling. SW and MT locations were numbered, rising with increasing distance across each terrace from the adjacent hillslope. End-members varied between field sites (Table 2.5) and are explained in further detail in subsequent sections. For each sample collected *in-situ* measurements of pH, electrical conductivity (EC), and acid neutralizing capacity (ANC) were carried out in the field. ANC was established using the inflection point titration method (Rounds, 2006).

Separate sub-samples were collected for major ion analysis (Na^+, K^+, Ca^{2+}, Mg^{2+}, SiO_2, Cl^-, NO_3^-, and SO_4^{2-}). Samples were filtered using 47 mm Whatman® MicroPlus cellulose nitrate membranes (0.45 μm pore size) into 30 ml Nalgene™ high-density polyethylene (HDPE) sample bottles immediately after collection and stored frozen. Analysis of cations (Na^+, K^+, Ca^{2+}, and Mg^{2+}) was carried out using a Dionex DX 500 and anions (Cl^- and SO_4^{2-}) a Dionex ICS 2000 (instrumental precision < 0.25 ppm). SiO_2 was determined colorimetrically using a UV-Vis Spectrophotometer following the method outlined by (Fishman and Friedman, 1989). All major ion analysis was carried out within 28 days of samples being defrosted, and samples were stored in darkness at 4 °C for the duration of the analysis. Sub-samples (2 ml) were also collected for stable isotope (δ^2H) analysis undertaken on a continuous-flow Isoprime™ mass spectrometer at the University of Birmingham, UK. δ^2H was determined using a chrome reduction method on a Eurovector Elemental Analyzer, for which internal precision is < 1 ‰.

Site	Sample points	End-members
MF Toklat	SW1, SW2, SW3, MT1, MT7, MT14	DF, DF Spring, GR, GM, GW, HF, Precip, SP
East Fork	SW1, SW2, SW3, MT1, MT2, MT3	GR, GW, HF, HS,
Teklanika	SW1, SW2, SW3, MT1, MT2, MT3	HS, Tek
Gorge Creek	SW1, T1, T2	DF, GC, HF

Table 2.5: Sampling locations and identified end-members for all field sites. Three surface water (SW) and three groundwater (MT) locations were sampled at all sites except GC

2.3.4.1 MF Toklat

During 2013 and 2014 extensive sampling was undertaken on the MF Toklat field site. SW samples were collected at sites SW1 (LT1), SW2 (LT2), and SW3 (LT3), and groundwater samples at sites MT1, MT7, and MT14 (Figure 2.4b). Samples collected from UT2, UT4, and UT5 were used to calculate mean GW composition for the vertical groundwater input end-member to the terrace (Figure 2.4a). Importantly UT sites were upstream of the colluvial deposit at the base of the terrace where two additional end-members were also identified (DF & DF spring). This meant the geochemical compositions of upstream GW and the nearby colluvial deposit could be separated. Other possible end-members identified and sampled included; summer rainfall (Precip.); winter snowpack (SP); buried ice; glacial meltwater (GM) from headwater glaciers; and the main glacial MF Toklat River (GR) (Figure 2.4a).

SP samples were only collected in 2014, when the monitoring period overlapped with late spring melt and a snowfall event in August 2014. Precip. was sampled using a rainwater collector located ~5 Km NW of the site at an NPS road camp. Due to the remote, inaccessible nature of field sites it was not possible to install autosamplers at individual field sites to collect rain samples. Collecting summer rainfall at the road camp ensured samples were collected both regularly and promptly after storm events. Precipitation δ^2H composition was calculated as a weighted average applying the cumulative incremental weighting approach (McDonnell *et al.*, 1990; Tekleab *et al.*, 2014):

$$\delta^2 H = \frac{\sum_{i=1}^{n} p_i \delta_i}{\sum_{i=1}^{n} p_i} \quad (3)$$

where p_i is the rainfall total (mm) and δ_i is δ^2H (‰).

2.3.4.2 EF

During the 2014 monitoring period sampling was carried out at EF on six separate occasions. Surface water (SW1-3) and groundwater (MT1-3) sites were sampled on the terrace (Figure 2.8). End-members identified and sampled included; upstream vertical groundwater input to the terrace (GW), sampled using a piezometer installed at the site; hillslope flow (HF) from adjacent to the terrace; hillslope seepage (HS) at the base of the hillslope; and the main glacial East Fork River (GR) (Figure 2.8).

2.3.4.3 Tek

Sampling of the Tek field site occurred on four separate occasions during the 2014 monitoring period. Surface water (SW1-3) and groundwater (MT1-3) sites on the terrace were sampled (Figure 2.10). Hillslope seepage (HS) from the adjacent valley-side and the main glacial

channel of the Teklanika River (Tek) were the only identified end-members for the field site (Figure 2.10).

2.3.4.4 GC

The GC field site was visited five times for sampling during the 2014 monitoring period. Surface water samples were collected on the terrace at SW1 and groundwater samples at T1 and T2 (Figure 2.12). Identified end-members for the field site included a colluvial deposit which extended directly onto the terrace (DF); hillslope flow from the adjacent valley side (HF); and flow from the non-glacial Gorge Creek (GC) (Figure 2.12).

2.4 DATA & STATISTICAL ANALYSIS

2.4.1 Terrace water balance

For water balance estimates the study site was conceptualised as a floodplain terrace unit and adjacent hillslope block (Figure 2.15). Based on this conceptualisation, the summer water balance of the terrace was interpreted as:

$$S_{terrace} = P + SWE_{max} + PF + Q_{vertical} - ET - Q_{surface} - Q_{subsurface} \quad (4)$$

where $S_{terrace}$ was terrace aquifer storage; P represented summer precipitation; SWE_{max} was maximum snow water equivalent (prior to spring melt); PF was summer permafrost melt; $Q_{vertical}$ a vertical upstream groundwater influx (from the paraglacial floodplain); ET was actual evapotranspiration; $Q_{surface}$ was surface stream runoff from the terrace; and $Q_{subsurface}$ was subsurface runoff from the terrace. P, SWE_{max}, and ET fluxes were estimated for both the terrace and hillslope areas, while PF was estimated only for the hillslope block (permafrost was not present on the terrace; see section 2.1.1). $Q_{vertical}$ represented subsurface flow recharging the terrace from the upstream floodplain, as opposed to the adjacent hillslope

block. The specific water source composition of $Q_{vertical}$ was unknown with a number of components potentially contributing to the flux. These included those associated with upstream hillslope areas (P-ET, PF, & SWE_{max}) and glacial melt from headwater glaciers (GM). As the terrace was elevated above the active floodplain all perceptible recharge to the terrace occurred through the subsurface. Therefore direct input of GM (and other upstream components) from the main glacial river channels were not considered as a separate component, as their contribution would be contained within $Q_{vertical}$.

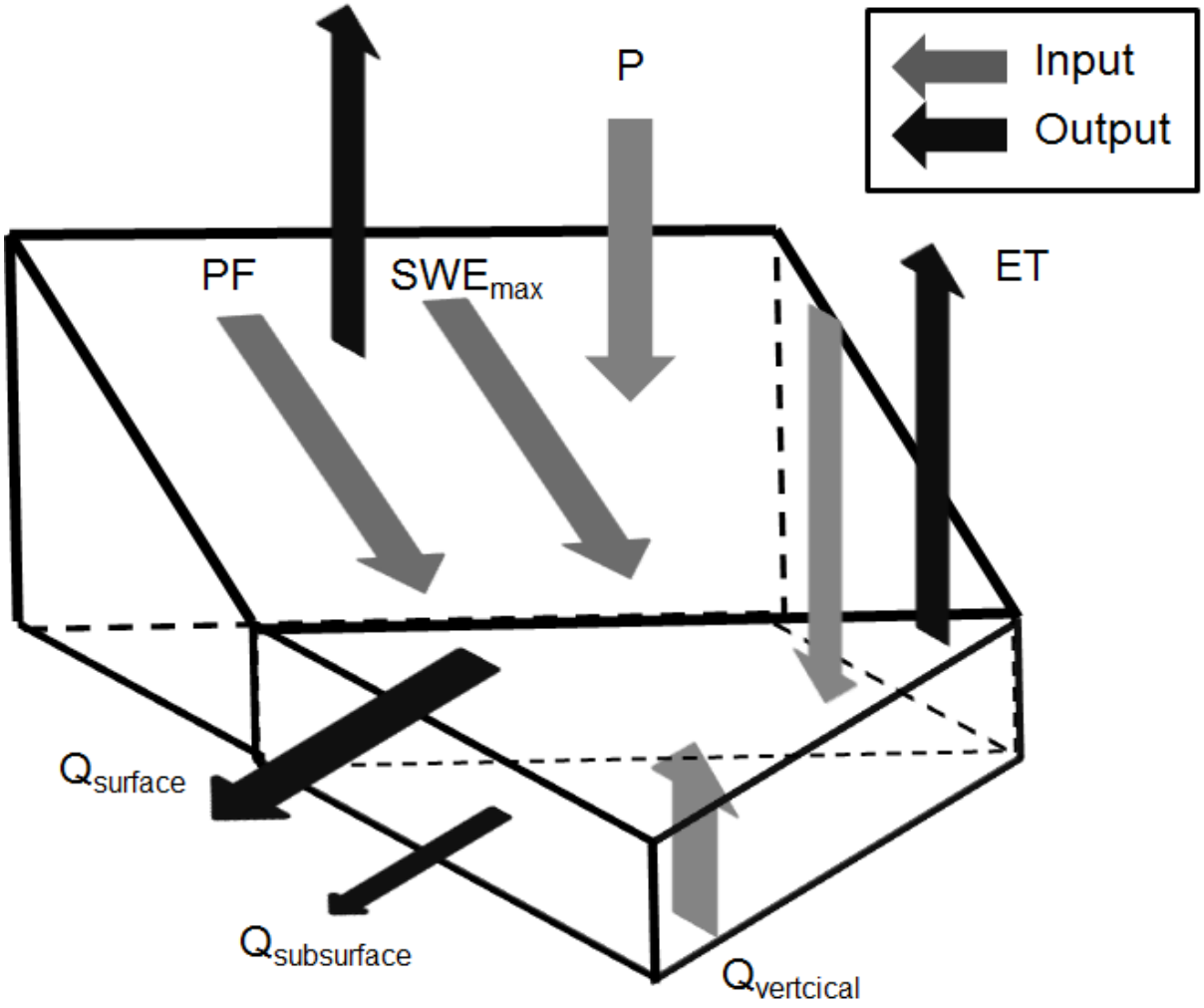

Figure 2.15: Conceptual model for fluxes included as part of water balance estimates for the terrace and adjacent hillslope. Grey coloured arrows indicate inputs into the system and black arrows are representative of outputs

Each component of the water balance was calculated as a daily estimate from 1st June to 31st August 2014. SWE_{max} and PF were the only exceptions, which were each estimated as average seasonal fluxes. P, ET and SWE_{max} were estimated using meteorological data obtained from an automated weather station situated ~5 km NW of the site (WRCC., 2014b). Meteorological data was recorded hourly and included; air temperature (°C), relative humidity (%), soil temperature (°C), incoming solar radiation (W m^{-2}), accumulated precipitation (m), and snow depth (m). ET was estimated using the Penman-Monteith equation (Drexler *et al.*, 2004; Monteith, 1965). Surface and atmospheric resistivity values used for the calculations were taken from Oke (1987) for open grass (70 s m^{-1}), which best reflected overall catchment vegetation cover. Using assumed values for hydrological land use groups is an approach which has been applied by others (Dunn and Mackay, 1995; Stutter *et al.*, 2006).

SWE_{max} was calculated using the degree-day melt temperature-index method (DeWalle and Rango., 2008). Snowpack density measurements for SWE_{max} calculations were taken at the beginning of the field season (22nd–24th May) from late-lying coverage on the hillslope. A CPVC corer (Internal diameter = 30 mm / Length = 45 mm) was inserted into the snowpack and completely filled. The sample was then weighed using a digital scale and its mass (excluding corer) divided by the corer volume to obtain snowpack density. Measurements at three individual locations on three separate days were made with a mean density of 667.18 Kg m^{-3} (σ = 59.59 Kg m^{-3}) obtained. SWE_{max} calculations and precipitation (P) were compared between two meteorological stations that covered the broad range of elevations across the terrace and associate hillslope. Meteorological data from the Toklat weather station (~5 km NW of the site) used in the above calculations (elevation = 890 m) was compared with data from an automated weather station located at Eielson Visitor Center (WRCC., 2014a), ~19 km WSW of the site (elevation = 1113 m).

Estimates of seasonal permafrost melt (PF) from the hillslope block were based on coverage and active thinning rates reported by Yocum *et al.* (2006) (see section 2.1.1), and which were in line with ice-melt measurements made within the catchment (personal observation). PF flux was estimated assuming mean percentage coverage of 50%, thinning of 1.25 m, and a soil layer porosity of 37% (σ = 1%). A maximum value was calculated assuming 80% coverage and 1.5 m active thinning, with a minimum assuming 20% coverage and 1.0 m active thinning.

$Q_{vertical}$ was calculated for the terrace using the median $K_{1.0}$ and measured vertical hydraulic gradients (VHG). $Q_{subsurface}$ used the same median $K_{1.0}$ and the measured horizontal hydraulic gradient (HHG). $Q_{surface}$ was estimated from stage-discharge measurements completed at sites LT1, LT2, and LT3 and estimates for three other streams on the terrace that appeared comparable in size and behaviour to site LT2. Variability in $Q_{vertical}$ was determined from the standard deviation in measured *K* across the terrace. Errors in $Q_{surface}$ were determined by varying discharge of ungauged streams between the largest and smallest streams gauged across the terrace. LT1 and LT3 were the largest and smallest streams on the terrace respectively (personal observation) and estimates of total stream discharge were derived by taking these streams as analogues for the three remaining streams on the terrace, thus providing potential minimum and maximum total $Q_{surface}$ values.

Groundwater levels were monitored manually at approximately twice weekly intervals at each nested site from July 6th to September 2nd in 2013 (Julian Day (JD) 187 to 245), and May 22nd to September 6th in 2014 (JD 142 to 249). In addition, three pressure transducers (Models In-Situ® Inc. miniTROLL SSP-100 and TruTrack WT-HR 500) provided continuous groundwater levels, at 15 minute intervals, for piezometers MT3, MT7, and MT13 in both field seasons. Discharges at sites LT1, LT2, and LT3 (Figure 2.4b) were estimated by

determining individual stage-discharge relationships, and monitoring stage was logged at 15 min intervals by Solinst® Leveloggers (Model 3001 Levelogger Junior Edge). Stream discharge was measured a minimum of once a week using a SENSA RC2 Water Velocity Meter and the mean-section method.

2.4.2 Two-component hydrograph separations

Two-component hydrograph separations were carried out at all field sites for both SW and MT sampling locations. These separations were conducted to establish spatial variation in the contribution to flow from adjacent valley sides and upstream GW to terraces. Identified end-members used were; GW at all sites; DF at MF Toklat and GC; HF at EF; and HS at Tek. Mean values were used for respective end-members. Separations were carried out using a form of the steady-state mass-balance equations (5) and (6), which was applied to separate stream flow into two component based on identified end-member concentrations (Blaen *et al.*, 2014; Sklash and Farvolden, 1979; Sueker *et al.*, 2000):

$$Q_s = Q_{DF} + Q_{GW} \tag{5}$$

$$C_S Q_S = C_{DF} Q_{DF} + C_{GW} Q_{GW} \tag{6}$$

where Q (m^3 s^{-1}) is discharge, C is tracer concentration and the subscripts *S*, *DF*, and *GW* refer to the stream, debris fan, and groundwater respectively.

The uncertainty for each component was estimated using the method of Genereux (1998), based on a Gaussian error propagation (7):

$$W_{fDF} = \sqrt{\left[\frac{C_{GW} - C_S}{(C_{GW} - C_{DF})^2} W_{C_{DF}}\right]^2 + \left[\frac{C_S - C_{DF}}{(C_{GW} - C_{DF})^2} W_{C_{GW}}\right]^2 + \left[\frac{-1}{(C_{GW} - C_{DF})^2} W_{C_S}\right]^2} \tag{7}$$

where *W* is uncertainty and *f* the mixing fraction. Standard deviations for end-member mean solute values were multiplied by their respective student t-distribution to provide uncertainty calculations at a 95% confidence level. Uncertainty for stream samples was calculated as the analytical precision (Genereux, 1998), as individual separations were completed for each stream sample.

2.4.3 Mean residence times

For the MF Toklat field site stable isotope data was available for both 2013 and 2014, making it possibly to consider mean residence times (MRT) for surface water sites and identified end-members. However, determining MRT for stream waters on the MF Toklat terrace would be problematic given sampling occurrence, both spatially and temporally, was coarse and the sampling period short (McGuire and McDonnell, 2006). First order approximations of MRT for the MF Toklat field site were calculated using the sine wave approach, fitting seasonal patterns in both streamflow and precipitation δ^2H (McGuire *et al.*, 2002; Rodgers *et al.*, 2005; Tekleab *et al.*, 2014). For this approach predicted δ^2H was defined as:

$$\delta = C_0 + A\left[\cos\left(ct - \varphi\right)\right] \quad (8)$$

where δ is predicted δ^2H [‰] value, C_0 weighted mean annual measured δ^2H [‰], A is annual amplitude for predicted δ^2H [‰], c an angular frequency constant (0.017214 rad d^{-1}), t is time after the beginning of the sampling interlude (days), and φ is the phase lag (in radians) for predicted δ^2H. A periodic regression analysis using sine and cosine conditions was used to assess Eq. (4) (Tekleab *et al.*, 2014):

$$\delta = c_0 + \beta_{cos}\cos(ct) + \beta_{sin}\sin(ct) \quad (9)$$

β_{cos} and β_{sin} are regression coefficients that are applied to calculate the input and output amplitude signals $\left(A = \sqrt{\beta^2 \cos + \beta^2 \sin} \right)$, and therefore the phase lag, $\tan \varphi = \left| \frac{\beta_{sin}}{\beta_{cos}} \right|$.

MRT was estimated from the fitted sine wave input and output signals as:

$$T = c^{-1} \left[\left(\frac{A_2}{A_1} \right)^{-2} - 1 \right]^{0.5} \quad (10)$$

where *T* is MRT (days), A_1 amplitude of precipitation δ^2H [‰], and A_2 is stream flow amplitude δ^2H [‰].

2.4.4 Principal component analysis

Principal component analysis (PCA) for major ion (Na^+, K^+, Ca^{2+}, Mg^{2+}, SiO_2, NO_3^-, Cl^-, and SO_4^{2-}) data was used to identify flow paths at all sites for both SW and GW points. PCA achieves this by determining causal relationships in the multivariate geochemical data set, taking into account all variables measured (Vogt and Muniz, 1997). PCA has been successfully applied by others (Gordon *et al.*, 2015) to establish the influence of geochemical weathering signals in surface waters and establish flow paths. All data were normalised using the log(x + 1) approach, a method outlined by Sokal and Rohlf (1995) and which has been used by others (Doering *et al.*, 2012). For each site PCA was carried out on SW and identified end-member samples, with end-members varying between sites (Table 2.5). Principal components with a variance < 1 were removed, meaning PC1 and PC2 were retained and plotted for all sites

CHAPTER 3: PREFERENTIAL FLOW PATHWAYS WITHIN PARAGLACIAL FLOODPLAINS: HYDROGEOMORPHIC CONTROLS UPON THE OCCURRENCE AND STABILITY OF BIODIVERSITY HOTSPOTS

3.1 SCOPE OF CHAPTER

Preferential flow pathways (PFPs) have been proposed as supporting groundwater (GW) –fed streams on paraglacial floodplains; and which are important biodiversity hotspots (Chapter 1). However, understanding of the hydrological dynamics which support PFPs and related GW-fed stream is minimal (Chapter 1). This chapter aims to address this research gap. Focusing on a floodplain terrace on the MF Toklat River, DNPP, Alaska, understanding of the spatiotemporal nature of GW-stream recharge through PFPs was developed; and used to guide water balance analysis which estimated fluxes that influenced GW-recharge on the terrace.

Hydrofacies with high hydraulic conductivity (*K*) and which were associated with strong vertical hydraulic gradients (VHGs) were identified. Their presence highlighted the importance of PFPs to GW-fed stream occurrence. GW-recharge on the terrace during summer was gradual and continuous, and streams exhibited non-flashy responses to storm events. Water balance estimates indicated precipitation (snowmelt and rainfall) and permafrost melt from adjacent hillslopes could contribute significantly to GW-fed streams. The size of these fluxes and non-flashy nature of GW-fed streams was suggestive of colluvial deposits (e.g. talus cones) acting as important conduits of flow, which extended the residence time of hillslope runoff.

A conceptual summary bringing together the understanding developed of the role of PFPs and valley side water sources is presented. This work raises concerns regarding the long-term stability of these biodiversity hotspots given predicted impacts of climate change upon hydrologic regimes and sediment yields in paraglacial catchments. It has also highlighted the need for improved understanding of hillslope runoff contribution to GW-fed streams, and the role of PFPs in hillslope-floodplain connectivity.

3.2 INTRODUCTION

Fluvioglacial deposits present across paraglacial floodplains exhibit complex hydrological connectivity, characterised by extensive lateral and vertical groundwater-surface water (GW-SW) interactions (Anderson, 1989; Poole *et al.*, 2002; Stephenson *et al.*, 1988). Where groundwater rises to the floodplain surface important riverine habitat patches occur (Ward *et al.*, 2002). As a result GW-SW behaviour exerts significant influence on floodplain aquatic habitats (Arscott *et al.*, 2002; Robinson and Doering, 2012), riparian vegetation occurrence (Caldwell *et al.*, 2015; Doering *et al.*, 2012), and biogeochemical dynamics (Anderson, 2007; Cooper *et al.*, 2002) within paraglacial catchments. Extensive networks of subsurface hydrological pathways support this complex hydrological connectivity and constitute important channels of flow in these environments (Malard *et al.*, 2002; Poole *et al.*, 2002; Ward *et al.*, 1999). Termed paleochannels (Stanford and Ward, 1993), they are also referred to as preferential flow pathways (PFPs) (Anderson *et al.*, 1999; Goutaland *et al.*, 2013).

PFPs are the result of channel avulsion in braided river systems, that causes channel abandonment during high flow (Poole *et al.*, 2002). Fine sediments are rapidly deposited as floodwaters retreat, leaving the abandoned channel buried. Gravel and cobble-rich deposits that once formed the exposed stream channel then provide high transmissivity flow pathways through the subsurface, confined by lower *K* sediments (Poole *et al.*, 2002). PFPs are the major control upon GW-SW interactions within paraglacial floodplains (Stanford and Ward, 1993), and where they intercept the floodplain surface groundwater (GW) –fed streams (biodiversity hotspots) are known to occur (Caldwell *et al.*, 2015). The geomorphic controls that determine the presence of PFPs, and therefore control the hydrology of paraglacial floodplains, are important in ensuring the stability and persistence of GW-fed streams (Lorang and Hauer, 2007).

The complexity of hydrological connectivity in paraglacial systems is not only limited to the floodplain, with multiple water sources and pathways having been identified on valley slopes (Carey *et al.*, 2013; Carey and Woo, 2001) and within colluvial deposits (Caballero *et al.*, 2002; Muir *et al.*, 2011). Colluvial deposits (e.g. talus slopes) have received increasing attention as important water sources and conduits of flow in paraglacial catchments (Clow *et al.*, 2003; Gordon *et al.*, 2015; Hood and Hayashi, 2015; Liu *et al.*, 2004; Roy and Hayashi, 2009). Furthermore, these deposits can account for considerable water storage, thereby contributing significantly to baseflow during summer months (Muir *et al.*, 2011; Tetzlaff and Soulsby, 2008). Within paraglacial catchments permafrost, where present, adds a complexity to hydrologic dynamics as it is both a water source and significant control upon flow paths (Carey and Quinton, 2005; Quinton *et al.*, 2009). In response to anthropogenic climate change and rising surface temperatures in high latitude regions permafrost layers are thinning (Carey *et al.*, 2013; Mann *et al.*, 2010). The increasing depth of the active layer in summer months will open up deeper groundwater flow paths on hillslope (Carey *et al.*, 2013; Douglas *et al.*, 2013), generating further complexity in the hydrological connectivity of paraglacial environments.

Despite the recognised importance of colluvial deposits as valuable aquifers (Weekes *et al.*, 2015), and shifting groundwater flow paths on paraglacial valley sides (Boucher and Carey, 2010), the influences of valley side flow upon biodiversity hotspots has not been appropriately considered, with an emphasis remaining on stream-aquifer connectivity within the floodplain unit (Gordon *et al.*, 2015). Furthermore, despite the established role of PFPs in sustaining GW-fed streams (Lorang and Hauer, 2007), their role in GW-SW interactions across floodplains (Malard *et al.*, 2002), and recognition of their sensitivity to climate change (Poole *et al.*, 2002), no consideration of their contribution to hillslope-floodplain connectivity

(Bracken and Croke, 2007) has been made. Regardless of repeated calls for further conceptualisation of paraglacial floodplains in three dimensions (Malard *et al.*, 2002) and increased consideration of lateral hydrological connectivity (Poole, 2010), a paucity remains in our understanding of hillslope-floodplain connectivity and the possible role of PFPs within paraglacial environments connecting GW-fed streams with the hillslope.

Focusing on a paraglacial floodplain terrace with an extensive network of GW-fed streams on the MF Toklat River within DNPP, Alaska, this chapter addresses these research gaps, and considers the fundamental hydrogeomorphic controls upon PFPs and associated biodiversity hotspots. Fieldwork focused on monitoring groundwater levels on the terrace and establishing hydrofacies present, aiming to: (1) capture the spatiotemporal pattern of GW-fed stream recharge through PFPs on the terrace during summer months; (2) quantify groundwater recharge of the terrace and valley side fluxes during summer months; and (3) develop a conceptual model of the water sources supporting terrace aquifer recharge.

3.3 STUDY SITE

Fieldwork was carried out in 2013 and 2014 on the MF Toklat field site. For further details see section 2.1.1.

3.4 METHODOLOGY

Lithofacies were identified on the terrace using the methods outlined in section 2.3.1. These were linked to surface hydraulic conductivity ($K_{0.0}$) to establish hydrofacies. Details on how $K_{0.0}$ was calculated are provided in section 2.3.2.1. This data was utilised alongside subsurface hydraulic conductivity ($K_{1.0}$; see section 2.3.2.2) measurements and hydrometric monitoring (including stream discharge and groundwater levels; see section 2.3.3.1) to produce a terrace water balance. A detailed breakdown of the water balance is provided in section 2.4.1.

3.5 RESULTS

3.5.1 Lithofacies and hydrofacies characterisation

Seven separate hydrofacies were identified on the MF Toklat terrace (Table 3.1). With the exception of soil layers (P), all deposits were gravel dominated, clast-supported, and had massive stratification (Gcm). Differentiation occurred between deposits where some were cobble (c) rich gravels, whilst others were sand (s) rich. Two hydrofacies were identified as having a bimodal (b) grain size distribution. Percentage clay content between gravel dominated hydrofacies was minimal with a range of mean values between 1 and 5%. Contrasts in sediment texture regarded percentage gravel and sand compositions. Hydrofacies Gcm had the highest mean gravel (90%) and lowest sand (9%) composition. Sand rich gravel deposits (sGcm) exhibited a much lower mean gravel content (60%) and subsequent higher sand content (35%).

Higher sand content was linked to lower *K* values (Pearson correlation, $r = -0.57$, $n = 20$, $p < 0.01$) (Table 3.1). Mean values of log *K* for Gcm and sGcm were -3.60 m s^{-1} ($\sigma = 1.62$) and -3.81 m s^{-1} ($\sigma = 0.91$) respectively. Highest *K* values were associated with Gcm and cobble-rich gravel deposits (cGcm), -3.71 m s^{-1} ($\sigma = 0.54$) with a clear positive correlation in gravel content and log *K* (Pearson correlation, $r = 0.57$, $n = 20$, $p < 0.01$). In contrast hydrofacies with a bimodal sediment distribution (sGcm, b; Gcm, b) were associated with lower *K* values of -4.68 m s^{-1} ($\sigma = 1.23$) and -5.05 m s^{-1} ($\sigma = 1.07$) respectively. Porosity values were comparable across all gravel dominated deposits (Table 3.1) ranging from 24 to 33%. Gcm (33%) and cGcm (28%) had the highest porosities and were also the deposits with highest gravel content.

	cGcm	cGcm, b	Gcm	sGcm, b	sGcm	Gcm, b	P
No. of sites	3	5	6	12	5	1	3
% Gravel	0.84	0.65	0.90	0.69	0.60	0.82	0.04
σ	0.07	0.04	0.04	0.11	0.12	-	0.02
% Sand	0.15	0.32	0.09	0.28	0.35	0.17	0.83
σ	0.07	0.05	0.04	0.09	0.11	-	0.05
% Clay	0.01	0.02	0.01	0.04	0.05	0.01	0.14
σ	0.01	0.01	0.01	0.03	0.02	-	0.06
Log k (m/s)	-3.71	-3.98	-3.60	-4.68	-3.81	-5.05	-4.03
σ	0.54	0.33	1.62	1.23	0.91	1.07	-0.15
% Porosity	0.28	0.28	0.33	0.27	0.26	0.24	0.35
σ	0.02	0.05	0.05	0.04	0.06	-	0.13

Table 3.1: Identified hydrofacies on the MF Toklat terrace with associated sediment texture breakdown, log *K* values, and percentage porosity

3.5.2 Vertical variation in hydrofacies

Detailed sedimentary profiles produced for the terrace (see section 2.3.1.1) showed that vertical variation in hydrofacies present in exposed terrace outcrops occurred. Digitised hydrofacies layers were added to profile images (Figure 3.1) to provide a visualisation of vertical variation. A low *K* hydrofacies (sGcm, b) with high sand and clay content (Table 3.1) was identified at Profile 3, next to a GW-fed stream within SC2 (Figure 2.4b). Overland flow from a nearby colluvial deposit during storm events washed fine sediments into SC2 (personal observation). For this unit sediments at the surface which were sampled to determine texture may not have been representative of subsurface sediment texture. Particularly as for remaining outcrops at the terrace base (Profiles 1 & 2) high *K* hydrofacies (sGcm and Gcm) were prominent in upper layers.

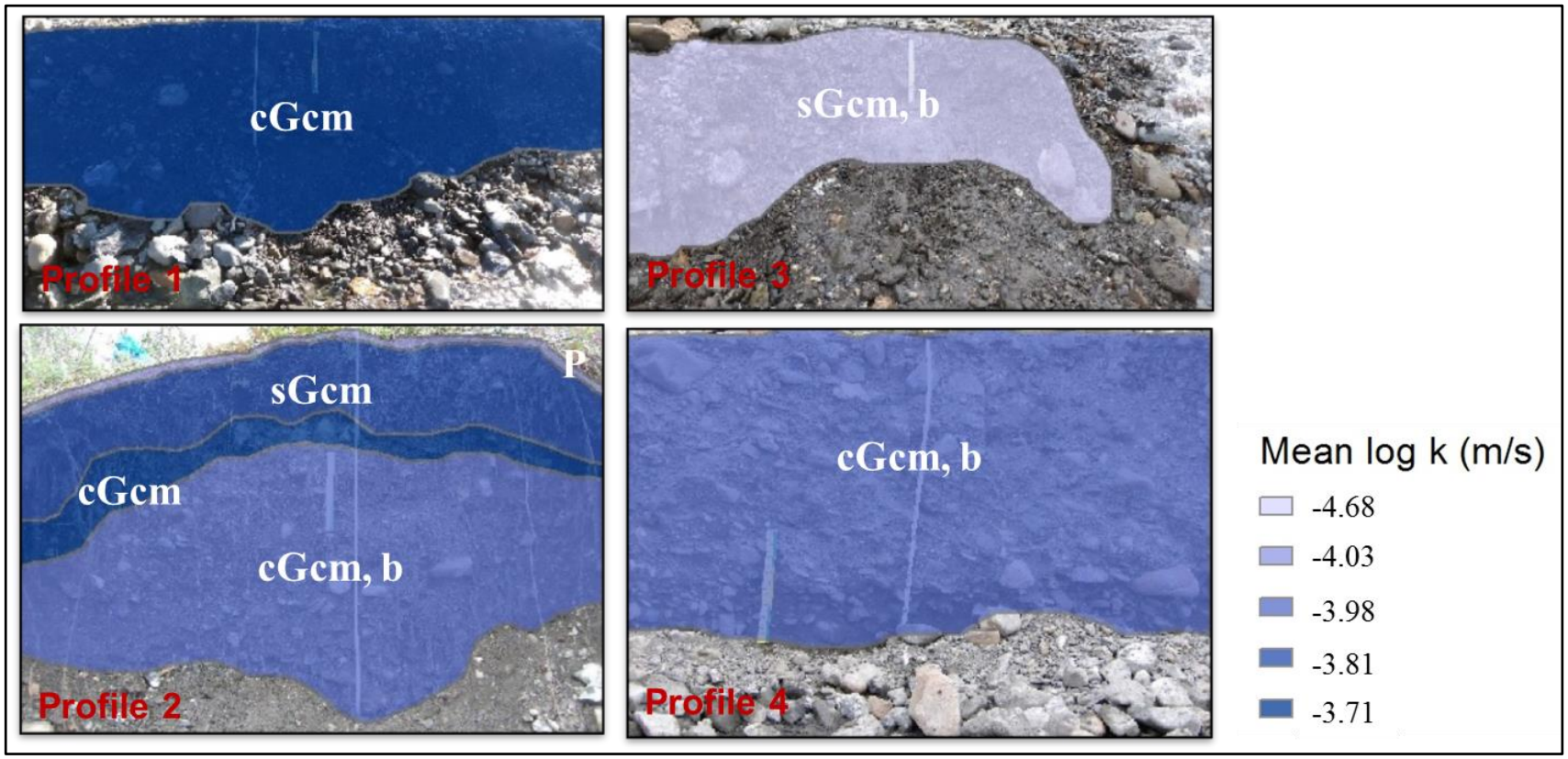

Figure 3.1: Digitised hydrofacies layers placed onto sedimentary profiles of exposed terrace carried out on the MF Toklat terrace. Higher *K* units were observed in upper layers at terrace base in Profiles 1 and 2. Low *K* units were present near GW-fed streams (Profile 3).

3.5.3 Lateral spatial distribution in hydraulic conductivity

Along the middle transect (MT) mean log $K_{0.0}$ varied by over three orders of magnitude (ranging from -2.54 to -5.81 m s^{-1}; Figure 3.2a), with hydraulic conductivities clustered into high, low, and soil layer hydraulic groupings (high, n = 7, -3.5 < Log K< -2.5; low, n = 5, -6.0 < Log K < -5.0; soil layer, n = 2, -4.2 < Log K < -3.8). Mean log $K_{0.0}$ was -3.55 m s^{-1} (σ = 1.10) for the high grouping, -5.45 m s^{-1} (σ = 0.72) for low, and -4.04 m s^{-1} (σ = 0.14) for soil coverage. Significant variation in $K_{0.0}$ was also observed within individual sites, with 50% of sites showing variation over one order of magnitude (Figure 3.2a). $K_{1.0}$ was significantly lower than $K_{0.0}$ at sites (Paired t-test; p < 0.001)), but showed a similar range in K over ~4 orders of magnitude (Figure 3.2b). Log $K_{1.0}$ ranged between -3.93 m s^{-1} and -7.90 m s^{-1}. No significant correlation was observed between $K_{0.0}$ and $K_{1.0}$ (Pearson correlation; p > 0.05). Spatial heterogeneity for log $K_{0.0}$ was lower across the upper transect (UT) (Appendix Bi). Values of log $K_{0.0}$ at UT sites were within ~1 order of magnitude of each other and fell between the two groupings observed along the middle transect (between log -4.0 m s^{-1} and -5.0 m s^{-1}). At UT mean log $K_{1.0}$ values were all lower than $K_{0.0}$ for respective sites (Appendix Bi) and were comparable with the majority of MT $K_{1.0}$ values (between log -4.5 0 m s^{-1} and -6.5 m s^{-1}).

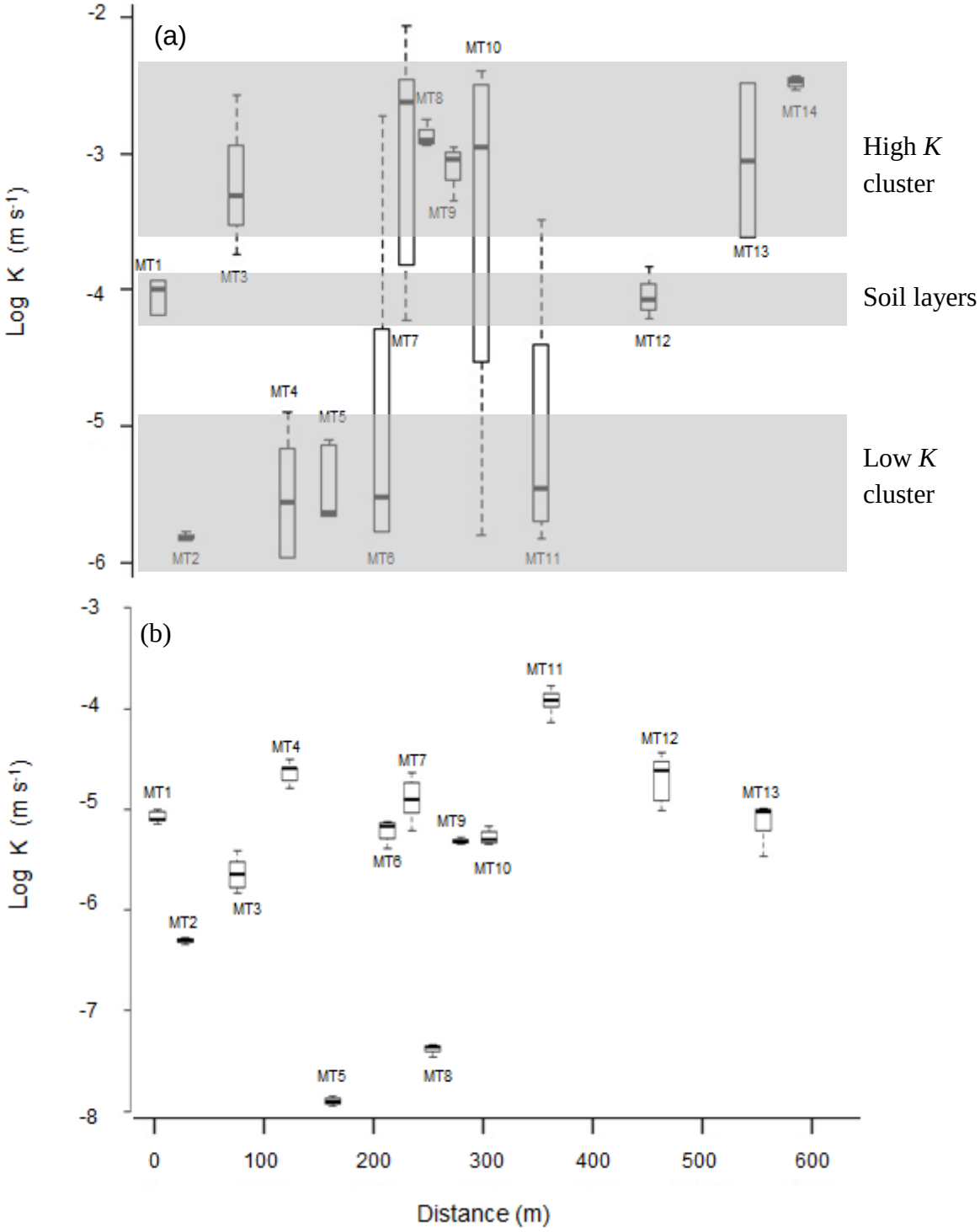

Figure 3.2: (a) $K_{0.0}$; and (b) $K_{1.0}$ hydraulic conductivity values for individual middle transect (MT) sites. Grey shaded areas for (a) separate groupings of low and high *K* sediments, and soil layers. X-axis shows increasing distance across the transect from the hillslope

3.5.4 Groundwater Storage

Summer precipitation (June – August) totalled 229.5 mm in 2013 and 348.3 mm in 2014. More detailed meteorological data is provided in appendix Ai. Groundwater levels rose across the MF Toklat terrace over both the 2013 and 2014 study periods (Figure 3.3), reflecting an increase in water storage ($S_{terrace}$) across the terrace. Water levels did not demonstrate a flashy response to individual rain or snowmelt events during the summer months (Figure 3.3). Across the middle transect (MT) water levels rise ranged between 0.12 m and 0.75 m in 2014, rising above the surface at 10 of the 14 sites (Table 3.2). A similar response was observed through the shorter 2013 measurement period.

At the upper transect (UT), groundwater levels rose within the top 1 m later in the season, between June 27th and July 19th (JD 178 to 200) in 2014 (Figure 3.4a). Sites UT4 and UT5, furthest from the hillslope, were the first where a rise in groundwater levels to within 1.0 m of the surface was observed. Water levels rose to intersect the surface at sites UT2 and UT4. This rise from a depth of 1 m to the surface occurred over 18 days and 21 days respectively (Figure 3.4a). This rise in water level across UT occurred later in 2013 (Figure 3.4b). Water levels rose to intersect the surface at UT4 on 24th August (JD 236) in 2013 and July 20th (JD 201) in 2014, a difference of 35 days. The rate of water level rise was also much quicker during 2014, rising from 0.80 m to 0.05 m depth over ~12 days. Compared to a water level rise from 0.90 m to 0.03 m over ~37 days during 2013 (Figure 3.4b)

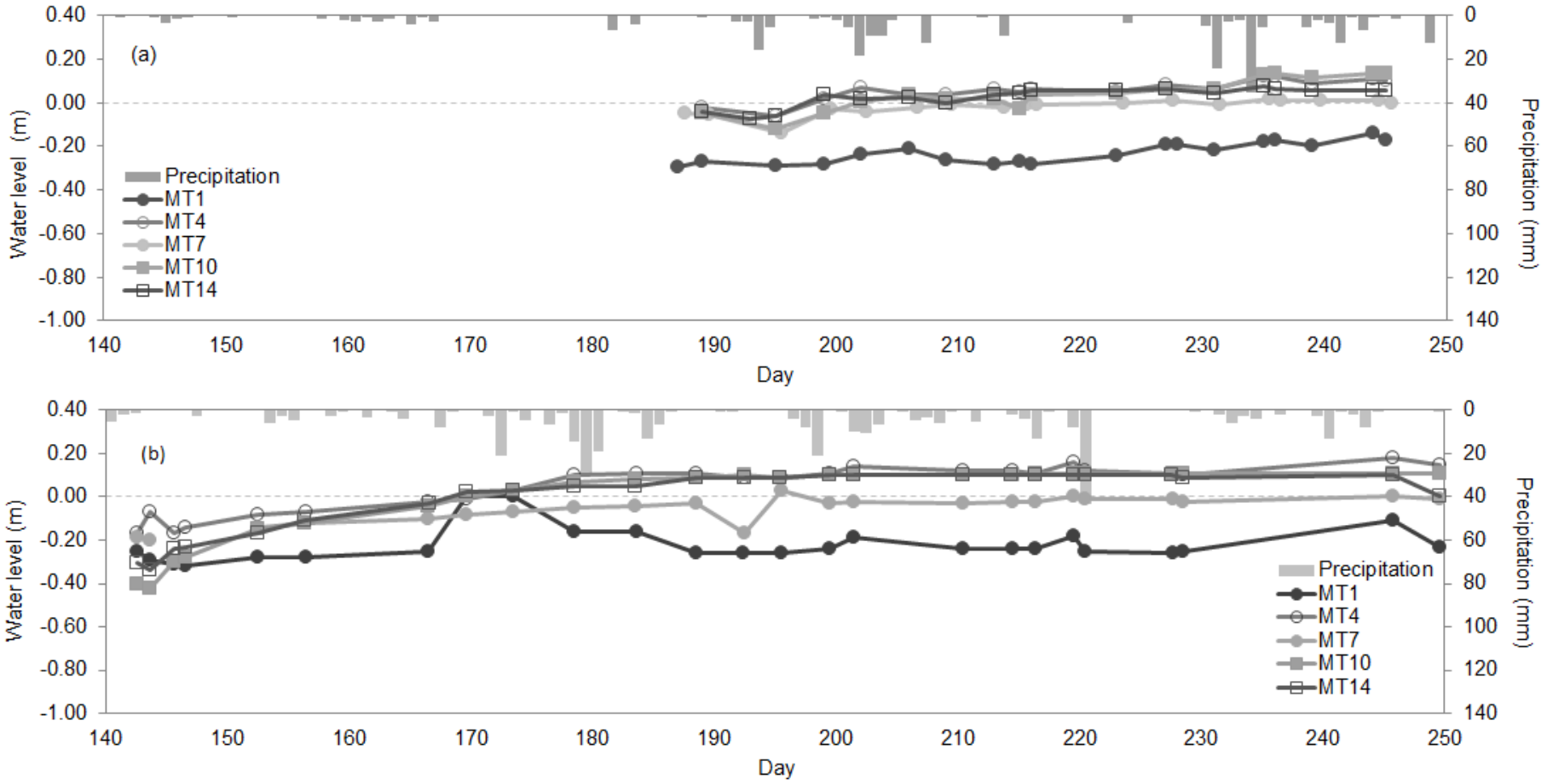

Figure 3.3: Precipitation and GW levels for selected middle transect (MT) sites during (a) 2013 and (b) 2014. Data presented for all MT sites from piezometers installed at 1.0 m depth. GW across the terrace did not exhibit a flashy response to storm events in either year

	Water level above/below the surface (m)													
Date	MT1	MT2	MT3	MT4	MT5	MT6	MT7	MT8	MT9	MT10	MT11	MT12	MT13	MT14
08/07/2013	-0.27	-0.23	-0.03	-0.02	0.00	-0.02	-0.05	-0.02	-0.04	-0.05	-0.32	-0.86	-0.13	-0.08
02/09/2013	-0.17	-0.14	**0.08**	**0.10**	**0.15**	**0.09**	0.00	**0.20**	**0.03**	**0.14**	**0.07**	-0.43	-0.04	**0.06**
22/05/2014	-0.25	-0.32	0.01	-0.17	-0.11	-0.21	-0.19	-0.13	-0.42	-0.40	-0.30	-0.86	-0.11	-0.30
02/09/2014	-0.11	**0.13**	**0.11**	**0.18**	**0.18**	**0.14**	0.00	n.a.	**0.09**	**0.11**	**0.08**	-0.29	**0.19**	**0.10**

Table 3.2: GW levels at the beginning and end of monitoring periods for middle transect (MT) sites during 2013 and 2014. Values in **bold** indicate where GW levels rose above the surface

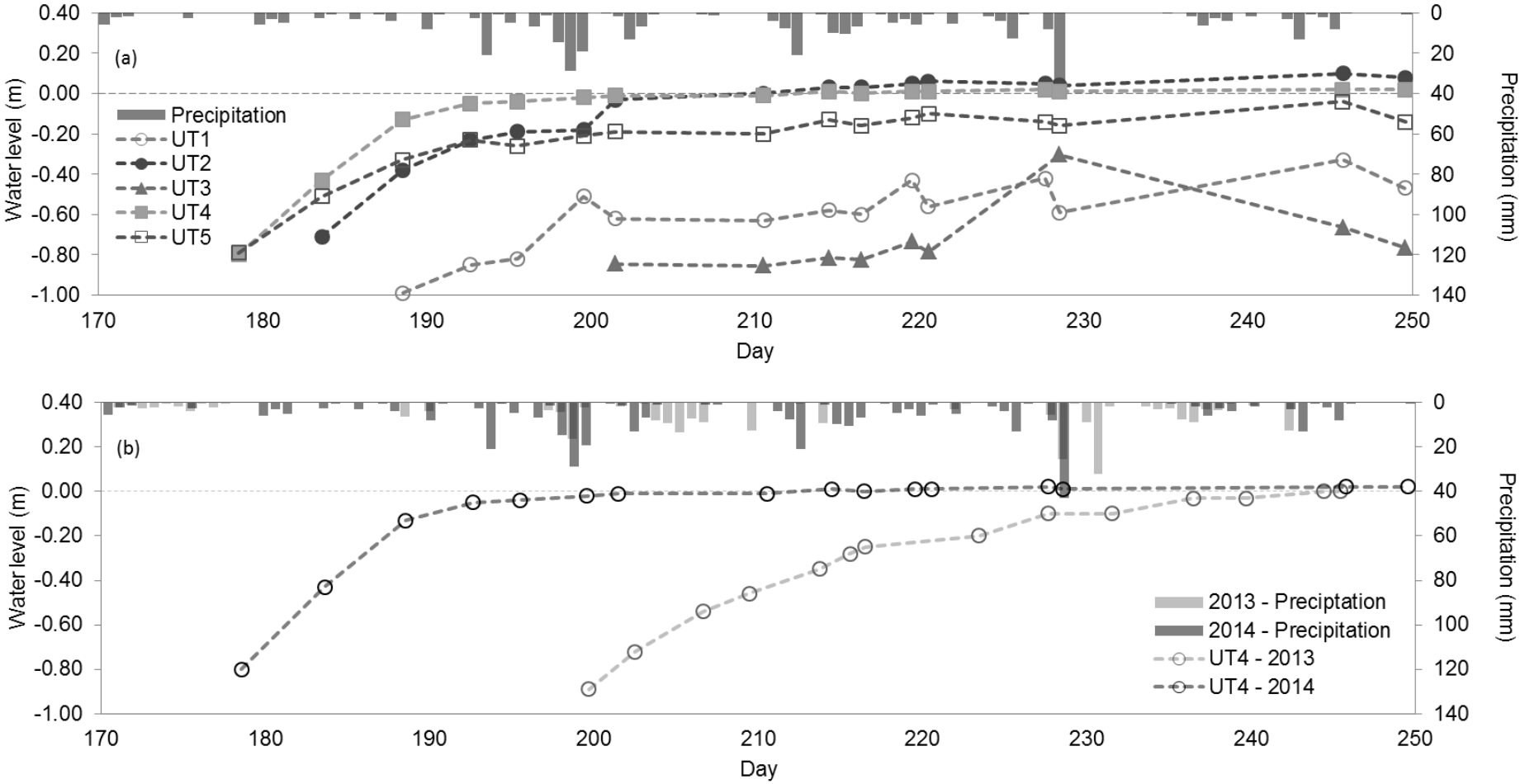

Figure 3.4: GW responses for upper transect (UT) sites during (a) 2014 and (b) a comparison of responses at site UT4 during 2013 and 2014. GW levels rose earlier and at a faster rate during 2014

3.5.5 Vertical hydraulic gradient

Across the middle (MT) and (UT) upper transects both positive and negative vertical hydraulic gradients (VHGs) were observed (Figure 3.5). While individual sites showed a clear temporal variation in VHG (notably MT1, MT4, MT8, MT9, MT11, and MT14), the magnitude of this variability was small compared to the spatial variations between sites (-0.2 to 0.3), due to PFP presence. Only MT2 showed a temporal variability comparable to that across the middle transect (μ = -0.19, σ = 0.26).

The high temporal variation in VHG at MT2 is a probable consequence of the unique circumstances of the channel within which this piezometer nest was located. Unlike other GW-fed streams on the terrace the channel was frequently inundated with overland flow from a nearby colluvial deposit during rain events (personal observation) that washed fine clay and silt deposits into the channel. These events resulted in the piezometers at MT2 being flooded with fine sediments which may have reduced their effectiveness and raises uncertainties regarding the reliability of VHG measurements for the site. Consequently the results for this piezometer nest were not considered further.

For both transects negative VHG gradients (indicative of downward movement of water) were observed at sites nearest the hillslope (MT1, MT3 and UT1). Negative gradients at these sites may be indicative of downward groundwater input from lateral subsurface flow pathways along the hillslopes adjacent to the terrace. Across the remainder of the upper and middle transects (with the exception of site MT7) VHGs were positive (indicative of upward movement of water), reflective of a vertical groundwater flux from further upstream to the surface of the terrace.

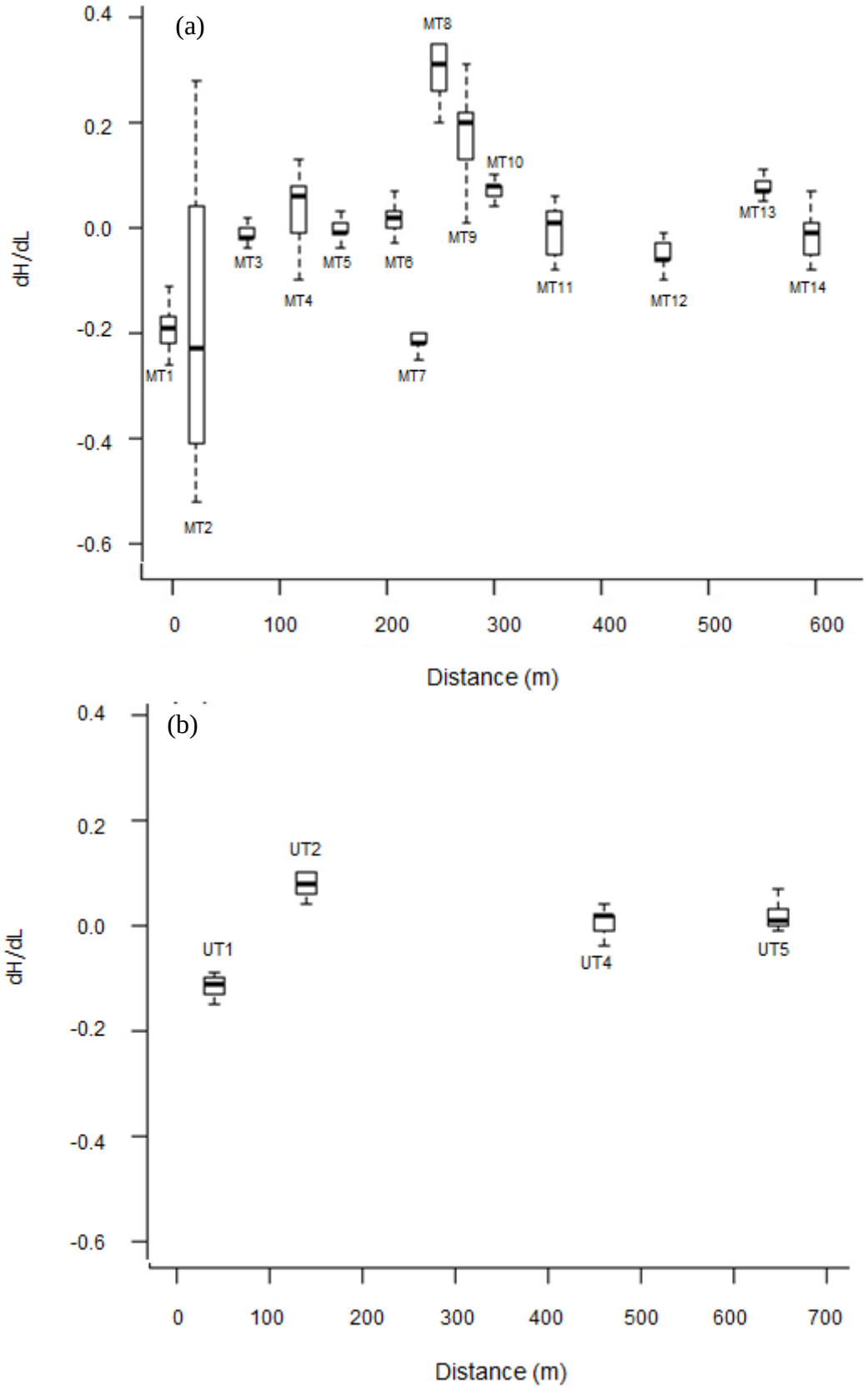

Figure 3.5: Vertical hydraulic gradients (dH/dL) across; (a) the middle transect (MT); and (b) the upper transect (UT) during 2014. Positive values are indicative of upward water movement.

Hydrofacies with high mean *K* were associated with stronger VHGs (Figure 3.6; one-way ANOVA, $p < 0.001$), reflecting their role as PFPs. Tukey-Kramer pairwise comparison tests showed statistically significant difference (95% confidence interval) in VHGs between all hydrofacies, with the exception of pairings sGcm and P, and sGcm, b and Gcm, b. These pairings were not significantly different from each other. The relationship between high *K* values and strong VHGs was also observable for individual sites. The highest mean $K_{0.0}$ values across MT sites were identified at MT8, MT9, MT10, and MT14 where the strongest positive vertical hydraulic gradient values were also observed (Figure 3.2a; Figure 3.5a).

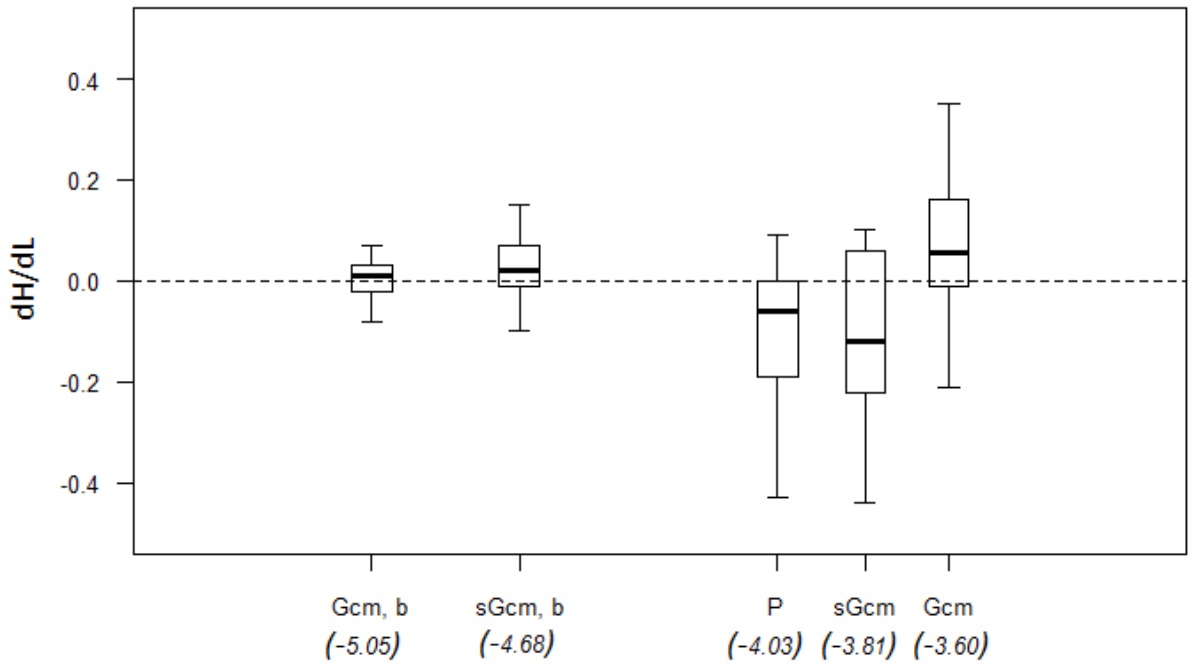

Figure 3.6: Vertical hydraulic gradients (dH/dL) for hydrofacies where gradients were available. Stronger gradients (positive and negative) are observed for hydrofacies with higher mean log *K* (values in brackets).

3.5.6 Water balance

Groundwater ($Q_{vertical}$) provided the largest estimated input to the floodplain terrace (Figure 3.7). $Q_{vertical}$ in July and August was approximately double the flux estimated for June. SWE_{max} from the adjacent hillslope and terrace area provided a comparable estimated input to $Q_{vertical}$ over summer months. Net precipitation and permafrost represented comparatively small inputs to the terraces storage. Stream flow from the terrace provided the only substantial loss from the storage, accounting for 20% of water inputs. Horizontal subsurface flow ($Q_{subsurface}$) did not provide a significant export from storage. Taking into account maximum terrace width (~600 m) and an aquifer depth of 100 m total $Q_{subsurface}$ flux equalled ~2.5 x 10^4 m^3, two orders of magnitude less than any other estimated flux. The remaining 80% was stored within the river terrace.

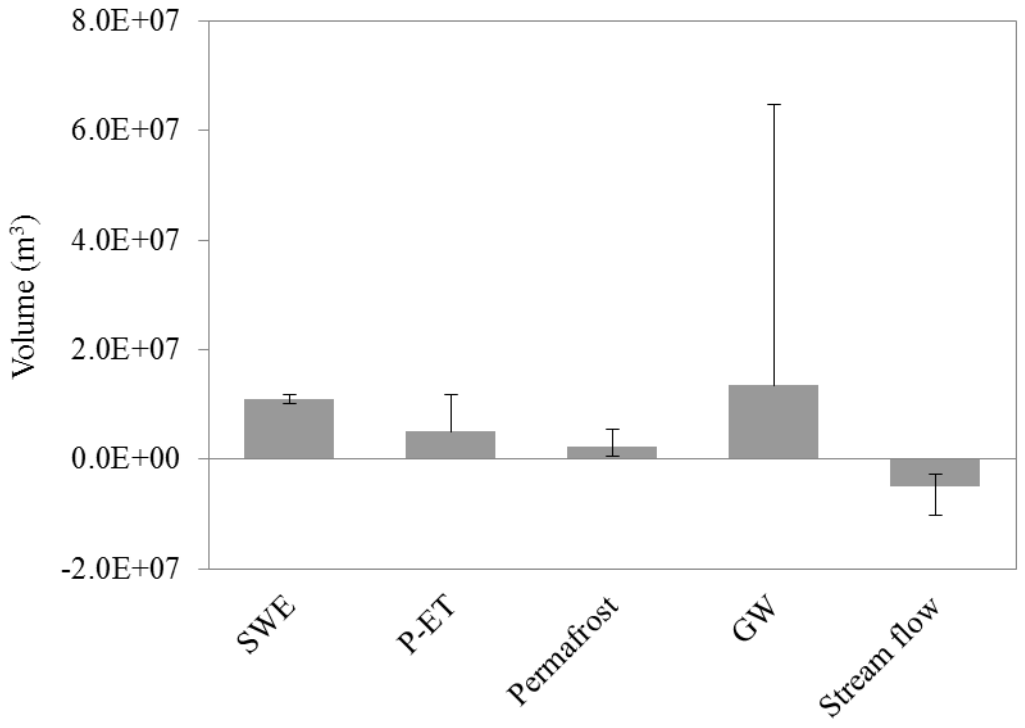

Figure 3.7: Total water balance estimate for terrace and adjacent valley side area during 2014. Horizontal subsurface flow ($Q_{subsurface}$) did not account for significant export of aquifer storage, and was several orders of magnitude lower than any other estimated flux

For June, July, and August the total water table rise based on estimated mean values and a specific yield of 29% was 19.81 (10.06 m excluding snow and permafrost melt). This water table rise was observed across the study site by the movement up-valley of the stream head positions. The furthest rise observed was 912 m up-valley, with an elevation increase of 20.85 m over the 2014 study period. This provides evidence to suggest that the calculated water balance is approximating the increase in floodplain storage over the study period.

Large margins of error were associated with each of the given fluxes. The largest error was associated with $Q_{vertical}$ (380%), due to the high variability in measured *K* across the terrace. Large errors were also calculated for estimated P-ET (134%). This error was principally related to variability in rainfall between the two weather stations for which meteorological data was compared. SWE_{max} was comparable between the two weather stations which meant error for this flux was considerably less than for other fluxes (14%). Margins of error for permafrost and streamflow were 90% and 74% respectively.

3.6 DISCUSSION

Given the recognised importance of PFPs to the occurrence of GW-fed streams this chapter has sought to further explore and establish the key hydrogeomorphic controls upon GW-fed streams. Furthermore, for the first time, estimates of the hydrological fluxes which sustain the discharge of GW-fed streams in paraglacial floodplains have been quantified. The discussion focuses on these advances and considers wider questions of hillslope-floodplain connectivity in conceptualising this process understanding.

3.6.1 Preferential flow pathways and groundwater recharge

The results found a clear spatial heterogeneity in *K* both laterally and vertically on the terrace. Spatial variation in *K* ranged over 3-4 magnitudes laterally across the terrace. Further,

to varying over a scale of hundreds of metres, $K_{0.0}$ also varied substantially at individual sites. $K_{0.0}$ was observed to range over 3 to 4 orders of magnitudes on a scale of tens of centimetres. Such large variability from the cm to the km scale for a single geomorphic unit (i.e. the terrace) highlights that terraces should not be treated as a single homogenous unit (Miller *et al.*, 2014). Rather the significant heterogeneity in *K* observed points to individual hydrostratigraphic units (Maxey, 1964) providing distinct subsurface flow pathways through the terrace units.

Log *K* values for identified hydrofacies varied over several orders of magnitude and were comparable with those from other studies (Heinz and Aigner, 2003a). Concurrent high *K* hydrofacies with moderate to strong VHGs was suggestive of specific hydrofacies units across the terrace acting as conduits of flow (PFPs) which, highlight their importance for GW-SW interactions and sustaining GW-fed streams (Caldwell *et al.*, 2015). Strong vertical hydrologic exchanges (VHE) associated with high *K* hydrofacies (PFPs) across the terrace maintained a large positive water input through the summer ($Q_{vertical}$). Horizontal subsurface flow ($Q_{subsurface}$) through the terrace was minimal and so the large $Q_{vertical}$ flux provided by VHEs, associated with PFPs, highlights the importance of the latter when characterising the hydrology of paraglacial floodplains (Poole *et al.*, 2006).

3.6.2 Valley side water sources

Observed groundwater recharge on the terrace in 2013 and 2014 was relatively consistent and continuous, exhibiting minimal response to individual storm events. However, groundwater levels rose at UT4 much earlier in the season, and at a faster rate, in 2014 compared to 2013. Earlier and faster rates of groundwater rise on the upper transect in 2014, during periods of high precipitation and low temperatures (low melt) (see section 2.2), compared with 2013,

during low precipitation and high temperature (high melt), suggests the importance of summer precipitation to the terrace aquifer. This suggests that recharge may be predominantly rain-fed, or driven; which is typically observed only in temperate systems (Allen *et al.*, 2010). However, the non-flashy, gradual response of groundwater levels is indicative of the retention of event water within the headwaters (Kirchner, 2003). This may reflect the influence of colluvial deposits (Clow *et al.*, 2003), alpine meadow (Clow and Sueker, 2000), or fractured bedrock (Liu *et al.*, 2004) as important conduits within these systems that increase residence times and minimise flashy responses to aquifer recharge on the floodplain (Weekes *et al.*, 2015). Particularly given these landscape units were an extensive presence within the MF Toklat catchment (see section 2.1.1).

SWE_{max}, P-ET, and PF flux estimates for the adjacent valley side and terrace area were sufficiently large enough to account for groundwater recharge on the terrace. Given these estimates and steady, continuous, groundwater recharge on the terrace; the retention and gradual discharge of groundwater on valley sides (Baraer *et al.*, 2015) could make an important contribution to sustaining GW-fed stream flow on the terrace. Particularly as colluvial deposits, alpine meadow, and fractured bedrock are all hydrological stores present on the adjacent valley side (see section 2.1.1).

3.6.3 Conceptualising understanding

Identified high *K* hydrofacies and associated strong VHGs highlighted the importance of PFPs in supporting biodiversity hotspots through high groundwater inputs. Previous work on the terrace had assumed the importance of upstream glacial meltwater in supporting GW-fed streams (Crossman *et al.*, 2011). Upstream water sources are undoubtedly an important water source to the terrace aquifer; $Q_{vertical}$ was the single largest water source estimated to support

terrace aquifer recharge. Furthermore, given the uncertainty in the size of the flux (due to the range of observed *K* values) $Q_{vertical}$ to the terrace aquifer could be considerably greater.

However, it may not be appropriate to assume that this large upstream GW flux is derived predominantly from glacial meltwater, given the large upstream catchment area (114 Km^2) and limited glacial coverage (5.3%) of the MF Toklat (Crossman *et al.*, 2012). Water balance analysis has shown that the contribution of non-glacial meltwater sources (SWE_{max}, PF, and P-ET) from adjacent valley sides and terrace areas alone could equal or exceed the $Q_{vertical}$ input from upstream to the terrace. Given that 94.7% of the catchment area upstream of the terrace is non-glacierised it seems appropriate to infer that non-glacial meltwater (and rainfall) sources (from valley sides) may also represent an important component of $Q_{vertical}$, alongside glacial meltwater. Upstream of the terrace extensive colluvial deposits, alpine meadow, and fractured bedrock (of the Cantwell Formation) are ubiquitous within the MF Toklat catchment. Their occurrence and identification as valuable hydrologic stores, delaying water release and increasing residence times (Hood and Hayashi, 2015) raises the prospect that they make a significant contribution to the $Q_{vertical}$ flux supporting GW-fed streams on the terrace. This would have the effect that GW-fed stream recharge on the terrace would be primarily rain-fed, or driven, rather than by upstream glacial meltwater as previously assumed.

A conceptual summary of the water balance analysis is presented in Figure 3.8. The role of PFPs as the dominant subsurface flow path connecting upstream groundwater input to GW-fed streams on the terrace is emphasised. The contribution of adjacent valley side flow to terrace aquifer recharge is also highlighted. Colluvial deposits, alpine meadows, and fractured bedrock have all been identified as potentially significant hydrological stores on valley sides, and would make a significant contribution to sustaining GW-fed streams on the terrace. Although all three hydrological units are present on the valley sides adjacent to the terrace

(see section 2.1.1), the recent literature has heavily emphasised the role of superficial colluvial deposits in particular as important hydrological units in paraglacial environments. (Baraer *et al.*, 2015; Hood and Hayashi, 2015; Weekes *et al.*, 2015).

Clow *et al.* (2003) highlighted the nature of talus slopes as the primary groundwater reservoir in a small alpine headwater catchment, with a potential storage capacity greater than the total annual discharge. They estimated that talus deposits had porosities between 43% and 60% and *K* ranging 6.5 – 9.4 x 10^{-3} m s^{-1}. Similarly Muir *et al.* (2011) estimated *K* for colluvial deposits between 1.0 – 3.0 x 10^{-2} m s^{-1}. While sediments below alpine meadows have been found to be highly porous (~60%) they also exhibit extremely low *K* properties (~2.5 x 10^{-7} m s^{-1}) (McClymont *et al.*, 2010). Likewise, although the fractured volcanic bedrock of the Cantwell formation may have a porosity up to 40% (Singhal and Gupta, 2010), *K* properties are likely to range between 3.0 x 10^{-4} and 8.0 x 10^{-9} m s^{-1} (Domenico and Schwartz, 1990). Although this demonstrates alpine meadow and fractured bedrock can provide important groundwater aquifers on valley sides, their lower *K* values suggest they cannot act as conduits of flow in the same way as colluvial deposits.

Due to the prevalence of colluvial deposits on the valley sides adjacent to the MF Toklat terrace it is considered that they are the most important groundwater store and channel of subsurface flow on valley sides. While fractured bedrock and alpine meadow may provide important aquifers for groundwater on the valley sides the rain-driven nature of recharge, which indicates a fast response to storm events, suggests these low *K* hydrological units could not provide the dominant subsurface flow paths as colluvial deposits can.

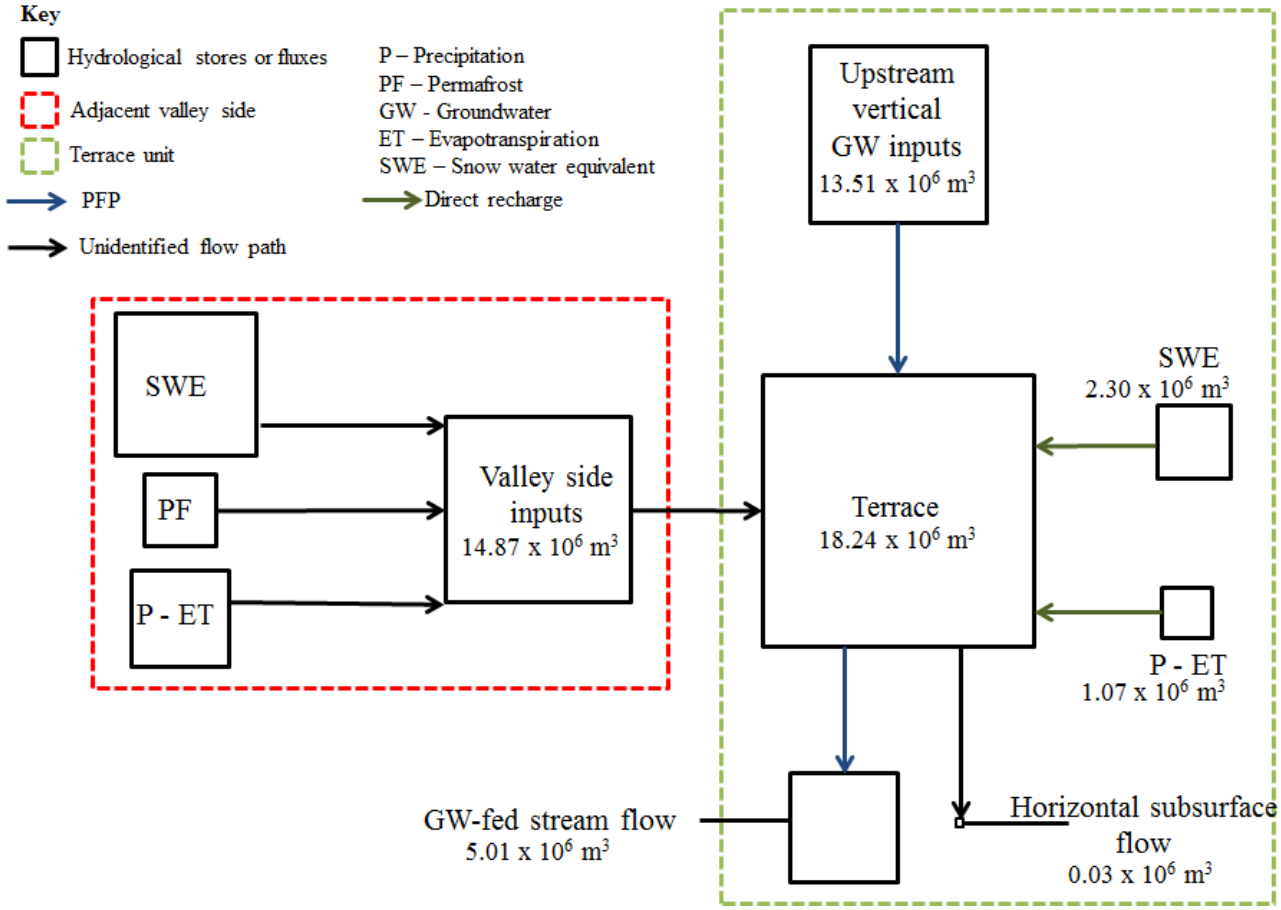

Figure 3.8: Conceptual summary of water balance analysis. Hydrological stores and fluxes presented are proportional relative to their calculated size. The conceptualisation demonstrates how hydrological fluxes from the adjacent valley side could equal or exceed groundwater recharge from upstream of the terrace unit. Colluvial deposits, alpine meadow, and fractured bedrock on valley sides could provide valuable aquifers, retaining groundwater on valley sides; with colluvial deposits then acting as important conduits of flow to sustain GW-fed streams. Given the combination of large catchment area, minimal glacial coverage, and prevalence colluvial deposits, alpine meadow, and fractured bedrock upstream of the terrace; hillslope runoff sources may provide a larger component of upstream input to GW-fed streams on the terrace than previously thought. Glacial meltwater may be a less influential component of these streams, which are instead predominantly ran-fed, or driven, from valley-side runoff sources. The minimal export of groundwater through horizontal subsurface flow reflects the channelization of groundwater across the terrace that leads to the emergence of GW-fed streams, and which account for almost all groundwater exported from the terrace. The lack of diffuse flow across the terrace combined with the presence of high *K* hydrofacies (associated with strong VHGs) highlights the important role of PFPs as concentrated conduits of flow through the terrace. Given the significance of valley side inputs and importance of PFPs to GW-fed stream occurrence identified in this chapter the potential role of PFPs in hillslope-floodplain connectivity should be further explored.

3.6.4 Implications of conceptual understanding

Given the possible connection between hillslope runoff and GW-fed streams that has been identified, PFPs have an important role in hillslope-floodplain connectivity that delivers hillslope runoff to GW-fed streams and sustains perennial flow. Such a role has not previously been considered and raises a number of important issues. Firstly which shifts in the hydrologic regimes of paraglacial catchments, in response to climate change, are of most concern to the long-term stability of GW-fed streams? Current understanding emphasizes the detrimental impacts of declining upstream meltwater (snow and glacial) contributions (Deb *et al.*, 2015). While upstream meltwater may provide an important component of subsurface groundwater recharging the terrace, our water balance analysis also suggests alterations in valley side runoff (due to shifting precipitation patterns and declining permafrost coverage etc.) may have important implications for GW-fed streams on floodplain margins.

Secondly glaciers and their associated meltwaters are a vital source of sediment to paraglacial floodplains. Glacial retreat will have profound implications on sediment load and transport within these systems (Gurnell *et al.*, 2000; Klaar *et al.*, 2015). Following deglaciation a short-term peak in paraglacial sedimentation yields is succeeded by an ensuing decline, as sources of sediment are depleted or stabilise (Church and Ryder, 1972; Orwin and Smart, 2004). Declining sediment yields will have a detrimental impact upon the main paraglacial river channels (Marren and Toomath, 2014). Diminishing avulsion processes and channelization of flow will restrict the development of new PFPs across floodplains (Poole *et al.*, 2006). Furthermore avulsion processes are important for the renewal and 'reactivation' of existing PFPs (Poole *et al.*, 2002). A reduction in these infrequent, but important flood events on terraces, may result in the establishment of invasive plant roots (Gurnell *et al.*, 2000) and infiltration of suspended sediment from surface water (otherwise removed by avulsion

processes) within existing PFPs; constraining their hydraulic conductivity and effectiveness as channels of flow (Poole *et al.*, 2002). This may already be occurring on the MF Toklat terrace base where mature vegetation has developed at the terrace base (see section 2.1.1), and fine sediments have accumulated in GW-fed streams where overland flow from adjacent valley-sides has directly entered channels (see section 3.5.2).

As a consequence hydrologic connectivity across paraglacial floodplains could be restricted, with subsequent negative implications for the stability of GW-fed streams (Caldwell *et al.*, 2015). If PFPs are essential to hillslope-floodplain connectivity then such alterations may impact the perennial nature of GW-fed streams, and these changes would be damaging to their role as biodiversity hotspots in paraglacial environments.

3.7 SUMMARY

Spatial heterogeneity in *K* and the connection between strong VHGs and high *K* hydrofacies have clearly demonstrated the importance of PFPs to sustaining biodiversity hotspots on floodplain terraces. Novel water balance analysis has indicated that while vertical groundwater fluxes from upstream are a major component of GW-fed stream recharge, greater consideration must also be given to valley side runoff (e.g. precipitation and permafrost) as key water sources. Our analysis indicated that fluxes of these water sources from the adjacent hillslope and terrace area alone have the potential to support a significant amount of terrace aquifer recharge. Furthermore, valley side runoff could also provide a significant component of upstream groundwater to the terrace alongside glacial meltwater.

Combining this new understanding has for the first time raised consideration of the role provided by PFPs in hillslope-floodplain connectivity. A first-order attempt to conceptualise the understanding gained from this work has been presented, and which; (1) emphasises the

importance of PFPs to GW-fed streams; and (2) acknowledges the potential significance of hillslope runoff processes in supporting GW-fed stream recharge. This interpretation advances the prospect of revising our considerations of the fundamental hydrologic and hydrogeomorphic controls upon GW-fed streams within paraglacial floodplains, and the implications of climate change upon their long-term role as biodiversity hotspots. There is a need to validate the conceptual summary developed through; (1) identification of individual valley side flow paths; (2) quantification of that flow; and (3) more clearly establishing the role of PFPs in hillslope-floodplain connectivity within paraglacial catchments. These research gaps are addressed in subsequent chapters.

CHAPTER 4: HILLSLOPE-FLOODPLAIN CONNECTIVITY IN PARAGLACIAL CATCHMENTS: COLLUVIAL DEPOSITS REGULATING FLOODPLAIN HYDROLOGICAL DYNAMICS

4.1 SCOPE OF CHAPTER

PFPs have been linked to GW-fed stream presence within paraglacial floodplains (Chapter 1). In Chapter 3 PFPs were identified as an important hydrogeomorphic control upon GW-fed streams. In addition hillslope runoff from adjacent valleys-side areas was highlighted as a potentially valuable source of flow to GW-fed streams; with colluvial deposits proposed as important stores and conduits of hillslope runoff to GW-fed streams (Chapter 3). Moreover, the significance of hillslope runoff to GW-fed streams has raised questions over the role of PFPs in hillslope-floodplain connectivity (Chapter 3).

This chapter addresses the importance of colluvial deposits as conduits of flow and aquifers that enable sustained flow of GW-fed streams. Furthermore, it focuses on the role of PFPs in providing hydrological connectivity between hillslope and floodplain. During summer 2013 and 2014 surface-water (SW) and groundwater (GW) behaviour across a floodplain terrace on the MF Toklat River, DNPP, Alaska, were investigated. SW, GW, and identified end-members were sampled for pH, electrical conductivity (EC), acid neutralizing capacity (ANC), major ions, and stables isotopes (δ^2H).

Spatial patterns in water chemistry and two-component hydrograph separations demonstrated the importance of flow from colluvial deposits to GW-fed streams. Spatiotemporal patterns in geochemical signatures of surface waters highlighted the presence of multiple, discrete flow paths (PFPs) on the floodplain that connected GW-fed streams to the hillslope. Mean residence time (MRT) estimates suggested this flow was dominated by ‘old’ water and that colluvial deposits represented important aquifers. The results highlight that more attention must be given to the consequences of changing climate on hillslope flow in paraglacial catchments and establishing first-order controls on GW-fed streams. They also provide support for the interpretation that GW-fed stream recharge in summer is rain-fed or driven.

4.2 INTRODUCTION

GW-fed streams on paraglacial floodplains are valuable biodiversity hotspots which support increased taxonomic richness and abundance within aquatic ecosystems (Lencioni and Spitale, 2015; Robinson and Doering, 2012). Furthermore, their presence supports riparian vegetation that is integral to aquatic-terrestrial linkages in paraglacial environments (Paetzold *et al.*, 2005). Paraglacial catchments and their associated hydrologic regimes are particularly sensitive to anthropogenic climate change in the 21st century (Baraer *et al.*, 2012; Barnett *et al.*, 2005). However, the hydrological dynamics which support GW-fed streams remain poorly understood and subject to considerable uncertainties (Levy *et al.*, 2015) and consequently the full implications of climate change for these valuable floodplain habitats are unknown.

PFPs through paleochannels across paraglacial floodplains (Stanford and Ward, 1993) have been identified as important to GW-fed stream occurrence (Caldwell *et al.* 2015; Chapter 3). They are a substantial channel of subsurface flow across floodplains (Anderson *et al.*, 1999) and GW-fed streams form where they extend to the surface (Poole *et al.*, 2002). The role of PFPs in GW-SW interactions along river corridors is well established (Malard *et al.*, 2002; Miller *et al.*, 2014). However, their importance in the wider context of maintaining lateral hydrologic connectivity, and particularly hillslope-floodplain connectivity (Bracken and Croke, 2007), has remained unconsidered. Alongside glacial melt (GM), hillslope runoff is increasingly recognised as an important part of the water balance in paraglacial catchments (Baraer *et al.* 2015; Weekes *et al.* 2015; Chapter 3) although the specific pathways followed by hillslope runoff remain poorly understood (Gordon *et al.*, 2015). Hence there is a need to deliberate further the role of PFPs in connecting hillslope runoff to GW-fed streams in paraglacial environments as outlined in Chapter 3.

The importance of hillslope runoff in paraglacial catchments raises a number of questions on valley side flow pathways. Colluvial deposits (e.g. talus cones) are widespread in paraglacial catchments (Ballantyne, 2002b); and alongside alpine meadow and fractured bedrock (see section 3.6.3) have been recognised as valuable hydrological stores (McClymont *et al.*, 2012), retaining groundwater in the catchment headwaters and increasing mean water residence time (Weekes *et al.*, 2015). Declining glacial meltwater discharge (Milner *et al.*, 2009) will increase the relative importance of these stores in future (Baraer *et al.*, 2012). It has been observed that GW-fed streams do not exhibit a flashy response to storm events, and that hillslope runoff water sources are sufficient to sustain streamflow and GW recharge on paraglacial floodplains (Chapter 3). Hillslope runoff in paraglacial settings is snow- and rain-fed dominated (Caballero *et al.*, 2002) which typically creates flashy stream responses to storm events (Addy *et al.*, 2011). Non-flashy behaviour would then suggest that hydrological storage, retention, and gradual release of hillslope runoff on valley sides (Weekes *et al.*, 2015) is important to sustaining GW-fed streams. There is a need to address this research gap, quantifying the hillslope runoff contribution to GW-fed streams and the dynamics of water storage on the valley side; and ultimately determine how runoff from this source connects to the floodplain.

Chapter 3 raised the potentially greater significance of colluvial deposits as both hydrological stores and conduits of flow over alpine meadow and fractured bedrock on hillslopes (see section 3.6.3). Subsequently this chapter focuses on ascertaining the significance of colluvial deposits to streamflow, and their interactions with PFPs, which may be integral to hillslope-floodplain connectivity. Drawing upon an analysis of the geochemical and isotopic composition of waters sampled within a catchment on the MF Toklat River, DNPP, Alaska the objectives of this chapter are to; (1) characterise the role of PFPs in hydrological

connectivity between valley side runoff and GW-fed streams; (2) determine if colluvial deposits are important stores and conduits for hillslope runoff to GW-fed streams; and (3) quantify the contribution of colluvial deposits to GW-fed stream discharge.

4.3 STUDY SITE

Fieldwork was carried out on the MF Toklat terrace during 2013 and 2014 (see section 2.1.1).

4.4 METHODOLOGY

Hydrometric monitoring (stream discharge and groundwater levels) was conducted on the MF Toklat terrace during both years, details are provided in section 2.3.3.1. Geochemical and isotopic tracers were applied to establish water sources and flow pathways to the field site. Details on sampling protocol and laboratory analysis are provided in section 2.3.4. Sampling strategy is outlined in section 2.3.4.1. Two-component hydrograph separations were used to quantify flow contribution from colluvial deposits to discharge, further information can be found in section 2.4.2. Finally mean residence times (MRT) were estimated to establish the possible role of colluvial deposits as GW aquifers on valley-sides (see section 2.4.3).

4.5 RESULTS

4.5.1 Stream discharge

Stream discharge for sites SW1, SW2, and SW3 and precipitation during the 2013 and 2014 monitoring periods are presented in Figure 4.1. Precipitation was higher in June, July, and August (348.3 mm) in 2014 compared with 2013 (229.5 mm). Overall discharge remained relatively stable and consistent at SW1 and SW2 during both years, with the exception of discrete responses to individual storm events. During 2014 discharge at SW1 showed a much greater response to individual storm events on 26th June and 6th August (JD 177 & 218) compared to equivalent events in 2013 on 19th and 22nd August (JD 231 & 234).

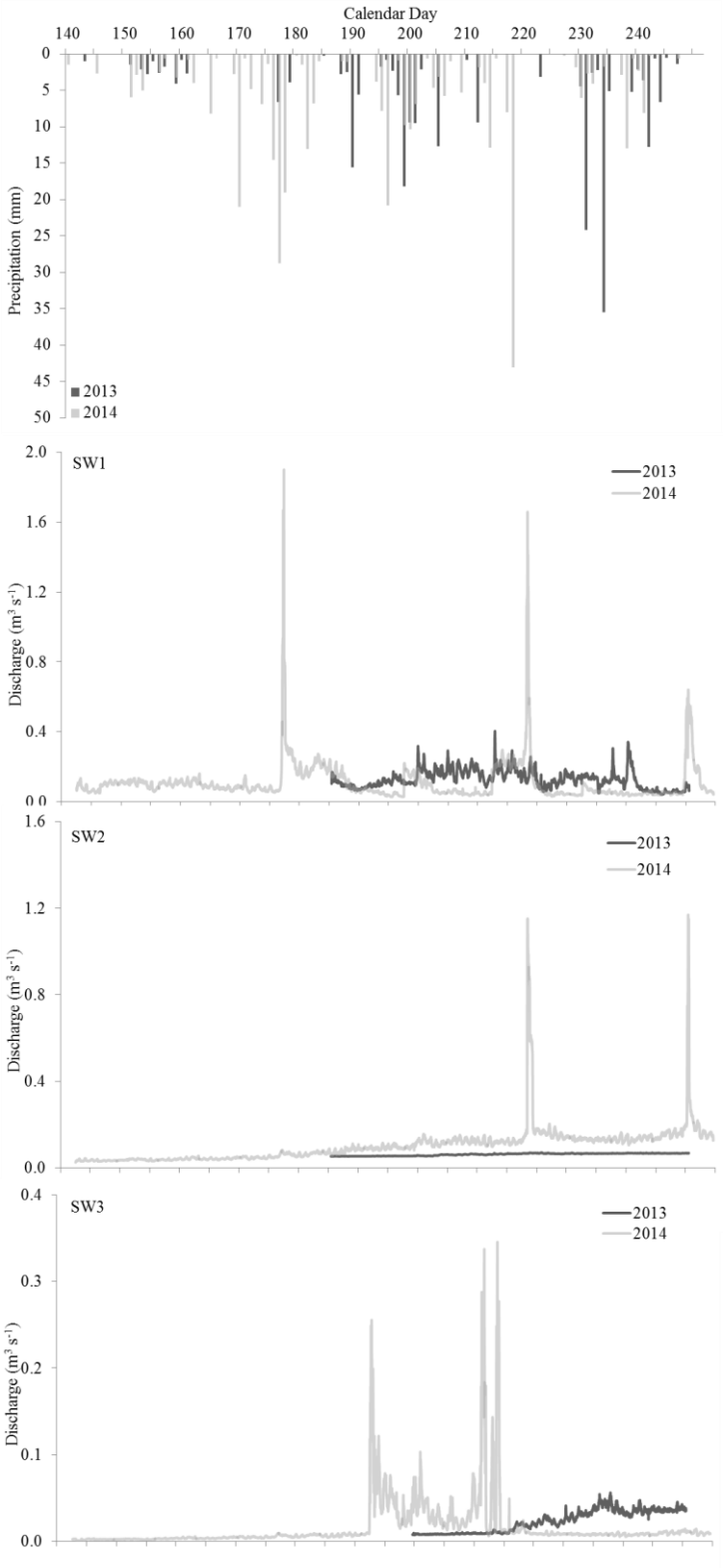

Figure 4.1: Precipitation for the MF Toklat and stream discharge at sites SW1, SW2, and SW3 during 2013 and 2014. Discrete responses to individual storm events were observed at SW1 and SW2 during 2014, caused by overland flow from adjacent hillslopes flowing across the terrace and into individual channels. Similar responses to storm events during 2013 were not observed as overall precipitation during summer months was 34.1% lower and so hillslopes were not sufficiently saturated to cause overland flow responses. Increases in discharge at SW3 between JD 192 – 215 in 2014 and after JD 215 in 2013 were caused by backwater from the main glacial

Similarly at SW2 responses to storm events on 6th August and 2nd September (JD 218 and 245) during 2014 were observed, while no response to individual storm events was recorded during 2013. The responses observed at SW1 and SW2 during 2014 were most likely caused by overland flow from adjacent hillslopes flowing onto the terrace and directly into those channels during individual storm events (personal observation). There was a 51.8% increase in precipitation for June, July, and August between 2013 and 2014, which may explain why similar responses in stream discharge to storm events during 2013 were not observed. Reduced precipitation may have meant hillslopes were not sufficiently saturated to cause overland flow in response to individual storm events.

Discharge at SW3 remained very low throughout 2014, with the exception of a period between 11th July and 3rd August (JD 192 to 215; Figure 4.1). This coincided with the occurrence of backwater formation at the terrace base (nearest SW3), caused by the main glacial river switching to a channel nearer the terrace (see Figure 2.4a). Backwater from the main river inundated the base of SW3, resulting in discharge data for this site to become distorted during this period. A similar response occurred during 2013 and caused the observed increase in discharge from 3rd August (JD 215) at SW3.

4.5.2 Groundwater behaviour

Groundwater response for selected sites in 2013 and 2014 are presented in Figure 4.2 with associated precipitation data for both years. Seasonal groundwater level response across the full width of the terrace (Sites MT3, MT7, and MT14) displayed similar behaviour during both years. At all sites water levels rose steadily through the summer before plateauing at, or just above, the surface (Figure 4.2). During both years groundwater levels rose at a similar rate and time at site MT7. In contrast, at sites MT3 and MT14, on the terrace margins, groundwater levels rose earlier in the year, at a faster rate, and to a higher level above the surface in 2014 compared with 2013. At MT3 groundwater levels rose to the terrace surface on 18th July (JD 199) in 2013 and 22nd May (JD 142) in 2014. At MT14 this occurred on 18th July (JD 199) in 2013 and 18th June (JD 169) in 2014.

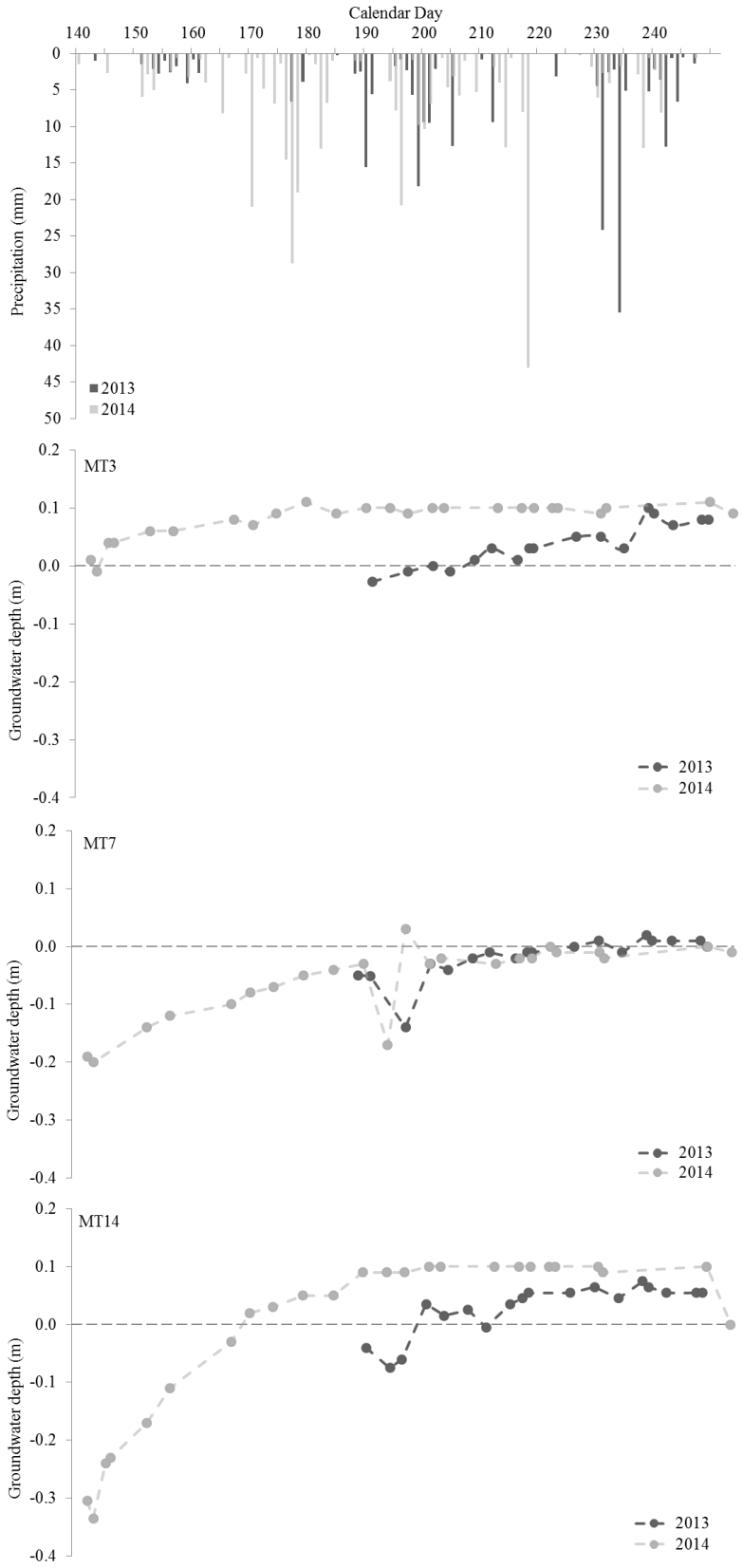

Figure 4.2: Precipitation for the MF Toklat and groundwater levels at sites MT3, MT7, and MT14 during 2013 and 2014

4.5.3 Geochemical composition of waters

Combined mean values, and associated standard deviations (σ), for measured hydrochemical and stable isotope variables during 2013 and 2014 for surface water (SW) sites, selected groundwater sites (MT), and identified end-members are presented in Table 4.1. Identified terrace end-members include hillslope flow (from a debris fan (DF) up-valley of GW streams), and groundwater (GW) flow that included vertical inflow from the terrace area upstream of the debris fan. This separation allowed the characterisation of flow specifically from the individual DF. In addition hydrochemical and stable isotope variables for summer precipitation (Precip.) and winter snowpack (SP) are presented.

Mean values indicated distinct spatial variations in water chemistry with respect to both surface water and groundwater across the terrace (Table 4.1). Sites nearest the hillslope (SW1 & MT1) were associated with elevated ANC, sodium, potassium, silica, and higher ratios of both $[Mg^{2+} + Ca^{2+}]$ vs SO_4^{2-} and K^+ vs Si. $[Mg^{2+} + Ca^{2+}]$ vs SO_4^{2-} ratios were >1 for almost all surface water, groundwater and end-member samples collected on the terrace (Figure 4.3). Sites further from the terrace (SW3 & MT14) showed increased calcium and magnesium levels. In addition to observed spatial variation in water chemistry across the terrace temporal patterns in water chemistry were also observed. This temporal variation is most apparent in observed mean EC values and associated σ (Table 4.1), reflecting inter-annual and seasonal trends in solutes of surface-water and groundwater as well as identified end-members. There were clear differences in the chemistry of identified flow paths (end-members) supporting flow on the terrace (Figure 4.4). Identified hillslope input (DF) exhibited elevated bicarbonate, sodium, and potassium, in contrast to lower concentrations in GW input to the terrace. GW concentrations of sulphate, calcium, and magnesium were considerably greater than those of hillslope input.

Site	EC		ANC		Na^+		K^+		Mg^{2+}		Ca^{2+}		SiO_2		Cl^-		NO_3^-		SO_4^{2-}		δH		Mg^{2+}:Ca^{2+}		K^+:Si		$[Mg^{2+}+Ca^{2+}]$:SO_4^{2-}	
	(µS)	σ	(meq l^{-1})	σ	(meq l^{-1})	σ	(meq l^{-1})	σ	(meq l^{-1})	σ	(meq l^{-1})	σ	(meq l^{-1})	σ	(meq l^{-1})	σ	(meq l^{-1})	σ	(meq l^{-1})	σ	(‰)	σ		σ		σ		σ
SW1	**529**	*73*	**3.65**	*0.22*	**0.51**	*0.21*	**0.058**	*0.083*	**2.16**	*0.59*	**1.47**	*0.59*	**0.095**	*0.034*	**0.085**	*0.024*	**0.94**	*2.32*	**1.91**	*0.79*	**-159.63**	*2.64*	**1.59**	*0.48*	**0.37**	*0.69*	**2.19**	*1.06*
SW2	**556**	*97*	**2.75**	*0.21*	**0.45**	*0.19*	**0.038**	*0.010*	**2.36**	*0.74*	**1.83**	*0.68*	**0.082**	*0.028*	**0.131**	*0.077*	**0.78**	*1.47*	**2.67**	*1.29*	**-161.82**	*1.91*	**1.35**	*0.30*	**0.26**	*0.15*	**1.92**	*1.26*
SW3	**586**	*69*	**2.75**	*0.15*	**0.19**	*0.07*	**0.041**	*0.015*	**3.17**	*1.20*	**2.13**	*0.94*	**0.070**	*0.022*	**0.053**	*0.050*	**0.67**	*1.27*	**3.46**	*1.16*	**-162.07**	*2.03*	**1.55**	*0.38*	**0.31**	*0.19*	**1.58**	*0.52*
MT1	**553**	*66*	**16.56**	*15.72*	**0.47**	*0.18*	**0.060**	*0.026*	**2.30**	*0.57*	**1.30**	*0.52*	**0.100**	*0.036*	**0.084**	*0.045*	**0.30**	*0.51*	**1.65**	*0.68*	**-156.60**	*5.96*	**1.95**	*0.71*	**0.32**	*0.18*	**2.38**	*0.78*
MT7	**495**	*54*	**16.75**	*36.40*	**0.38**	*0.18*	**0.043**	*0.011*	**2.19**	*0.63*	**1.63**	*0.60*	**0.080**	*0.027*	**0.097**	*0.048*	**1.98**	*6.42*	**2.24**	*0.85*	**-162.02**	*2.07*	**1.49**	*0.60*	**0.30**	*0.16*	**2.33**	*2.90*
MT14	**562**	*66*	**7.11**	*9.87*	**0.19**	*0.08*	**0.040**	*0.015*	**2.81**	*0.66*	**2.03**	*0.70*	**0.067**	*0.026*	**0.058**	*0.019*	**6.04**	*22.16*	**3.39**	*1.18*	**-162.39**	*2.41*	**1.46**	*0.37*	**0.33**	*0.17*	**1.51**	*0.41*
DF	**475**	*100*	**4.15**	*0.91*	**2.07**	*0.96*	**0.054**	*0.015*	**0.89**	*0.29*	**0.58**	*0.26*	**0.127**	*0.041*	**0.046**	*0.018*	**0.57**	*2.02*	**0.81**	*0.32*	**-150.35**	*2.21*	**1.70**	*0.66*	**0.30**	*0.15*	**1.94**	*0.69*
GW	**602**	*52*	**4.71**	*2.67*	**0.18**	*0.07*	**0.046**	*0.008*	**3.45**	*0.86*	**1.58**	*0.51*	**0.068**	*0.021*	**0.053**	*0.022*	**0.34**	*1.04*	**2.41**	*0.90*	**-159.67**	*2.27*	**2.35**	*0.78*	**0.49**	*0.21*	**3.87**	*7.38*
Precip.	**48**	*29*	**0.18**	*0.16*	**0.04**	*0.08*	**0.014**	*0.017*	**0.12**	*0.31*	**0.20**	*0.23*	**0.004**	*0.005*	**0.056**	*0.031*	**0.04**	*0.05*	**0.09**	*0.20*	**-133.70**	*29.83*	**0.39**	*0.37*	**4.17**	*4.95*	**5.52**	*7.62*
GM	**270**	*233*	**2.05**	*1.65*	**0.08**	*0.08*	**0.019**	*0.008*	**0.28**	*0.12*	**0.60**	*0.15*	**0.03**	*0.03*	**0.04**	*0.01*	**0.02**	*0.01*	**0.27**	*0.32*	**-162.76**	*2.36*	**0.46**	*0.09*	**0.64**	*0.33*	**4.85**	*4.32*
SP	**128**	*158*	**0.16**	*0.13*	**0.04**	*0.04*	**0.018**	*0.018*	**0.25**	*0.54*	**0.25**	*0.39*	**0.002**	*0.004*	**0.045**	*0.007*	**4.40**	*10.71*	**0.14**	*0.21*	**-164.40**	*15.30*	**0.44**	*0.43*	**15.10**	*14.31*	**2.70**	*1.26*

Table 4.1: Physicochemical properties of sampled surface water (SW), middle transect (MT), and identified end-members sites for 2013 and 2014 sampling periods. Combined mean values (**in bold**) and associated standard deviations (*in italics*) are presented. Debris fan (DF) and upstream groundwater (GW) flow were used for two-component hydrograph separations. Summer precipitation (Precip.), winter snowpack (SP), and glacial melt (GM) geochemical and isotopic signatures are also presented. Precip. samples were collected using a rain collector at a road camp ~5 km downstream (NE) of the site (within the same catchment), and isotopic composition was calculated as a weighted average using the method of McDonnell *et al.* (1990).

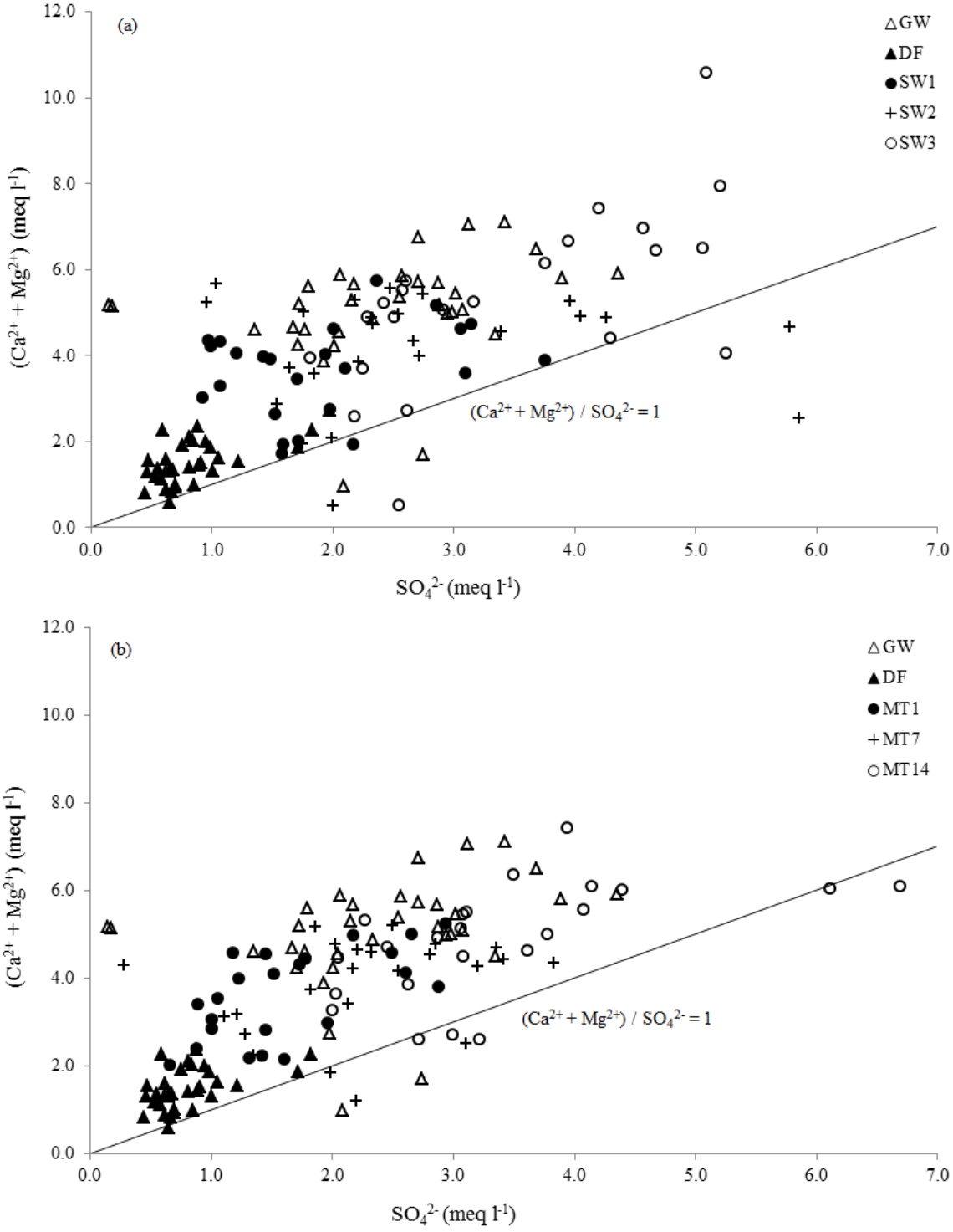

Figure 4.3: (Ca^{2+} + Mg^{2+}) vs SO_4^{2-} ratios for end-members (GW and DF); (a) surface water; and (b) middle transect sites. Plots show combined 2013 and 2014 data.

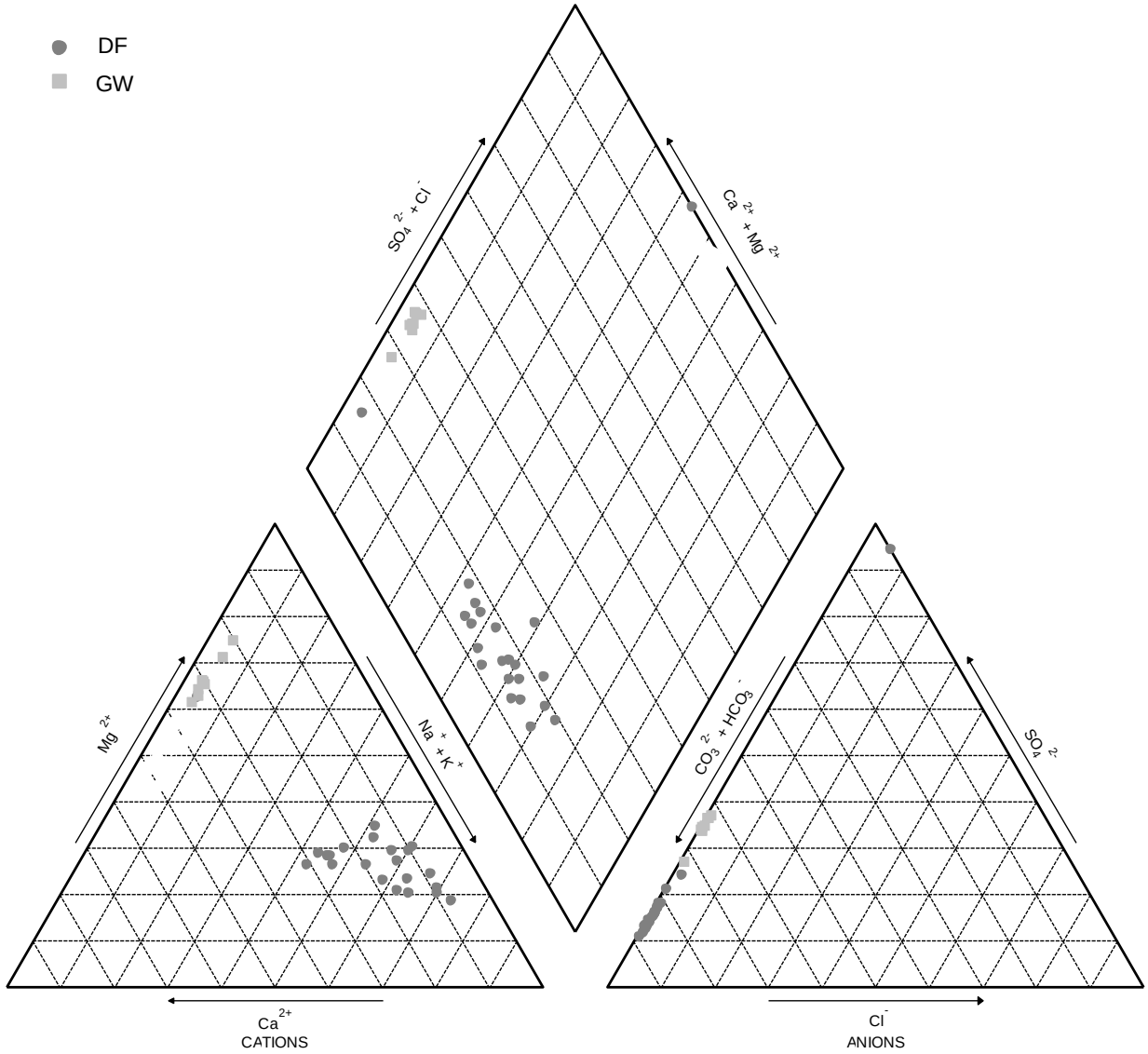

Figure 4.4: Piper diagram for two identified end-members within the MF Toklat catchment. A debris fan (DF) on the valley side upstream of the GW-fed streams and groundwater (GW) from up-valley.

Spatial variations in water chemistry across the terrace were evident: during both 2013 and 2014 there was a trend towards increasing calcium and sulphate with increasing distance across the terrace from the hillslope for both surface-water and groundwater (Figure 4.5). In contrast silica declined with increasing distance from the hillslope in both years (Figure 4.5). Mean calcium and sulphate across all sites and identified flow path end-members were higher in 2013 compared with 2014. This contrasts with mean silica which was considerably higher in 2014 compared with 2013. Mean [K:Si] was also considerably higher at all sites in 2014 compared with 2013. Furthermore, temporal variation in [K:Si] was also markedly greater in 2014 (Figure 4.5). During both years [K:Si] was elevated in GW compared with hillslope input.

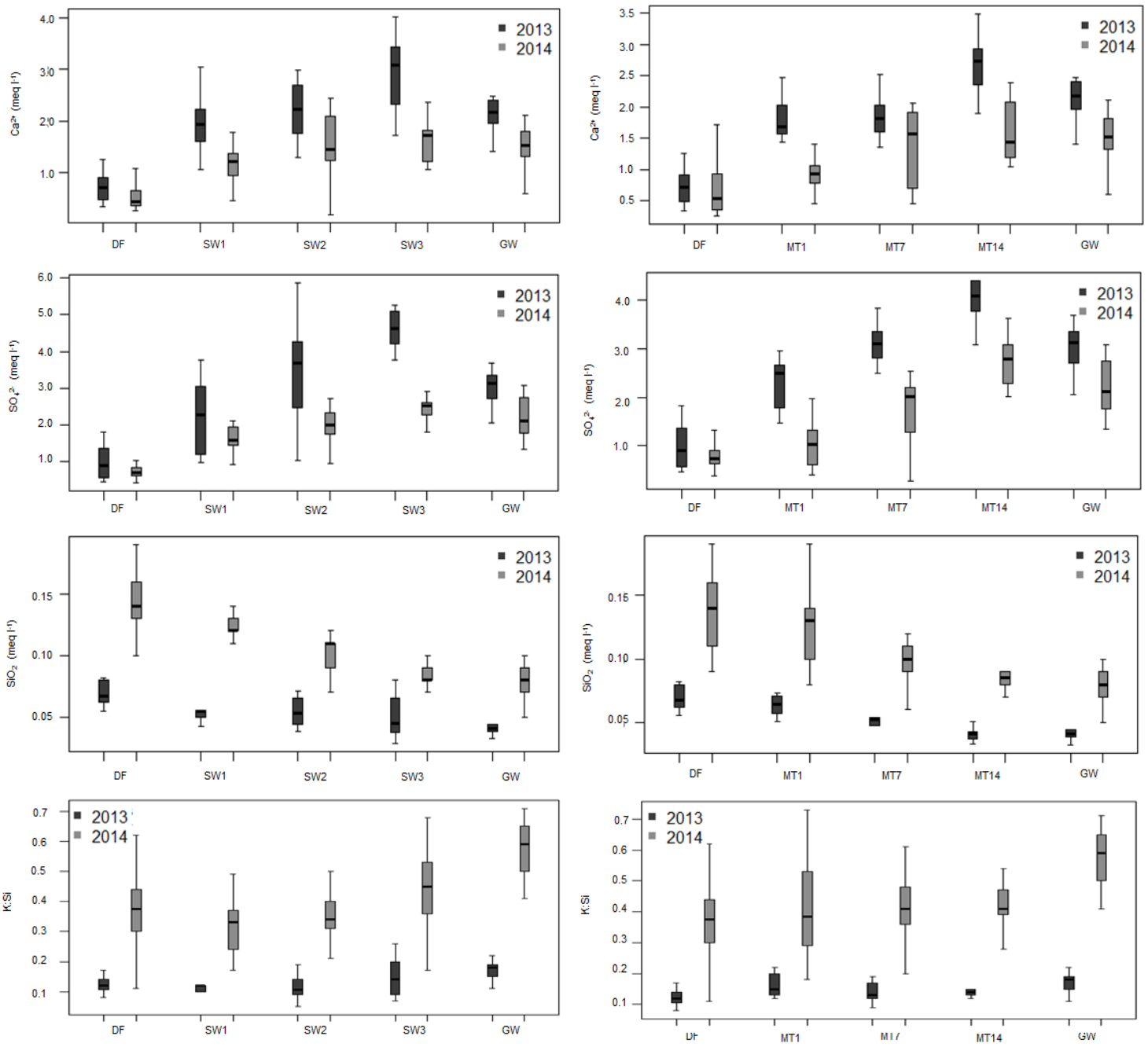

Figure 4.5: Boxplots for selected variables at SW and MT sites for 2013 and 2014, in addition to identified end-members DF and GW

4.5.4 Stable isotope composition of water

Temporal variations in δ^2H for surface water and groundwater sites in 2013 and 2014 are plotted in Figure 4.6. During 2013 there was no statistically significant trend in temporal δ^2H values in surface-water sites, whilst for groundwater there was a trend towards enrichment of δ^2H at MT1 (R^2 = 0.41, p = 0.06) and MT7 (R^2 = 0.59, p = 0.016) during the monitoring period. This trend was more apparent during 2014 in surface water: SW1 (R^2 = 0.61, p = 0.001), SW2 (R^2 = 0.50, p = 0.005), and SW3 (R^2 = 0.45, p = 0.013). It was also observed at GW sites MT7 (R^2 = 0.44, p = 0.01) and MT14 (R^2 = 0.33, p = 0.03). Only at MT1 was the trend not observed where between 24th May and 8th July (JD 144 & 188) there was a significant depletion in δ^2H. After 8th July (JD 188) δ^2H mirrored the behaviour of other GW sites, with a gradual enrichment in δ^2H (R^2 = 0.38, p = 0.08). A clear inter-annual difference in δ^2H is also evident with δ^2H more enriched across all sites during 2014 compared with 2013 (Figure 4.6).

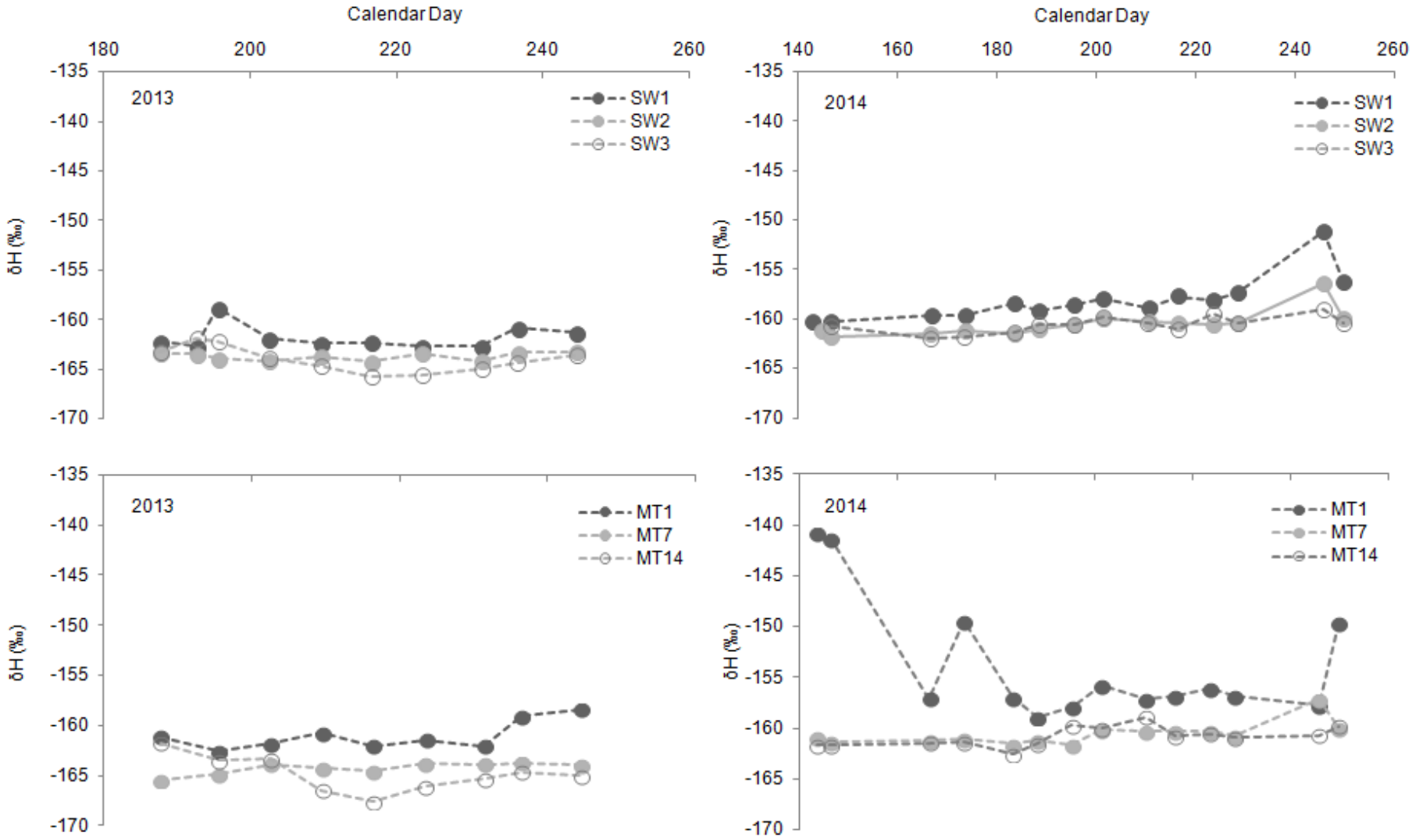

Figure 4.6: Temporal plots for δ^2H at surface water (SW) and groundwater (MT) sites in 2013 and 2014. Sampling period in 2013 was 6th July to 1st September (JD 187 – 244) and in 2014 was 22nd May to 2nd September (JD 142 – 245).

4.5.5 Hydrograph separations

Two-component separations, using sodium as a tracer of flow paths, at sites SW1, SW2, and SW3, were determined for 2013 (Table 4.2 & Figure 4.7) and 2014 (Table 4.3 & Figure 4.8). Mean contribution of DF flow to streams decreased with increasing distances from the hillslope in both years. At SW1 the mean contribution of DF was comparable in both years with values of 15.80% (2013; $\sigma = 7.31$) and 16.00% (2014; $\sigma = 12.00$). In contrast at SW2 and SW3 the mean contribution of DF during the season was slightly lower in 2013 compared to 2014. Mean uncertainty in 2013 (2014) was estimated at ±0.15 (±0.20), ±0.12 (±0.18), and ±0.09 (±0.06) for SW1, SW2, and SW3 respectively. Uncertainty associated with DF flow was greatest at SW1 during both years and declined with distance across the terrace, being lowest at SW3 in both years.

[Na^+]							
Site	**Q_{DF}(m^3 s^{-1})**		**Q_{GW} (m^3 s^{-1})**		**% DF**	**%GW**	
SW1	0.0193	*0.0123*	0.1007	*0.0357*	15.80	84.20	*7.31*
SW2	0.0033	*0.0026*	0.0215	*0.0125*	11.19	88.81	*4.77*
SW3	0.0002	*n.a.*	0.0037	*n.a.*	5.17	94.83	*n.a.*

	Uncertainity (95%)			**Mean uncertainity accounted for (%)**		
Site	**Mean**	**Max.**	**Min.**	**DF**	**GW**	**Stream**
SW1	0.15	0.26	0.08	68.56	30.66	0.79
SW2	0.12	0.15	0.08	56.16	43.04	0.81
SW3	0.09	0.09	0.09	21.24	77.98	0.77

Table 4.2: Mean discharge (Q) and percentage flow contribution for surface water (SW) sites from end-members DF and GW in 2013 (*Standard deviations in italics*). Associated uncertainty values are also presented

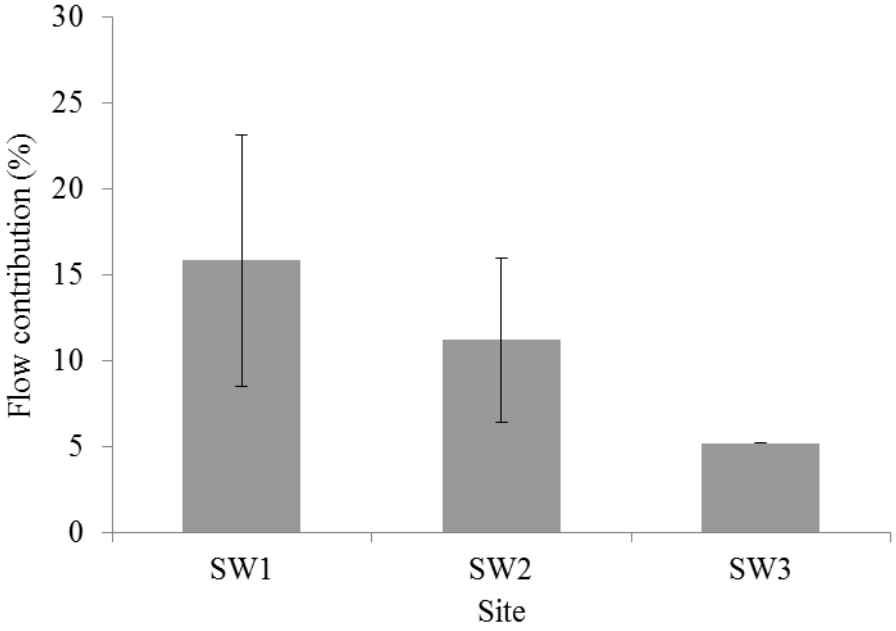

Figure 4.7: Estimated mean percentage flow contribution from end-member DF for surface water (SW) sites in 2013 and associated confidence intervals (standard deviations)

[Na^+]

Site	Q_{DF} (m^3 s^{-1})		Q_{GW} (m^3 s^{-1})		% DF	% GW	
SW1	0.0287	*0.0617*	0.0864	*0.0637*	16.00	84.00	*12.00*
SW2	0.0156	*0.0183*	0.0884	*0.0734*	15.00	85.00	*13.00*
SW3	0.0003	*0.0005*	0.0108	*0.0121*	2.00	98.00	*1.00*

	Uncertainity (95%)			Mean uncertainity accounted for (%)		
Site	**Mean**	**Max.**	**Min.**	**DF**	**GW**	**Stream**
SW1	0.20	0.59	0.07	81.28	18.23	0.49
SW2	0.18	0.61	0.06	75.37	24.11	0.52
SW3	0.06	0.07	0.06	13.66	85.63	0.71

Table 4.3: Two-component hydrograph separation results for 2014. See Table 4.2 caption for further details

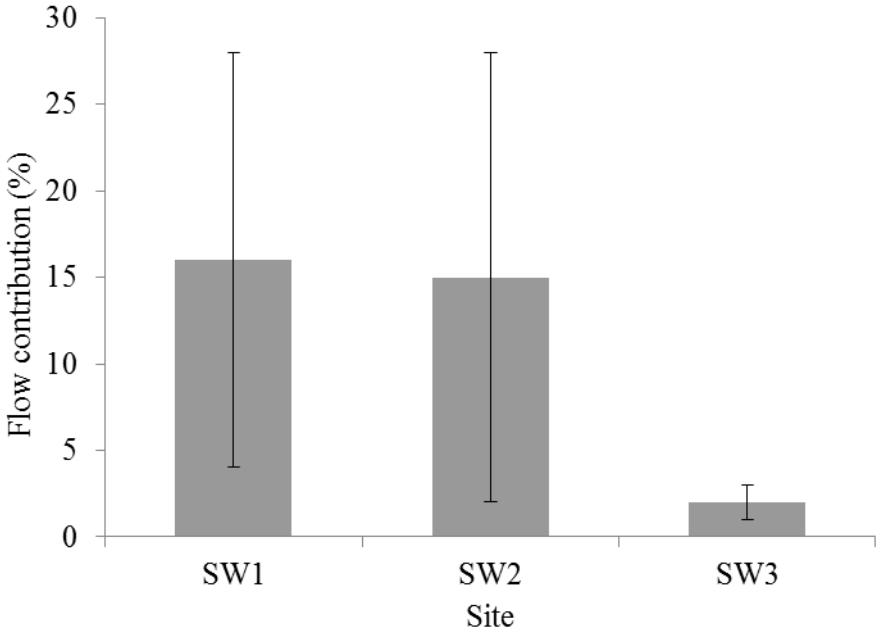

Figure 4.8: Estimated mean flow contribution from DF to surface water (SW) sites in 2014. Confidence intervals based on standard deviations.

4.5.6 Mean residence times

Estimated MRT values for sites SW1, SW2, and SW3, and identified end-members DF and the main glacial river channel (GR) are presented in Table 4.4. A trend towards longer MRT estimates, with increasing distance from the hillslope, was apparent. However, the associated R^2 and p values for these estimates indicate that the estimates are not statistically significant. In contrast statistically significant MRT estimates of 19.5 (R^2 = 026, p = 0.08) and 9.4 (R^2 = 0.49, p = 0.001) months were obtained for DF and GR respectively (Table 4.4).

				MRT			
	C_0	**A**	**Ψ**	**D**	**M**	**R^2**	***p***
Precip	-183.04	61.07	0.49	n.a.	n.a.	n.a.	n.a.
SW1	-154.98	5.60	0.07	631	20.7	0.14	0.214
SW2	-157.98	4.41	0.24	802	26.4	0.10	0.321
SW3	-158.80	3.63	0.57	976	32.1	0.06	0.564
GR	-151.11	12.18	0.14	285	9.4	0.49	0.001
DF	-146.27	5.96	0.01	592	19.5	0.26	0.08

Table 4.4: MRT estimates for SW sites, the main MF Toklat River (GR) and hillslope debris fan (DF). Table includes weighted mean annual measured δ^2H [‰] (C_0), annual amplitude for predicted δ^2H [‰] (A), phase lag [rad] (ψ), MRT estimate in days (D) and months (M), R^2, and p-values.

4.6 DISCUSSION

The results presented here have provided, for the first time, evidence of the direct role of PFPs in hillslope-floodplain connectivity between GW-fed streams and hillslope runoff in paraglacial catchments. Furthermore, the role of colluvial deposits in sustaining streamflow has been shown to be significant. The discussion explores these important findings further and considers their relevance to the conceptual summary developed in Chapter 3.

4.6.1 Hillslope-floodplain connectivity and the role of preferential flow paths

Spatial variation in stream and GW chemistry across the MF Toklat terrace may have been caused by differing geology across the terrace, which would influence the geochemical compositions of individual surface and groundwater sites (Soulsby *et al.*, 2004). However, the terrace was comprised of variations of the same lithofacies (massive, clast-supported gravel deposits; see section 3.5.1), and therefore it is unlikely differences in terrace geology were the cause of spatial variation. Instead it is suggested spatial differences are a strong indicator of the presence of multiple, discrete subsurface flow paths (Malard *et al.*, 1999). Rather than terrace geology it is variation in residence times along individual flow paths and the influence of varying water sources to each flow path which cause differences in geochemical compositions at sites (Ward *et al.*, 1999). This would strongly support the role of PFPs as conduits of flow across the floodplain (Poole *et al.*, 2002).

Furthermore, mean δ^2H values for SW and MT sites in 2013 and 2014 show that flow paths further from the hillslope were more depleted. As a conservative tracer the spatial differences in δ^2H between GW-fed streams highlight that the PFPs which sustain flow to them are connected to differing water sources (Soulsby *et al.*, 2000). Streams are therefore unlikely to have been sustained entirely by an individual water source, indicating that multiple water

sources (i.e. glacial meltwaters, snowmelt, rainfall, and permafrost) provide components of GW-fed stream discharge on the terrace.

A significant difference between 2013 and 2014 was summer precipitation (see section 2.2), with total summer precipitation 118.8 mm higher in 2014. This led to faster recharge of the terrace aquifer and higher groundwater levels on the terrace.. Compared to 2013 both SW and MT sites on the terrace were enriched in δ^2H during 2014. This was caused by higher rainfall levels during summer 2014 which provided an influx of 'new' water (Kirchner, 2003) that led to an increase in hillslope runoff to the terrace. This is evident from mean [δ^2H] values for DF (-150.35‰, σ = 2.21), which was more enriched than GW (-159.67‰, σ = 2.27). Temporal trends towards increasingly enriched [δ^2H] suggest that the GW-recharge which occurred across the terrace was rain-fed or driven, rather than by an increase in glacial meltwater fluxes to the terrace. Otherwise faster recharge of groundwater on the terrace may have been anticipated in 2013, instead of 2014, when mean temperatures were markedly higher (see section 2.2).

Geochemical signatures of SW and GW sites indicate a hillslope-runoff influence on GW-fed discharge across the terrace, and which is more dominant in streams nearest the hillslope. Throughflow on the hillslopes above the terrace was much greater in 2014 due to higher precipitation, indicated by higher [K:Si] values across all sites. Elevated [K:Si] ratios occur as a consequence of increased silicate weathering (Hodson *et al.*, 2002b), reflecting greater flow through the active soil layers on the hillslope; where silicate weathering dominates due to the depletion of carbonate minerals and increasing dominance of feldspar weathering (Clow and Sueker, 2000). Within the younger sediments of the floodplain [Mg^{2+} + Ca^{2+}] vs SO_4^{2-} ratios were predominantly >1 for all sites indicating coupled sulphide oxidation and carbonate dissolution as important weathering reactions. The additional H^+ released by sulphide

oxidation causes further hydrolysis (carbonate dissolution), resulting in elevated concentrations of Ca^{2+} and Mg^{2+} (Anderson, 2007; Cooper *et al.*, 2002). Ca^{2+} and Mg^{2+} dissolution kinetics are more rapid than for monovalent ions (Cooper *et al.*, 2002) and resultantly there is preferential hydrolysis as a consequence of sulphide oxidation (Tranter, 2003a). Therefore elevated [K:Si] ratios and lower Ca^{2+}-SO_4^{2-} in 2014, compared with 2013, suggests a reduction in the relative importance of GW flow from further up-valley on the floodplain, compared with adjacent hillslope input in 2014.

The physicochemical properties of SW and GW sites on the terrace are reflective of the importance of PFPs to GW-fed streams (Chapter 3). Furthermore, spatial variations highlight the importance of hillslope runoff to GW-fed streams, and are therefore suggestive of an important role provided by PFPs in hillslope-floodplain connectivity. In addition inter-annual differences in hydrochemistry indicate that the rate and timing of GW-fed stream recharge in summer months is strongly influenced by hillslope runoff. Along with temporal trends in δ^2H this supports the interpretation that GW-fed stream recharge is rain-fed and driven (see section 3.6.2).

4.6.2 Characterising the hydrological behaviour of colluvial deposits

Spatial variations in sodium and potassium across the terrace reflected the increasing influence of flow from colluvial deposits (DF) at sites nearer the hillslope. DF had much higher sodium and potassium concentrations, due either to increased feldspar weathering in the soil (Clow and Sueker, 2000), or cation exchange of calcium and magnesium with sodium and potassium. DF flow had lower mean EC (475 µS, σ =100), and when more dilute water is in contact with fine grained material exchange of divalent ions from solution for monovalent ions can occur (Tranter, 2003b). With increasing distance from DF across the terrace sulphate,

calcium, and magnesium increased in surface and groundwater. Up-valley GW had higher concentrations of these ions by comparison to DF, due to the presence of younger fluvioglacial deposits, which had not been leached of highly soluble carbonate and sulphide minerals (Anderson, 2007). The dominance of carbonate dissolution and sulphide oxidation in these deposits would explain elevated levels of sulphate, calcium, and magnesium in up-valley GW compared to DF. Spatial patterns in the geochemical composition of SW and GW sites across the terrace indicated flow from DF directly contributed to GW-fed streams on the terrace and that its influence was greatest on streams nearest the floodplain margin. This aligns with previous research which has highlighted colluvial deposits as important conduits of flow (Caballero *et al.*, 2002; Muir *et al.*, 2011; Roy and Hayashi, 2009).

MRT estimates for streamflow from DF (19.5 months; R^2 = 0.26) on the hillslope displayed a reasonable goodness of fit and were comparable with other studies (McGuire and McDonnell, 2006). MRT was estimated as 19.5 months for DF and was indicative of how colluvial deposits act to retain groundwater on valley sides and provide valuable aquifers (Clow *et al.*, 2003; Weekes *et al.*, 2015). In addition the MRT suggests that flow from DF is dominated by 'old' water, which is retained in the system from previous storm events (Buttle, 1994). MRT estimates for GW-fed streams did not provide reasonable goodness of fit from observed streamflow δ^2H signals. Although the sine wave approach is appropriate for sparse spatial and temporal tracer sampling (Tekleab *et al.*, 2014), the sampling period of ~15 months, with large gaps in the sampling record over winter was too short to capture the MRT for GW-fed streams adequately.

Spatial variations in geochemical signatures of SW and GW sites across the terrace have for the first time demonstrated the direct influence of flow paths through colluvial deposits upon GW-fed streams. Furthermore, MRT estimates for DF suggest that colluvial deposits can act

as important aquifers, retaining groundwater on paraglacial hillslopes (Muir *et al.*, 2011) and ensuring its gradual, sustained release to GW-fed streams on the floodplain. This may explain why GW-streams exhibited a non-flashy response to storm events, even though temporal behaviour of δ^2H suggest recharge is rain driven.

4.6.3 Quantifying streamflow contribution from colluvial deposits

The largest contribution to discharge of all streams remained GW flow from up-valley. This was in agreement with the large up-valley $Q_{vertical}$ flux estimated in the terrace water balance analysis (see section 3.5.6). The contribution to streamflow from DF did decline with increasing distance from the hillslope. The estimated mean contribution to discharge for SW1 and SW2 from this single colluvial deposit was >10% during both 2013 and 2014, and could have been as high as 28% at both sites based on 2013 estimates. These estimates align with the work of others which has identified the importance of colluvial deposits to sustaining streamflow in paraglacial catchments (Baraer *et al.*, 2015; Clow *et al.*, 2003; Liu *et al.*, 2004; Muir *et al.*, 2011; Roy and Hayashi, 2009); but which have not directly quantified their contribution to GW-fed streams specifically. Significantly DF accounted for flow from a single colluvial deposit, and there were an additional three colluvial deposits up-valley on the adjacent hillslopes adjacent to the terrace (see section 2.1.1). Therefore the total contribution to discharge of GW-fed streams from colluvial deposits on the valley sides adjacent to the MF Toklat terrace could be substantial.

4.6.4 Colluvial deposit influence on GW-fed streams: implications of shifting hydrological dynamics

This chapter has shown that flow from colluvial deposits on adjacent valley sides could make a significant contribution to GW-fed streams, and that PFPs provide an important role in connecting this flow. Considerations of the long-term implications of alterations in hydrologic

regimes of paraglacial catchments, as a consequence of climate change, has emphasised concerns regarding declining meltwater levels (Baraer *et al.*, 2012; Cable *et al.*, 2011; Finger *et al.*, 2012). However, when focusing specifically on GW-fed streams, particularly on floodplain margins (Lorang and Hauer, 2007), greater attention needs to be given to hillslope runoff and the importance of groundwater retained within colluvial deposits (Gordon *et al.*, 2015). This chapter also provides further evidence to support the interpretation made in Chapter 3 that recharge of GW-fed streams on the terrace is rain-fed, or driven. When considering the long-term stability of GW-fed streams greater attention should be given to shifting precipitation patterns and implications for hillslope runoff (Crossman *et al.*, 2013).

4.7 SUMMARY

The direct contribution of hillslope runoff, and in particular colluvial deposits, to GW-fed streams within paraglacial catchments has not previously been considered in detail. Consequently, the nature of hillslope-floodplain connectivity is largely unknown. Conceptual understanding developed in Chapter 4 suggests that flow from colluvial deposits may make a significant contribution to GW-fed streams and that PFPs may provide a critical role in hillslope-floodplain connectivity.

Spatial variation in surface and groundwater chemistry show the influence of multiple, discrete hydrological pathways across the terrace and has further highlighted the role of PFPs. In addition the spatiotemporal trends in the physicochemical properties of GW-fed streams have shown that hillslope runoff makes a valuable, direct contribution to GW-fed streamflow in the MF Toklat. Colluvial deposits have specifically been identified as an important source, and flow path, supporting GW-fed streams. MRT estimates using δ^2H as a tracer indicated that flow from colluvial deposits is dominated by ‘old’ water and that these deposits represent important aquifers for GW-fed streams within paraglacial catchments. Hydrograph

separations support this finding. Using [Na^+], the results suggest that a single colluvial deposit can contribute up to 28% of the total streamflow for GW-fed streams. Thus when considering the implications of changing water balances in paraglacial environments upon GW-fed stream networks greater consideration needs to be given to the streamflow contribution from colluvial deposits.

The application of geochemical and isotopic tracers at the MF Toklat has validated the conceptual summary developed in Chapter 3. It has identified the importance of flow from colluvial deposits and highlighted the significance of PFPs as conduits for hillslope-floodplain connectivity to GW-fed streams. This improved understanding of the hydrological dynamics and hydrogeomorphic controls supporting GW-fed streams within paraglacial catchments raises additional questions. Particularly the need to establish the key first-order control upon the occurrence of GW-fed streams. Determining whether hydrological dynamics (hillslope runoff) or hydrogeomorphic controls (PFPs) are most important to their long-term stability is critical to understanding the implications of climate change for GW-fed streams. This research gap is addressed in Chapter 5.

CHAPTER 5: FIRST-ORDER CONTROLS ON GROUNDWATER-FED STREAMS AND THEIR LONG-TERM STABILITY IN PARAGLACIAL CATCHMENTS

5.1 SCOPE OF CHAPTER

Chapters 3 and 4 focused on developing conceptual understanding of the hydrological connectivity and dynamics supporting GW-fed streams on paraglacial floodplains. PFPs were found to be important in controlling the occurrence of GW-fed streams and had an important role in hillslope-floodplain connectivity (Chapter 3). Hillslope runoff was identified as an important source of flow to GW-fed streams (Chapter 3 and 4), and colluvial deposits on valley sides were shown to account for significant water storage and conduits of hillslope runoff to GW-fed streams (Chapter 4).

This chapter aims to develop upon the conceptual understanding established and considers the first-order controls upon GW-fed streams occurrence. These have not previously been considered and remain a significant research gap. An intra-catchment scale study of GW-fed streams within DNPP was conducted to; (1) consider if PFPs were a persistent occurrence where GW-fed streams formed; (2) establish if hillslope runoff contribution to GW-fed streams was universal; and (3) outline the sensitivity of GW-fed streams to climate change given first-order controls.

The results presented in this chapter highlight the importance of PFPs as a first-order control upon GW-fed streams in paraglacial environment and raise questions about their long-term stability given anticipated impacts of glacial retreat upon PFPs. In addition the chapter demonstrates the importance of hillslope runoff, particularly flow through colluvial deposits, the significance of which is considered in the context of anticipated short to medium-term climate change.

5.2 INTRODUCTION

Within paraglacial catchments GW-fed streams have long been regarded as valuable riverine habitat patches (Tockner *et al.,* 2009; Ward *et al.,* 2002), that are both aquatic and terrestrial biodiversity hotspots (Crossman *et al.,* 2011). GW-fed streams on paraglacial floodplains are intrinsically linked to the presence of paleochannels (PFPs) (Stanford and Ward, 1993) and occur where these hydrogeomorphic structures intersect the floodplain surface (Caldwell *et al.,* 2015; Poole *et al.,* 2002; Poole *et al.,* 2006). Paleochannels infilled with deposits of high hydraulic conductivity (*K*) (Klingbeil *et al.*, 1999; Larned, 2012) are associated with strong vertical hydraulic gradients (Chapter 3), thus making them important PFPs across paraglacial floodplains. The importance of PFPs to GW-fed streams has been further identified by studying spatiotemporal differences in the geochemical and isotopic signatures of individual streams within GW-fed stream networks (Chapter 4). This has further highlighted their role as multiple, discrete subsurface flow pathways.

Geochemical and isotopic tracers have also highlighted PFPs as providing an important role in hillslope-floodplain connectivity (Poole, 2010) within paraglacial catchments (Chapter 4). This allows hillslope runoff to make an important contribution to the recharge of GW-fed streams alongside upstream meltwater components (Chapter 3 & 4). In particular Chapter 4 demonstrated the direct influence of flow from adjacent valley side colluvial deposits on GW-fed streams. Colluvial deposits are prevalent in paraglacial environments (Ballantyne, 2002b) and may constitute valuable aquifers in paraglacial systems which can retain, delay, and sustain the release of hillslope runoff to the floodplain (Baraer *et al.,* 2015; Caballero *et al.,* 2002; Clow *et al.,* 2003; Gordon *et al.,* 2015; Liu *et al.,* 2004; Muir *et al.,* 2011; Weekes *et al.,* 2015).

New understanding developed in Chapter 3 and 4 can be synthesised as; (1) having outlined the importance of PFPs to connecting GW-fed streams with hillslope runoff; and (2) identifying adjacent hillslope runoff as an important source of flow alongside up-valley groundwater (including a glacial meltwater component). However, we cannot currently ascertain if there is a key first-order control (Buttle, 2006; Devito *et al.*, 2005) upon GW-stream occurrence. This is a significant research gap given that PFPs and hillslope runoff (rain- and snow-fed) are sensitive to the implications of anthropogenic climate change in paraglacial catchments (Barnett *et al.*, 2005; Micheletti *et al.*, 2015; Zemp *et al.*, 2015). Declining downstream sediment loads due to continued deglaciation (Church and Ryder, 1972; Geilhausen *et al.*, 2013) will reduce channel avulsion processes which could have serious implications for the long-term stability of PFPs (and associated GW-fed streams; see section 3.6.4) (Poole *et al.*, 2002). Shifts in the hydrologic regimes of paraglacial catchments will lead to reduced winter snowpack, earlier snowmelt, and changes in the nature of summer precipitation (Nolin, 2012; Stewart, 2009) with implications for hillslope runoff (Carey *et al.*, 2013). These hydrological changes will place a greater emphasis on the capability of colluvial deposits to act as groundwater stores for hillslope runoff (Hood and Hayashi, 2015).

This chapter aims to address this research gap by establishing the first-order controls upon GW-stream occurrence within paraglacial floodplains. Furthermore, it considers the sensitivity of GW-fed streams to climate change through an intra-catchment scale study of GW-fed streams within DNPP. The objectives of the study were to: (1) establish if the occurrence of perennial GW-fed streams is connected to the persistent presence of PFPs; (2) determine if the direct contribution of hillslope runoff to GW-fed streams is universal at an intra-catchment scale; and (3) consider whether climate change impacts on PFPs or hillslope runoff will be more detrimental to the long-term stability of GW-fed streams.

5.3 FIELD SITES

An intra-catchment scale study was conducted between May and September 2014 in DNPP at four field sites; Middle Fork (MF) Toklat, East Fork Toklat (EF), Teklanika (Tek), and Gorge Creek (GC). Further details on all field sites are provided in section 2.1.

5.4 METHODOLOGY

Hydrometric monitoring was carried out at all field sites (see section 2.3.3) for the duration of the field season. In addition an extensive program of surface water, groundwater, and end-member sampling was carried out across all sites (see sections 2.3.4.1 - 2.3.4.4). Details on geochemical properties and stables isotopes measured, sampling protocol, and laboratory analysis are outlined in section 2.3.4. Principal component analysis (PCA) was applied to geochemical data collected for all field sites. PCA has been successfully utilised by others to breakdown multivariate data sets of geochemical properties and distinguish flow paths (Gordon *et al.*, 2015). Further details are provided in section 2.4.4. Two-component hydrograph separations were also used to establish hillslope runoff from adjacent valley-sides at all field site (see section 2.4.2).

5.5 RESULTS

5.5.1 Groundwater behaviour

Precipitation and GW levels for MF Toklat, EF, and Tek are presented in Figure 5.1. Precipitation data were obtained from an automated weather station on the MF Toklat (see section 2.2). At all sites GW was characterised by steady levels and exhibited non-flashy behaviour in response to storm events. Across all terraces GW levels were most consistent nearest valley sides. At EF and Tek a response in GW to certain storm events was observed at locations furthest from the valley side (MT3). The largest response in GW levels occurred between 25th and 27th June (JD 176 – 178) when 62.5 mm of precipitation was recorded in less than 72 hours. GW levels rose by 0.24 m and 0.31 m at MT3 for EF and Tek respectively (Figure 5.1). However, as the mean specific yield (S_y) for terrace sediments sampled on the MF Toklat (see section 2.3.1) was 29% (σ = 6%), such a response can be regarded as minimal, and reflecting the unresponsive nature of these systems to flashy storm events. Finally across all sites there was a clear spike GW levels on 2nd September (JD 245) which was in response to a late snowfall, and subsequent melt, event on 29th August (JD 241) (Figure 5.1).

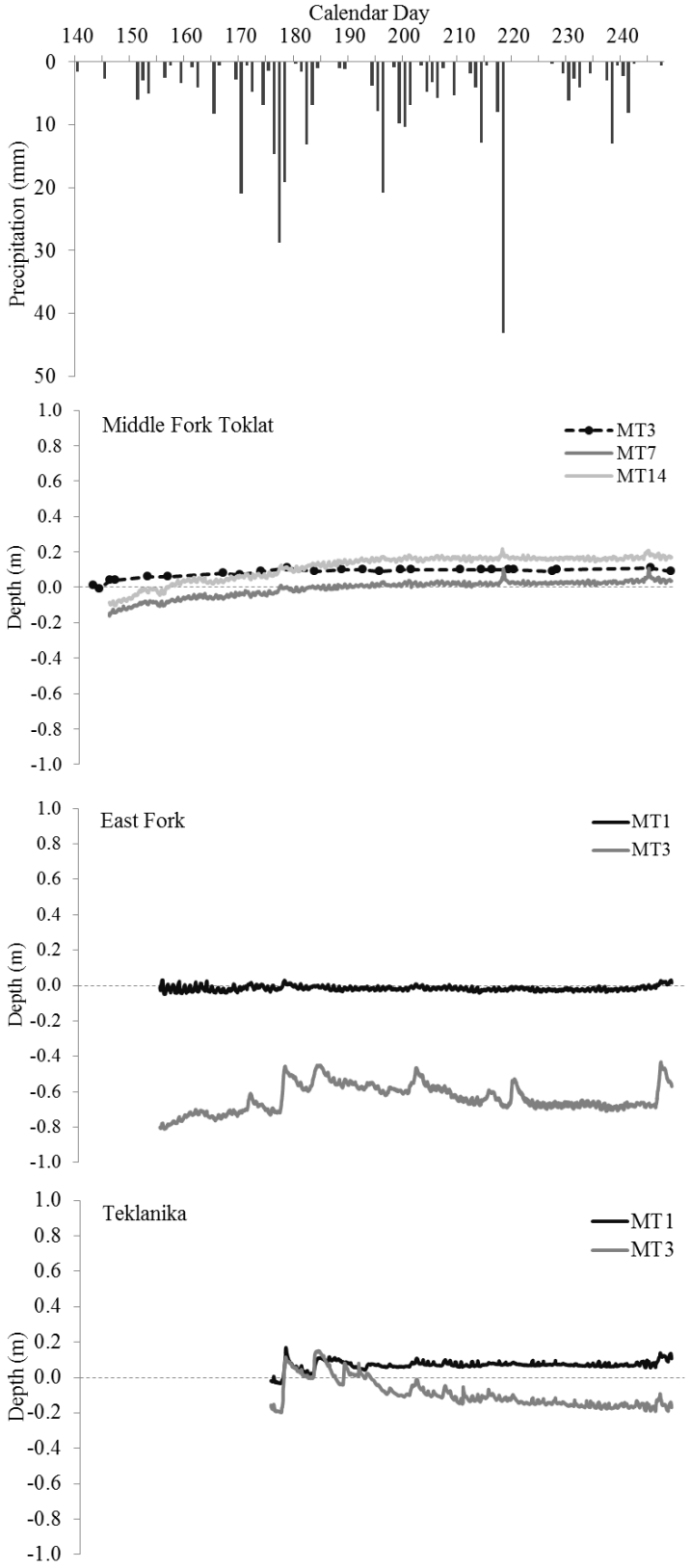

Figure 5.1: Total daily precipitation and groundwater levels at sites; Middle Fork (MF) Toklat, East Fork (EF), and Teklanika (Tek). GW levels inferred from pressure transducers at all locations with the exception of MT3 at MF Toklat, where manual spot measurement are presented.

5.5.2 Geochemical and isotopic signatures of terrace waters

5.5.2.1 Spatial observations

Bicarbonate was the dominant solute for both SW and MT locations at all sites (Figure 5.2). At MF Toklat sulphate concentrations were also high, unlike at Tek and EF where concentration in SW and GW were lower. Calcium and magnesium concentrations were comparable at EF, whereas at MF Toklat and Tek magnesium concentrations were much greater than calcium (Figure 5.2). A pattern observed in mean values of these solutes (Table 5.1). The influence of sodium and potassium upon the chemical composition of SW and GW was much greater at EF and Tek compared to MF Toklat (Figure 5.2). The least spatial variation in chemical composition between SW and MT was observed at EF (Figure 5.2). There is a clear difference in the geochemical signals of MT2 and MT3 at Tek compared to other MT and SW locations (Table 5.1). MT1 and SW locations at Tek had higher concentrations of sodium and potassium, while there was a shift towards elevated concentrations of calcium and magnesium at MT2 and MT3.

Spatial patterns in silica were replicated for both SW and MT locations at MF Toklat, EF, and Tek (Figure 5.3). Silica declined with increasing distance from the valley side across terraces. The exception was SW3 at Tek which displayed elevated silica (Figure 5.3). Across MF Toklat declines in mean silica for SW (0.036 meq l^{-1}) and MT (0.037 meq l^{-1}) were comparable. At EF the decline in mean silica was 33% greater in SW (0.049 meq l^{-1}) compared to MT (0.033 meq l^{-1}). Spatial variance was confirmed by differences in seasonal mean values, and was not limited to these variables, with other measured physicochemical properties also exhibiting spatial variation (Table 5.1).

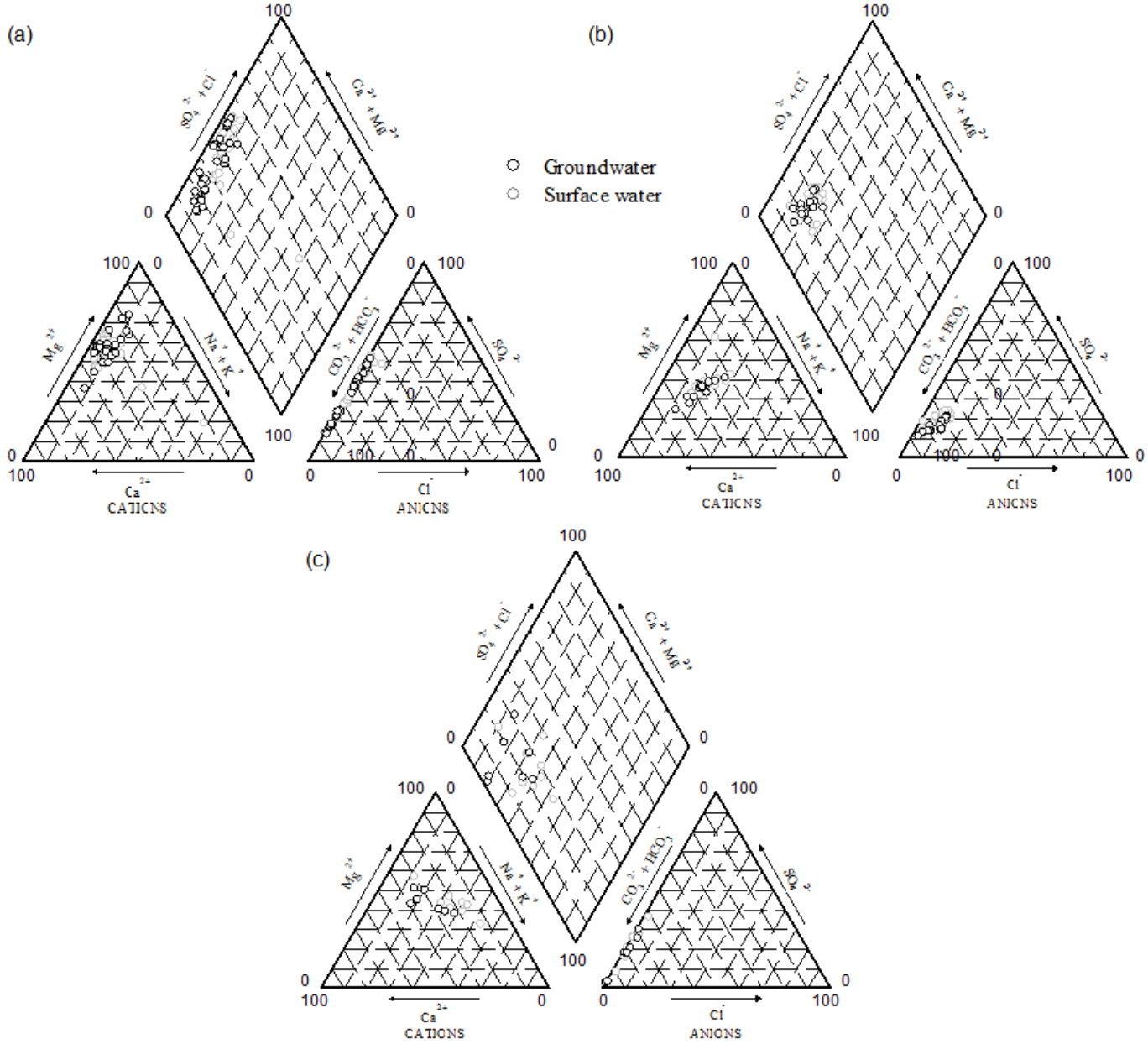

Figure 5.2: Piper plots for groundwater (MT) and surface water (SW) locations at sites (a) Middle Fork (MF) Toklat, (b) East Fork (EF), and (c) Teklanika (Tek)

	Na^+		K^+		Mg^{2+}		Ca^{2+}		SO_4^{2-}		SiO_2		δ^2H	
	(meq l^{-1})	σ	(meq l^{-1})	σ	(meq l^{-1})	σ	(meq l^{-1})	σ	(meq l^{-1})	σ	(meq l^{-1})	σ	(‰)	σ
MF Toklat														
SW1	**0.44**	*0.21*	**0.07**	*0.11*	**2.00**	*0.55*	**1.15**	*0.36*	**1.66**	*0.54*	**0.12**	*0.01*	**-158.10**	*2.30*
SW2	**0.41**	*0.22*	**0.04**	*0.01*	**2.15**	*0.82*	**1.54**	*0.63*	**2.02**	*0.49*	**0.10**	*0.02*	**-160.48**	*1.31*
SW3	**0.15**	*0.06*	**0.04**	*0.01*	**2.69**	*1.03*	**1.52**	*0.53*	**2.50**	*0.35*	**0.08**	*0.01*	**-160.58**	*0.84*
MT1	**0.35**	*0.13*	**0.05**	*0.02*	**2.01**	*0.56*	**0.99**	*0.35*	**1.23**	*0.35*	**0.12**	*0.03*	**-153.75**	*6.06*
MT7	**0.32**	*0.10*	**0.04**	*0.01*	**2.00**	*0.65*	**1.43**	*0.47*	**1.76**	*0.50*	**0.10**	*0.02*	**-160.57**	*0.97*
MT14	**0.17**	*0.18*	**0.04**	*0.01*	**2.50**	*0.63*	**1.62**	*0.59*	**2.73**	*0.62*	**0.09**	*0.02*	**-160.80**	*1.11*
East Fork														
SW1	**0.46**	*0.14*	**0.03**	*0.01*	**1.08**	*0.77*	**0.79**	*0.20*	**0.62**	*0.17*	**0.16**	*0.02*	**-156.83**	*2.86*
SW2	**0.33**	*0.10*	**0.03**	*0.01*	**0.70**	*0.17*	**1.04**	*0.23*	**0.61**	*0.12*	**0.12**	*0.02*	**-158.10**	*1.18*
SW3	**0.41**	*0.20*	**0.03**	*0.01*	**0.84**	*0.36*	**0.87**	*0.35*	**0.87**	*0.09*	**0.11**	*0.01*	**-158.63**	*2.20*
MT1	**0.41**	*0.19*	**0.03**	*0.01*	**0.75**	*0.32*	**0.80**	*0.27*	**0.55**	*0.10*	**0.14**	*0.02*	**-157.68**	*1.70*
MT2	**0.40**	*0.15*	**0.04**	*0.01*	**0.78**	*0.27*	**0.96**	*0.31*	**0.78**	*0.13*	**0.13**	*0.01*	**-158.35**	*1.27*
MT3	**0.41**	*0.15*	**0.05**	*0.05*	**0.77**	*0.27*	**1.25**	*0.20*	**0.66**	*0.22*	**0.10**	*0.02*	**-159.24**	*4.25*
Teklanika														
SW1	**1.45**	*0.49*	**0.03**	*0.01*	**1.66**	*0.47*	**1.03**	*0.25*	**0.94**	*0.39*	**0.16**	*0.02*	**-158.15**	*0.92*
SW2	**1.64**	*0.28*	**0.04**	*0.01*	**2.15**	*0.13*	**1.02**	*0.19*	**1.89**	*0.58*	**0.15**	*0.01*	**-157.71**	*0.62*
SW3	**2.02**	*1.39*	**0.03**	*0.01*	**1.56**	*0.84*	**0.54**	*0.27*	**1.94**	*0.34*	**0.19**	*0.01*	**-157.60**	*0.60*
MT1	**1.33**	*0.51*	**0.03**	*0.01*	**1.58**	*0.58*	**0.95**	*0.33*	**1.29**	*0.21*	**0.16**	*0.01*	**-158.48**	*0.88*
MT2	**0.49**	*0.10*	**0.04**	*0.01*	**1.51**	*0.25*	**1.00**	*0.27*	**1.62**	*0.46*	**0.12**	*0.04*	**-155.65**	*1.31*
MT3	**0.35**	*0.31*	**0.02**	*0.01*	**0.85**	*0.72*	**0.76**	*0.46*	**0.49**	*0.49*	**0.11**	*0.01*	**-157.52**	*1.82*

Table 5.1: Mean (**in bold**) and standard deviation (σ) values for selected geochemical and isotopic compositions for surface water (SW) and groundwater (MT) locations at sites MF Toklat, East Fork, and Teklanika

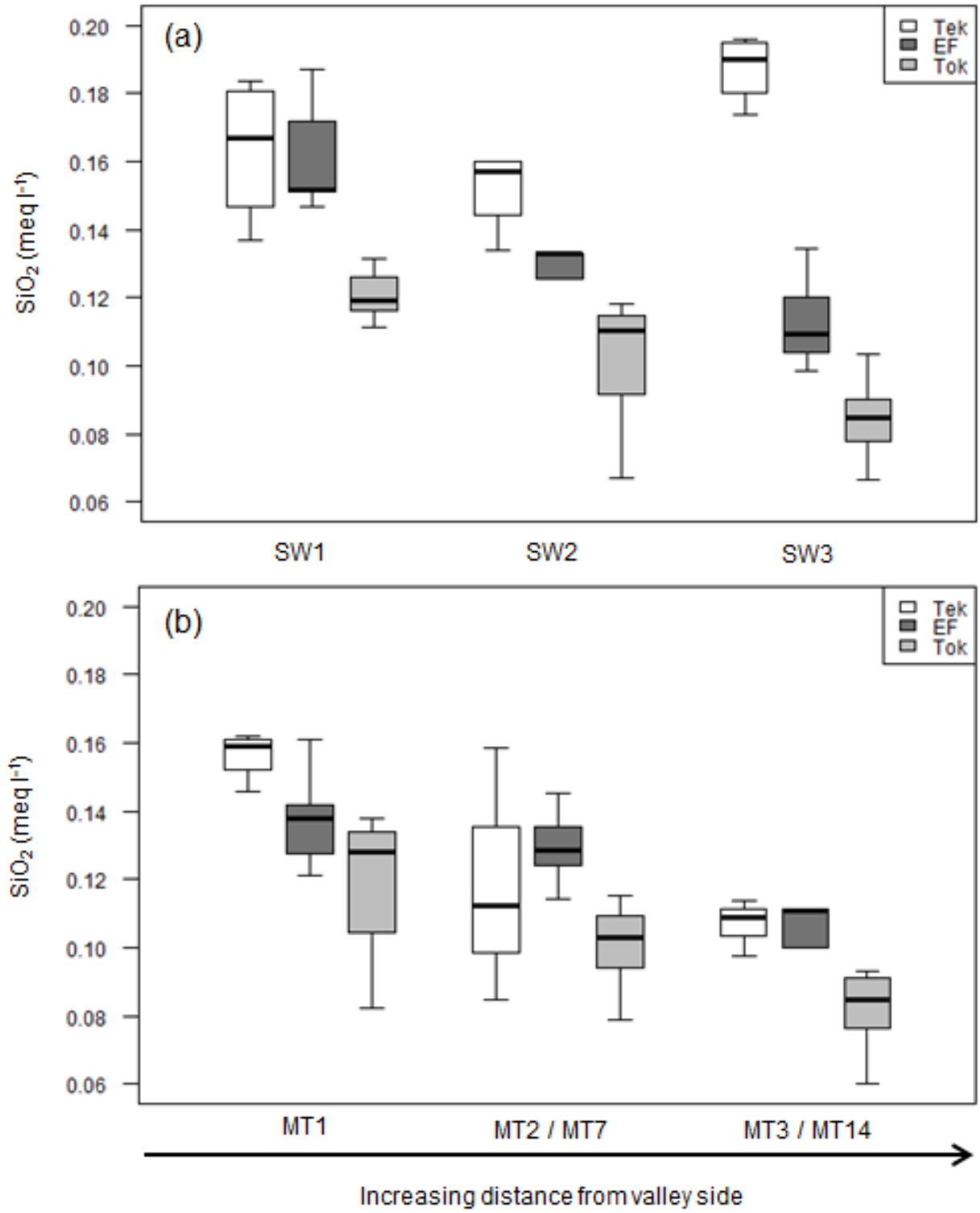

Figure 5.3: Spatial variation in silica (SiO_2) for (a) surface water (SW) and (b) groundwater (MT) locations at MF Toklat, East Fork, and Teklanika sites

5.5.2.2 Temporal trends

At MF Toklat MT1 (n = 14; p = 0.06; R^2 = 0.28) and MT7 (n = 14; p = 0.01; R^2 = 0.45) exhibited a seasonal trend towards increasing nitrate concentrations (Figure 5.4). This trend was replicated for MT1 at Tek (n = 4; p = 0.03; R^2 = 0.94). No seasonal trend in nitrate was observed at EF. At Tek there was a clear spatial difference with higher nitrate concentrations for MT1, in contrast to MT2 and MT3, which had comparable levels (Table 5.1). Figure 5.4 visibly highlights spatial patterns in nitrate and δ^2H at all sites. SW δ^2H signatures became more depleted with increasing distance from the valley side at MF Toklat and EF (Table 5.1). Similarly nitrate was elevated at MT locations nearest the valley sides at EF and Tek.

δ^2H for individual SW locations at MF Toklat showed a statistically significant ($p < 0.05$) seasonal trend towards isotopically lighter compositions (Figure 5.4). A trend replicated at SW1 at EF (n = 5; $p < 0.05$; R^2 = 0.90). For all sites a spike in δ^2H occurred after 28th August (JD 240), coinciding with a late snowfall and subsequent melt event. The spike was greater for SW locations at MF Toklat and EF, compared to a dampened signal observed at Tek (Figure 5.4). At MF Toklat the greatest change in δ^2H was observed at SW locations nearest the valley side, with the spike in δ^2H dampened with increasing distance from the hillslope. In contrast at EF large spikes were observed for SW locations across the full extent of the terrace while at Tek δ^2H for SW locations merged to the same value.

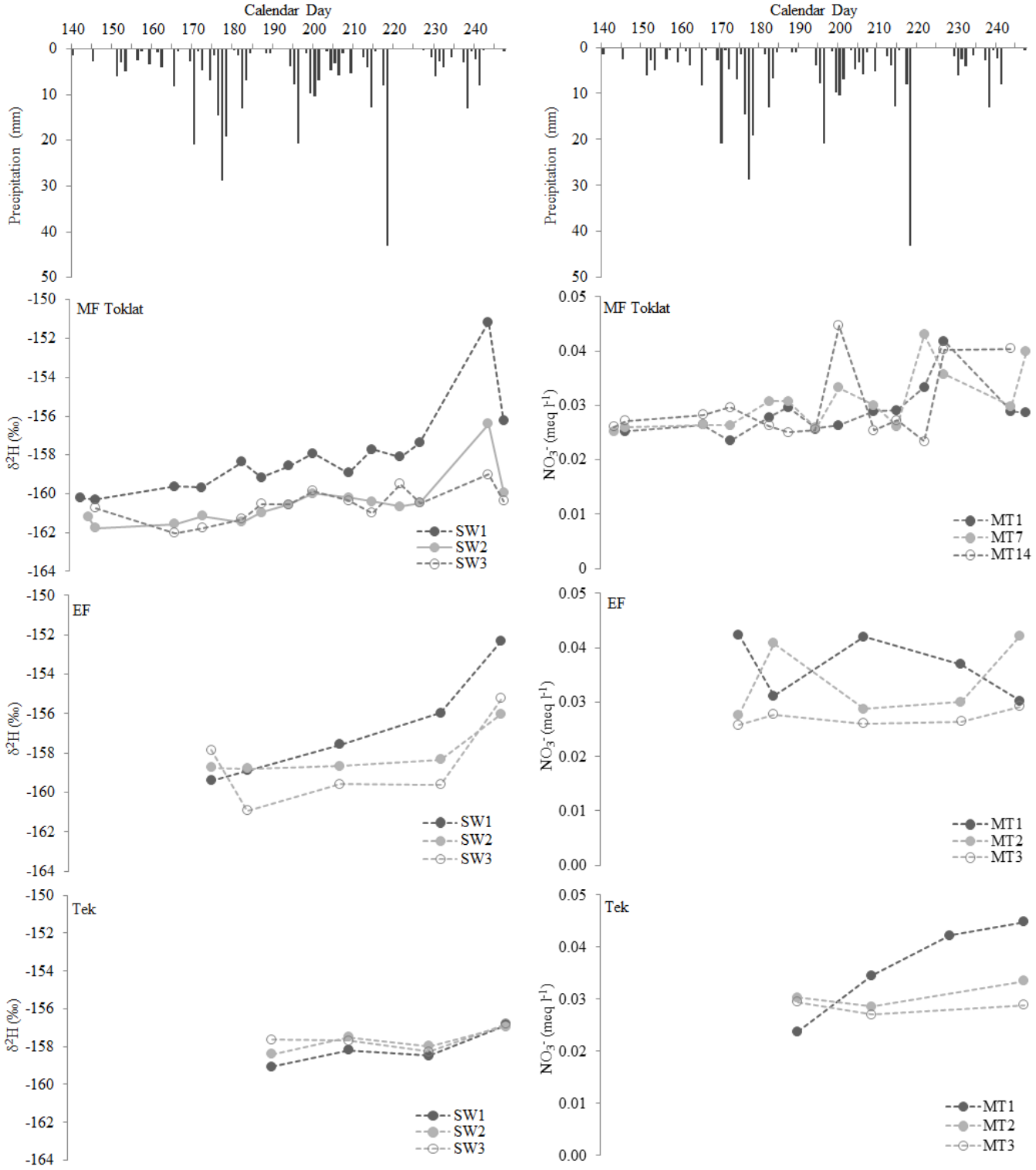

Figure 5.4: Total daily precipitation and temporal response of δ^2H at surface water (SW) and nitrate (NO_3^-) at groundwater (MT) locations for MF Toklat, EF, and Tek. Linear trends in seasonal response of δ^2H observed at MF Toklat for SW1 (R^2 = 0.61; p = 0.001), SW2 (R^2 = 0.50; p = 0.005), and SW3 (R^2 = 0.44; p = 0.013); and at EF for SW1 (R^2 = 0.90; p = 0.013). Linear trends in seasonal response of NO_3^- observed at MF Toklat for MT1 (R^2 = 0.28; p = 0.06) and MT7 (R^2 = 0.45; p = 0.01) and at Tek for MT1 (R^2 = 0.94; p = 0.03)

5.5.3 Principal component analysis

PCA was conducted for all sites, including GC. Variable plots (Figure 5.5) indicate significant differences in the geochemical signals and influences between sites. A full summary of individual variable correlations for PC1 and PC2 is provided in Table 5.2.

5.5.3.1 Variable plots

At MF Toklat (Figure 5.5a) there was a strong negative correlation along PC1 for silica (R^2 = -0.82; $p < 0.001$) and sodium (R^2 = -0.80; $p < 0.001$). This contrasted with a strong positive correlation along PC1 for magnesium (R^2 = 0.87; $p < 0.001$), sulphate (r^2 = 0.81; $p < 0.001$), and calcium (R^2 = 0.81; $p < 0.001$). Chloride (R^2 = 0.75; $p < 0.001$) and nitrate (R^2 = 0.83; $p < 0.001$) exhibited a strong positive correlation with PC2. Sodium (R^2 = 0.90; $p < 0.001$), magnesium (R^2 = 0.87; $p < 0.001$), potassium (R^2 = 0.82; $p < 0.001$), and calcium (R^2 = 0.79; $p < 0.001$) displayed strong positive relationships with PC1 at EF (Figure 5.5b). PC2 was positively correlated with silica (R^2 = 0.90; $p < 0.001$) and negatively with sulphate (R^2 = -0.43; $p < 0.05$).

PC1 at Tek was strongly positively correlated with sodium (R^2 = 0.85; $p < 0.001$) and potassium (R^2 = 0.81; $p < 0.001$), which were closely grouped, in addition to silica (R^2 = 0.81, $p < 0.001$) (Figure 5.5c). Magnesium (R^2 = 0.84; $p < 0.001$) and calcium (R^2 = 0.75; $p < 0.001$) aligned with a strong positive correlation along PC2, while nitrate (R^2 = -0.75; $p < 0.001$) was negatively correlated. Finally at GC magnesium (R^2 = 0.87; $p < 0.001$), calcium (R^2 = 0.61; $p < 0.004$) were positively correlated along PC1 (Figure 5.5d). Silica (R^2 = -0.87; $p < 0.001$) showed strong negative correlation along PC1. Sodium (R^2 = 0.81; $p < 0.001$) and chloride (R^2 = 0.79; $p < 0.001$) were positively correlated with PC2, while sulphate (R^2 = -0.76; $p < 0.001$) exhibited negative correlation.

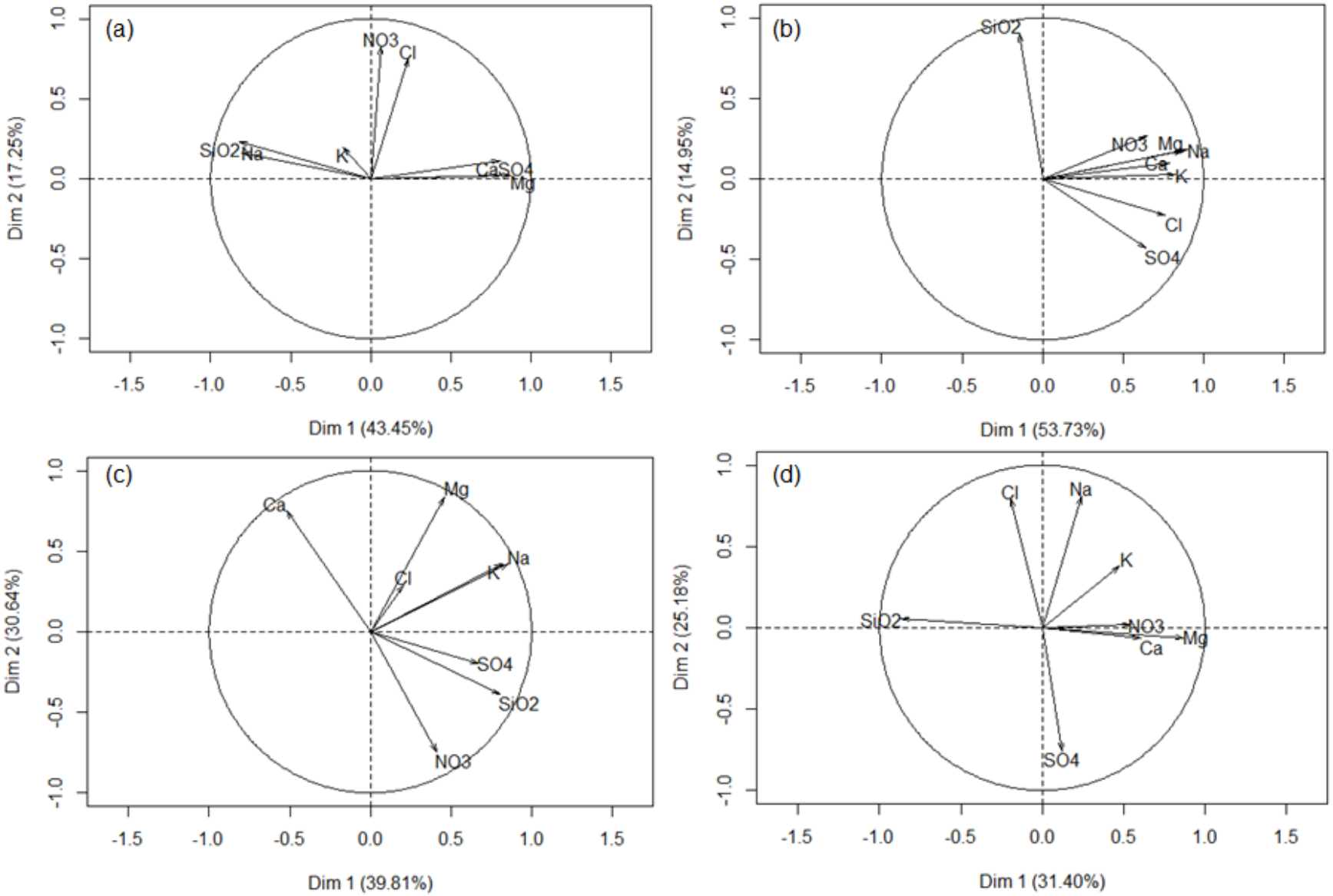

Figure 5.5: Variable plots for individual variables at sites; (a) Middle Fork (MF) Toklat; (b) East Fork (EF); (c) Teklanika (Tek);, and (d) Gorge Creek (GC). Principal Component (PC)1 (Dim1) and PC2 (Dim2) are presented with percentages indicated total variance explained by respective principal components

Site	PC1	R^2	*p* value	PC2	R^2	*p* value
MF Tok						
	Mg^{2+}	0.87	0.00E+00	NO_3^-	0.83	0.00E+00
	SO_4^{2-}	0.81	0.00E+00	Cl^-	0.75	0.00E+00
	Ca^{2+}	0.81	0.00E+00	SiO_2	0.23	2.88E-02
	Cl^-	0.24	2.45E-02			
	Na^+	-0.80	1.60E-21			
	SiO_2	-0.82	2.37E-23			
EF						
	Na^+	0.90	9.06E-12	SiO_2	0.90	9.52E-12
	Mg^{2+}	0.87	3.34E-10	SO_4^{2-}	-0.43	1.71E-02
	K^+	0.82	2.69E-08			
	Ca^{2+}	0.79	2.59E-07			
	Cl^-	0.76	1.10E-06			
	NO_3^-	0.65	1.08E-04			
	SO_4^{2-}	0.64	1.35E-04			
Tek						
	Na^+	0.85	1.85E-06	Mg^{2+}	0.84	4.61E-06
	K^+	0.81	1.22E-05	Ca^{2+}	0.75	1.35E-04
	SiO_2	0.81	1.83E-05	NO_3^-	-0.75	1.45E-04
	SO_4^{2-}	0.67	1.14E-03			
	Mg^{2+}	0.46	4.16E-02			
	Ca^{2+}	-0.52	1.92E-02			
GC						
	Mg^{2+}	0.87	3.03E-07	Na^+	0.81	8.35E-06
	Ca^{2+}	0.61	3.57E-03	Cl^-	0.79	1.77E-05
	NO_3^-	0.54	1.15E-02	SO_4^{2-}	-0.76	7.00E-05
	K^+	0.48	2.90E-02			
	SiO_2	-0.87	2.89E-07			

Table 5.2: Complete list of *P*-values and associated R^2 values at each site for individual variables along PC1 and PC2. Where *P-values* are listed as zero returned numbers were infinitesimally small.

5.5.3.2 Individuals plots

Individual plots and associated centroids are presented in Figure 5.6. At MF Toklat centroids were predominantly along PC1, with little deviation to PC2 (Figure 5.6a). Valley side flow (DF and HF) plotted along the negative PC1 axis, indicating the strong influence of silica and sodium. These end members had contrasting temporal behaviour, with DF showing the growing importance of sodium, silica, nitrate, and chloride, while HF displayed the reverse trend (Figure 5.6). In contrast SW locations on the terrace exhibited a greater influence of magnesium, calcium, and sulphate. SW1 and SW2, streams nearer the valley side, displayed greater influence of valley side end members; nitrate and chloride.

At EF the end member HS and SW1 showed the influence of silica on the positive PC2 axis. Sulphate exerted a larger control on SW2 and SW3 (Figure 5.6b). Upstream GW was weighted towards sodium, magnesium, calcium, and potassium on the positive PC1 axis. Temporal trends were prominent for SW1 and SW2, which showed an increasing influence of sodium, magnesium, potassium, calcium, nitrate and silica, along with declining significance of sulphate during the season (Figure 5.6b). Upstream GW exhibited an increasing importance of silica and declining influence of sulphate. At Tek HS was dominated by calcium (Figure 5.6c). SW2 was influenced by both calcium and magnesium, while SW1, SW3, and the main glacial river channel (Tek) exhibited the increasing influence of sodium, potassium, silica, and sulphate. Temporally SW1 and SW2 were increasingly influenced by nitrate and calcium throughout the season (Figure 5.6c).

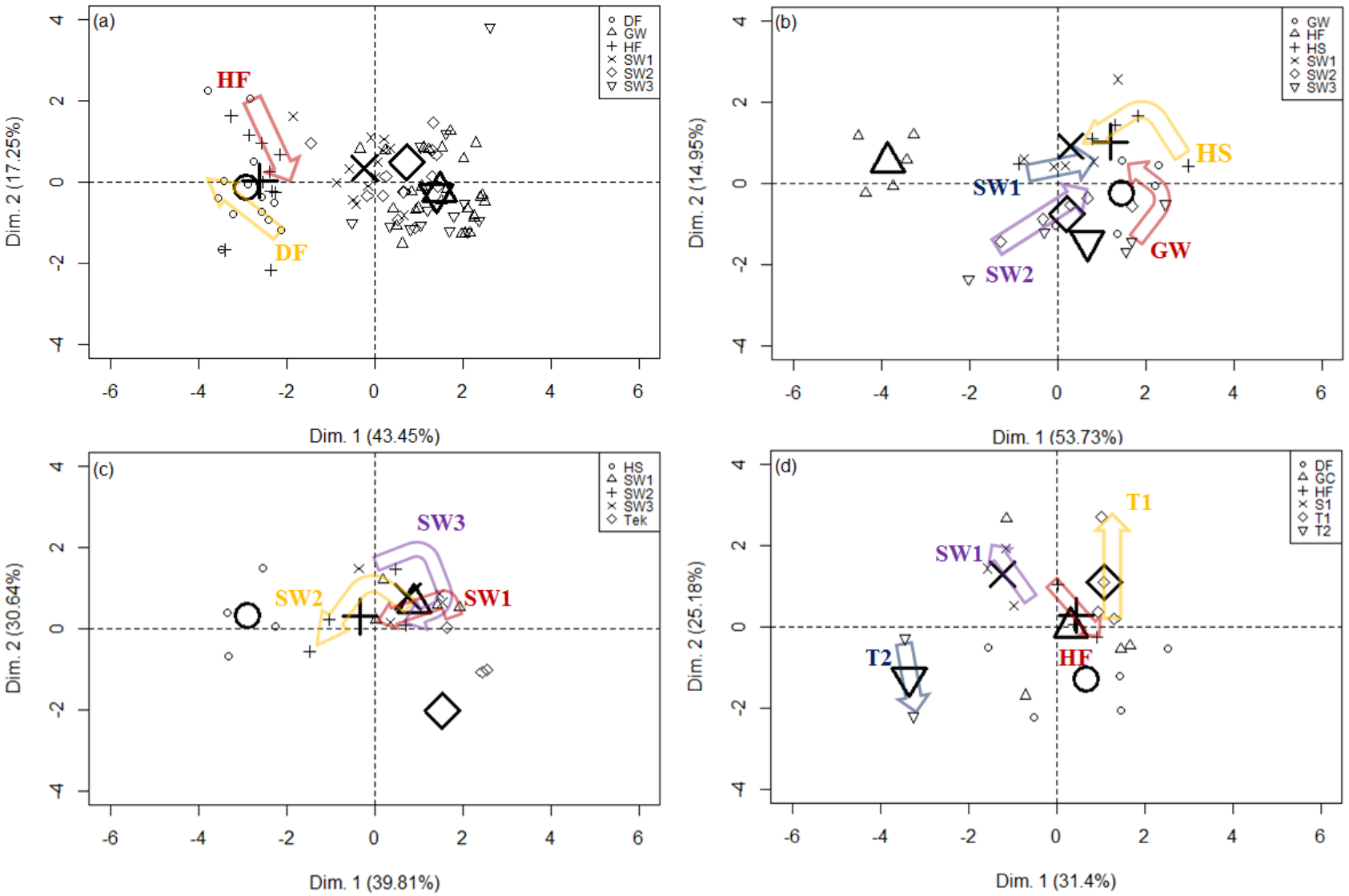

Figure 5.6: Individuals plots for sites (a) MF Toklat, (b) EF, (c) Tek, and (d) GC. Large symbols in bold are centroids for individual sample locations (e.g. SW1). Identified end members at sites included debris fans (DF), hillslope flow (HF), hillslope springs (HS), groundwater (GW). At (c) the main Teklanika River (Tek) was included and at (d) Gorge Creek (GC). Labelled arrows indicate temporal movement of individual locations over the season at sites where observed.

SW1 and T1 at GC were influenced by sodium and chloride (Figure 5.6d). SW1 was also influenced by silica and T1 by magnesium and calcium. Nitrate and chloride influence at T1 increased during the season, with a decline in the importance of sulphate. T2 was dominated by silica, with sulphate exerting increased influence later in the season. Finally, the end member HF was progressively influenced by nitrate, magnesium, and calcium throughout the season (Figure 5.6d).

5.5.4 Valley side flow contribution

The lowest uncertainties for two-component hydrograph separations were associated with MF Toklat and GC, reflecting better identification of end-members at these sites (Table 5.3). Across all sites the contributions to SW and MT at individual locations are broadly comparable (Figure 5.7). At MF Toklat, where flow from a single colluvial deposit was identified, estimated contributions to streamflow were lower than at any other site and there was a clear spatial decline in estimated valley side contribution with increasing distance across the terrace (Figure 5.7a). This trend was not replicated at other sites. Contributions to flow from a single colluvial deposit were much greater at GC, compared to the MF Toklat, where the estimated mean contribution to one SW location was 69% (Figure 5.7d). Estimated adjacent valley side contribution to flow was largest at Tek where mean estimates for SW ranged from 56% to 72% (Figure 5.7c). Mean valley side contribution at EF ranged between 38% and 41% for SW and MT locations, with the exception of SW2 where mean flow contribution was 53% (Figure 5.7b).

Site	Uncertainity (95%)			Mean uncertainity accounted for (%)		
	Mean	Max.	Min.	C_1	C_2	SW / GW
MF Toklat						
SW1	0.16	0.46	0.06	79.25	20.21	0.54
SW2	0.14	0.47	0.05	73.22	26.21	0.57
SW3	0.05	0.06	0.05	7.49	61.26	31.25
MT1	0.12	0.23	0.06	73.70	25.70	0.59
MT7	0.14	0.22	0.05	74.91	24.54	0.55
MT14	0.06	0.17	0.00	19.75	68.53	11.71
East Fork						
SW1	0.31	0.45	0.21	2.53	96.01	1.46
SW2	0.24	0.37	0.15	7.29	91.16	1.55
SW3	0.31	0.46	0.11	12.40	86.16	1.44
MT1	0.32	0.47	0.09	19.16	79.58	1.26
MT2	0.29	0.44	0.14	6.78	91.74	1.48
MT3	0.31	0.47	0.13	6.41	92.13	1.46
Teklanika						
SW1	0.40	0.46	0.35	33.14	62.61	4.25
SW2	0.35	0.40	0.32	32.13	62.60	5.27
SW3	0.39	0.42	0.34	9.97	84.60	5.43
MT1	0.36	0.39	0.34	4.87	89.71	5.42
MT2	0.31	0.31	0.31	17.26	76.64	6.10
MT3	0.33	0.37	0.28	19.64	74.60	5.76
Gorge Creek						
SW1	0.14	0.16	0.12	0.13	94.65	5.23
SW2	0.23	0.23	0.22	0.01	96.10	3.89
T1	0.15	0.18	0.10	0.13	94.74	5.13
T2	0.11	0.12	0.09	0.26	93.56	6.18

Table 5.3: Mean, maximum, and minimum uncertainty values at 95% confidence level. Mean uncertainty for individual components is also listed. At MF Toklat and EF component 1 (C_1) was debris fan (DF) and hillslope flow (HF) respectively. Component 2 (C_2) was upstream groundwater (GW). At GC C_1 was DF and C_2 was HF; and at Tek C_1 was HF and C_2 was upstream flow from the Tek River.

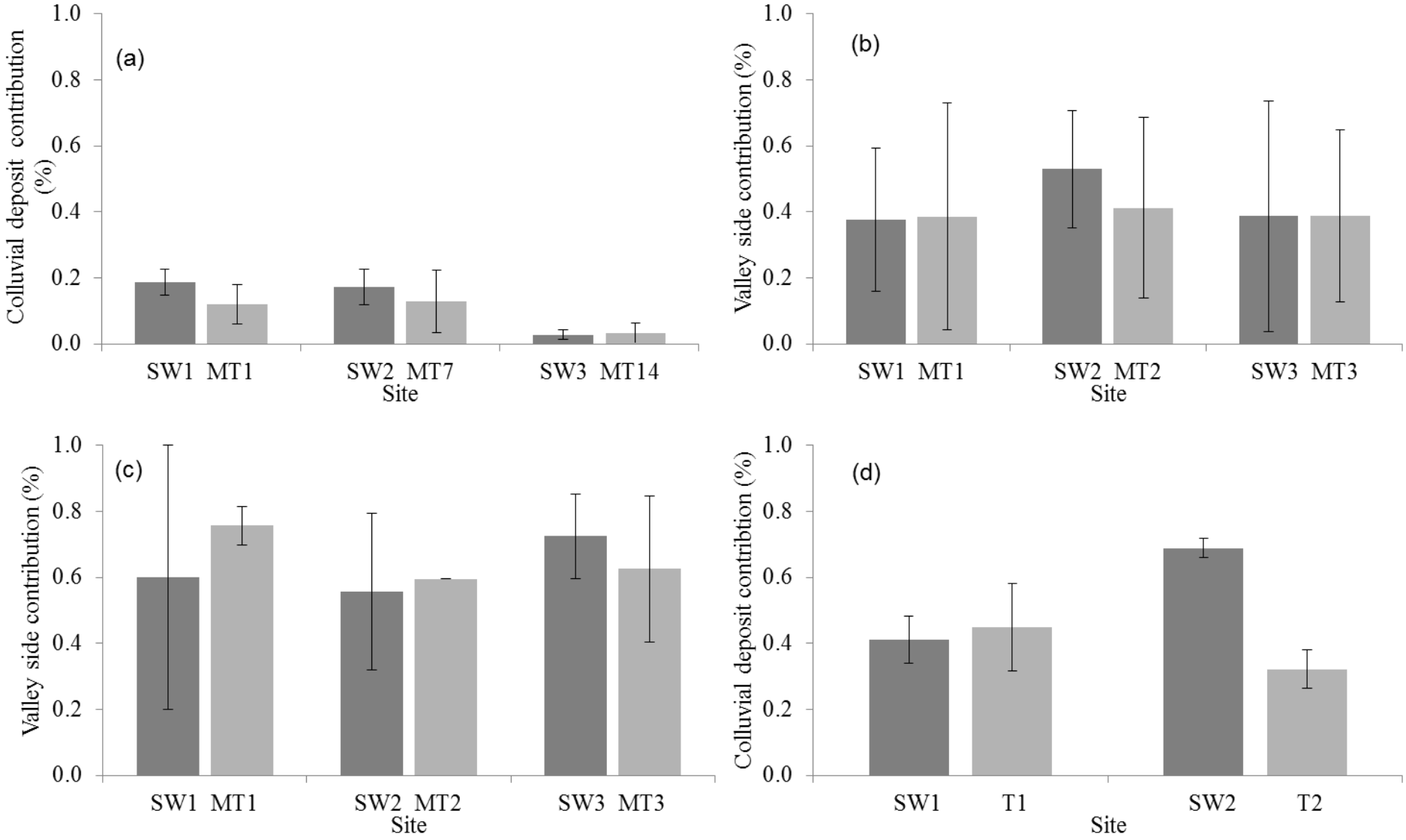

Figure 5.7: Two component hydrograph separations for surface water (SW) and groundwater (MT) locations at (a) MF Toklat, (b) EF, (c) Tek, and (d) GC. (a)/(d) separations show contribution from individual colluvial deposits. (b)/(c) provide a breakdown of flow from adjacent hillslope area, rather than from a single colluvial deposit.

5.6 DISCUSSION

This chapter has provided novel consideration of the first-order controls which influence GW-fed stream occurrence within paraglacial catchments. The discussion below considers the role of PFPs and hillslope runoff at an intra-catchment scale, before outlining the key first order controls upon GW-fed streams. In addition the implications of the understanding developed, when considering the consequences of climate change upon GW-fed streams are discussed.

5.6.1 Preferential flow pathway prevalence at the intra-catchment scale

At all sites inter-stream (SW) and groundwater (MT) differences in the spatiotemporal responses of geochemical and isotopic tracers reflected the significant control exerted by multiple, shallow subsurface flow paths across terraces (Chapter 4). Spatiotemporal differences in the conservative tracers of δ^2H composition and silica concentrations, between streams reflected variation in source contribution between shallow subsurface pathways across sites (Sueker *et al.*, 2000). Divergence in centroid positions from PCA output for individual streams at sites also suggested the presence of multiple, discrete flow paths. The contribution of flow from source waters with differing geochemical weathering signals (Gordon *et al.*, 2015) varied between individual streams and was the cause of divergence. This variation might be attributed to PFPs which influence differences in source contribution and subsequently could cause observed heterogeneity in hydrochemistry between streams (Nowak and Hodson, 2015).

The heterogeneity observed in the geochemical and isotopic properties of SW and MT at sites reinforces the concept of multiple, discrete flow pathways supporting GW-fed streams, and which may be related to PFP occurrence (Caldwell *et al.*, 2015; Poole *et al.*, 2002; Chapter 3; Chapter 4). Importantly though trends in spatial patterns for silica concentrations at GW and

SW sites were similar at MF Toklat, EF, and Tek. Given there is significant heterogeneity in bedrock geology between these catchments (Thornberry-Ehrlich, 2010; Wilson *et al.*, 1998) comparable geological settings at sites cannot necessarily be attributed as the cause of these similarities.

Geology is typically regarded as a more important hierarchal control on catchment runoff than geomorphology (Devito *et al.*, 2005). However, the similarity in spatial patterns of geochemical properties for GW-fed steams between field sites, and heterogeneity of geology at an intra-catchment scale, suggests that at a sub-catchment scale geomorphology is a more important first-order control upon GW-fed streams. It is suggested the cause of similarities in spatial patterns of water chemistry of GW-fed streams at sites is comparable surficial geomorphology settings between them. Furthermore, it is proposed that given spatial patterns in stream water chemistry point to multiple, discrete subsurface flow pathways across terraces (Malard *et al.*, 1999) there is a strong possibility PFPs are the cause of this, and therefore are the geomorphological structure which act as the predominant first-order control upon GW-fed stream occurrence.

5.6.2 Hillslope runoff influence on groundwater-fed stream recharge

Spatiotemporal patterns in surface and groundwater physicochemical properties and two-component hydrograph separations at sites highlight the significance of hillslope runoff. A strong seasonal trend towards enriched δ^2H composition at MF Toklat during 2014 was indicative of the increasing seasonal contribution to streamflow from waters that were predominantly rain-fed and which had followed shallow subsurface flow paths (Dahlke *et al.*, 2014; Quinton *et al.*, 2009; Chapter 4). This trend was replicated at EF (SW1). Seasonal increases in nitrate at MF Toklat (MT1 and MT7) and Tek (MT1) were observed, suggesting

a seasonal increase to GW recharge from shallow flow paths on adjacent valley sides. Colluvial deposits are underlain by fines and typically contain 'soil patches' that support biological and microbial activity which produce NO_3^- (Williams *et al.*, 1997). These can exert a significant influence on the solute composition of shallow flow paths through colluvial deposits, and which can be an important source of NO_3^- export in headwater catchments (Campbell *et al.*, 1995). For all sites SW and MT locations nearest the valley side showed seasonal temporal trends in physicochemical properties that are suggestive of the increased influence of hillslope flow. Spatial patterns also identified the importance of hillslope runoff to GW-fed streams. At MF Toklat, EF, and Tek there was a clear trend towards declining silica concentrations at SW and MT locations with increasing distance from the valley side. Elevated silica concentrations are attributed to the increased influence of hillslope runoff, where silicate weathering processes pre-dominate in the shallow soils due to the increased prominence of feldspar weathering and decline in importance of carbonate weathering (Clow and Sueker, 2000).

Increasing sulphate concentrations for SW locations with distance from the valley side, reflected the increased influence of upstream GW at these locations on terraces and its flow through younger, fluvioglacial sediments of the floodplain (Anderson, 2007; Cooper *et al.*, 2002; Chapter 4). This interpretation is supported by individual plots from PCA. PC1 at MF Toklat separated locations influenced by silicate weathering on the hillslope (DF and HS; high silica and sodium levels) from those influenced by carbonate dissolution and sulphide oxidation through floodplain flow paths (upstream GW; high calcium, magnesium, and sulphate levels) (Tranter, 2003b). Streams nearest the hillslope (SW1) showed an increased influence of silicate weathering, while those further away (SW2 and SW3) exhibited the dominance of carbonate dissolution and sulphate oxidation from upstream.

At EF an increased influence of silica along PC2 for HS and SW1, compared to the dominance of sulphate at SW2 and SW3 further across the terrace, reflects the differing influences of silicate weathering (hillslope runoff) (Hodson *et al.*, 2002a) and sulphate oxidation (floodplain) (Cooper *et al.*, 2002). Temporal trends towards an increased influence of silica and solutes associated with hillslope flow (nitrate, potassium, and sodium) at SW1, SW2, and for GW during the season support the inference, from the δ^2H composition, of increasing seasonal contribution of hillslope runoff to streamflow. Similar temporal patterns were observed at Tek, where all SW sites displayed the increased influence of hillslope runoff (HS).

It is clear that the direct contribution of hillslope runoff from adjacent valleys sides is not unique to the MF Toklat (Chapter 4). Two-component hydrograph separations produced higher estimates of flow contribution from the three other sites, although this may be due to the size of these terraces, which were much smaller. However, larger estimates suggest that previous work (i.e. Chapters 3 & 4) has potentially underestimated the significance of adjacent hillslope flow contribution to GW-fed streams. Given the importance of precipitation sources (winter snowpack and summer rainfall) to hillslope runoff in these catchment (see section 3.5.6) climate should be considered as a possible first-order control upon GW-fed steams of greater importance than surficial geomorphology (Buttle, 2006). Particularly as the upstream GW-input to terraces, separate of adjacent valley sides, would contain a hillslope-runoff component alongside glacial meltwaters (see section 3.6.3).

Due to the non-flashy response of GW levels to storm events observed at all sites (section 5.5.1), hillslope runoff must have been retained on valley sides and released gradually. Colluvial deposits, alpine meadow, and fractured bedrock were identified at all sites (see section 2.1) and are known to provide important aquifers (Weekes *et al.*, 2015). In addition

colluvial deposits contain discrete flow paths (Muir *et al.*, 2011; Roy and Hayashi, 2009), that are known to provide water directly to GW-fed streams (Chapter 4). Subsequently the landscape units necessary to retain precipitation inputs on valley-sides were present at all sites, raising the prospect of climate and hillslope runoff as the fundamental first-order control upon GW-fed streams.

5.6.3 Establishing first-order controls on groundwater-fed streams

This chapter has highlighted that at an intra-catchment scale, PFP prevalence and the occurrence of GW-fed streams are intrinsically linked. In addition it has emphasised the contribution of hillslope runoff to GW-fed streams, and the important role of alpine meadow, fractured bedrock, and particularly colluvial deposits in regulating flow. It is clear that both climate and surficial geomorphology are important controls upon the presence of GW-fed streams within paraglacial floodplains. However, when considering which may be the first-order control upon GW-fed streams it is suggested PFPs, and their associated hydrogeomorphic characteristics (Caldwell *et al.*, 2015; Poole *et al.*, 2002; Stanford and Ward, 1993; Chapter 3), are the fundamental first-order control. Typically climate and bedrock geology are considered more important hierarchal controls on overall streamflow from basins than surficial geomorphology (Buttle, 2006). However, such hierarchal orders do not reflect the controls on GW-fed streams specifically at a sub-catchment scale.

This intra-catchment study has shown that PFPs exert a universal spatiotemporal control on the physicochemical properties of GW-fed stream across catchments. This reflects their role as discrete conduits of flow within paraglacial floodplains (Miller *et al.*, 2014). Furthermore, while geochemical weathering signals identified in GW-streams through PCA highlight the important contribution of hillslope runoff to flow; they also clearly point to the important role

of PFPs in supporting hillslope-floodplain connectivity (Chapter 3; Chapter 4) which allows such a contribution. Consequently it is suggested PFPs are the key first-order control on GW-fed streams.

5.6.4 Implications of climate change for first-order controls and the long-term stability of groundwater-fed streams

If PFPs are the first-order control on GW-fed streams at the sub-catchment scale, then climate at the catchment scale will remain an important control given the influence it will have on PFPs. The long-term stability of GW-fed streams is dependent upon the persistent development of new PFPs and renewal of existing ones. Therefore a long-term decline in sediment loads within paraglacial catchments as a consequence of glacial retreat (Church and Ryder, 1972; Gurnell *et al.*, 2000), and subsequent reduction in avulsion processes (Marren and Toomath, 2014) that develop and maintain PFPs (Poole *et al.*, 2002) would be detrimental. A reduction in avulsion processes would also allow mature vegetation development and succession on floodplains (Klaar *et al.*, 2015). The development of associated soil profiles and deep root networks (Lorang and Hauer, 2007) would reduce the effectiveness of PFPs as conduits of flow (Poole *et al.*, 2002) and could have negative implications for the perennial nature of GW-fed streams.

This process may already be observable at Gorge Creek (GC). This catchment was de-glacierised and vegetation cover on the terrace was significantly denser and more mature than at any other site (see section 2.1.4). It was also the only terrace where all GW-fed streams were ephemeral in nature (personal observation), even though a large colluvial deposit provided ~69% of flow to an individual GW-fed stream on the terrace, indicating the prevalence of hillslope runoff. There are a number of possible causes for the ephemeral behaviour of streams; it may have been caused by greater evapotranspiration rates relating to

the denser, more mature vegetation on the terrace.(Nolin, 2012); or the lack of a glacial meltwater component from upstream may have restricted recharge (Brown *et al.*, 2006). Alternatively, this terrace was very large relative to its upstream catchment area (Table 2.1) and there may simply have not been sufficient hillslope runoff to recharge the terrace. However, alongside these possible causes the degradation of PFPs by vegetation and soil development (Poole *et al.*, 2002) and restriction of renewal by declining avulsion processes and channelization of flow (Marren and Toomath, 2014) should also be considered as contributing factors to ephemeral behaviour.

Glacial retreat and subsequent long-term declines in sediment loads will have negative implications for the development and renewal of PFPs within paraglacial environments. However, the time-scale of such changes will be over hundreds, or even thousands of years (Ballantyne, 2002a; Klaar *et al.*, 2015; Orwin and Smart, 2004). In the short- to medium-term, through the 21st Century, the more significant stress upon the stability of perennial GW-fed streams is likely to be alterations in the hydrological dynamics of paraglacial catchments in response to climate change (Brown *et al.*, 2006). Changing hillslope runoff characteristics may then be a more immediate concern for GW-fed streams. Winter snowpack is declining in paraglacial environments with earlier spring melt occurring (Mote *et al.*, 2005; Pederson *et al.*, 2013). Significant uncertainty exists regarding predicted responses in summer precipitation patterns, which exhibit regional heterogeneity (Rahman *et al.*, 2014). However, the increasing relative importance of summer precipitation and groundwater with declining meltwater levels is more certain (Baraer *et al.*, 2012; Tague and Grant, 2009).

Hillslope runoff decline due to these changes could impact the perennial nature of GW-fed streams, increasing the relative importance of colluvial deposits as groundwater stores on valley sides (Gordon *et al.*, 2015). Finally declining permafrost coverage on paraglacial

hillslopes (Lawrence and Slater, 2005) will also have implications for hillslope runoff. In the short-term thawing may increase hillslope runoff to GW-fed streams, but it will also connect hillslope runoff to deeper flow pathways (Boucher and Carey, 2010; Carey *et al.*, 2013). The consequences of which, for GW-fed streams, are entirely unknown.

5.7 SUMMARY

This chapter has, for the first time, considered first-order controls upon GW-fed streams within paraglacial catchments. Spatiotemporal patterns in the physicochemical properties of surface and groundwater on terraces at an intra-catchment scale demonstrated that PFPs provided discrete conduits of flow which supported GW-fed streams. In addition PCA output identified geochemical weathering signals in GW-fed streams associated with hillslope runoff and which reflected the important role of PFPs in hillslope-floodplain connectivity. Across the intra-catchment scale GW-fed streams showed non-flashy behaviour in response to storm events during summer months; even though two-component hydrograph separations indicated hillslope runoff contributed significantly to GW-fed streams. Large hillslope runoff contributions within paraglacial catchments might typically be expected to generate a flashy response in streams, and so the non-flashy behaviour of GW-fed streams reflected divergent pathways taken by hillslope runoff. It is suggested that colluvial deposits, alpine meadow, and fractured bedrock on valley sides may all provide important roles in groundwater retention and release on valley sides.

The chapter has identified PFPs as the key first-order control on the occurrence of GW-fed streams due to their fundamental role in hydrological connectivity across floodplains; and hillslope-floodplain connectivity within paraglacial environments. It has also raised concerns regarding the long-term consequences of glacial retreat and influence of climate on the stability of PFPs and the GW-fed streams they support. However, the important role of

hillslope flow identified in supporting GW-fed streams at an intra-catchment has underlined concerns, in the short- to medium-term, of the implications of shifting hydrological dynamics due to climate change upon them. There is a clear need for further research which; (1) considers the long-term stability of PFPs in paraglacial catchments experiencing glacial retreat; and (2) clearly establishes how the hydrological dynamics of hillslope runoff will shift on paraglacial valley sides.

CHAPTER 6: SYNTHESIS, IMPLICATIONS AND FUTURE DIRECTIONS

6.1 Introduction

GW-fed streams are valuable biodiversity hotspots within paraglacial environments for aquatic ecology (Brown *et al.*, 2003; Cauvy-Fraunie *et al.*, 2015). They also support riparian vegetation (Caldwell *et al.*, 2015; Soulsby *et al.*, 2005) that offers valuable terrestrial habitat (Paetzold *et al.*, 2005; Tabacchi *et al.*, 1998). Their existence on floodplains has been linked to the presence of PFPs (paleochannels) and where they intersect the topographic surface (Caldwell *et al.*, 2015, Poole *et al.*, 2002). Uncertainty regarding the sensitivity to climate change of the hydrological dynamics which support them (Brown *et al.*, 2006; Gordon *et al.*, 2015) has been the main motivation for this research. In particular, a greater insight into the hydrogeomorphic controls upon these GW-fed streams was a major focus. By addressing key research gaps, the consequences of anticipated shifts in the water balance of paraglacial environments in response to anthropogenic climate change during the 21st Century could be more fully understood.

Using a multi-faceted research approach, delivered at an intra-catchment scale, this thesis identified and dealt with three key interconnected research objectives. The hydrogeomorphic controls upon GW-fed streams within paraglacial floodplains was summarised in Chapter 3 (Objective 1). This understanding was used to estimate the water balance during spring, summer, and autumn months for a set of GW-fed streams on the MF Toklat River, DNPP, Alaska. Developing this understanding, the physicochemical properties of surface, groundwater, and identified end-members were used to estimate flow contribution from valley side colluvial deposits to GW-fed streams at the MF Toklat site (Chapter 4; Objective 2). In addition the role of PFPs to hillslope-floodplain connectivity was considered. Finally the knowledge developed was brought together in an intra-catchment study that considered the first-order controls upon GW-fed stream occurrence and their influence upon the sensitivity of

these biodiversity hotspots to climate change (Chapter 5; Objective 3). A synthesis of the key research findings and the implications of this research, along with potential future research, are outlined in this concluding chapter.

6.2 Key research findings

The research provided a number of unique perspectives on the hydrological dynamics of GW-fed streams within paraglacial floodplains by; (1) establishing the hydrogeomorphic controls upon GW-fed streams, including the identification and consideration of the role of PFPs to their occurrence; (2) examining the concept of hillslope-floodplain connectivity, and its role within paraglacial systems to sustaining GW-fed streams; and (3) consideration of first-order controls upon GW-fed stream presence. Major research findings were:

1. PFPs were the principal conduit of subsurface flow across paraglacial floodplains and where they intersect the topographic surface, with a sufficiently shallow water table, GW-fed streams occur (Chapter 3)
2. Valley side water fluxes (associated with winter snowpack and summer precipitation) from adjacent hillslope areas were an important component of the water balance for GW-fed streams (Chapter 3 & 4)
3. Colluvial deposits were valuable aquifers in paraglacial catchments, dominated by ‘old’ water, and can make a significant contribution to GW-fed stream discharge (Chapter 4)
4. The prevalence of PFPs as discrete flow pathways within paraglacial floodplains was observed at an intra-catchment scale. Indicative that PFPs, and their associated hydrogeomorphic properties, were an important first-order control upon GW-fed stream occurrence (Chapter 5)

5. Glacial retreat could have long-term consequences for the stability of PFPs, and subsequently the continued persistence of GW-fed streams within paraglacial catchments. However, in the short- to medium-term changes in hillslope runoff to GW-fed streams may have implications for their perennial nature (Chapter 5)

6.3 Conceptualising hydrological dynamics of groundwater-fed streams

An initial conceptual summary of understanding developed in Chapter 3 of the hydrological dynamics which influence GW-fed streams was presented in Figure 3.8. That summary emphasised the role of PFPs as conduits for vertical and lateral hydrologic exchange across paraglacial floodplains and which allow GW-fed streams to develop. It also conceptualised the role of PFPs in hillslope-floodplain connectivity, and proposed colluvial deposits on valley sides as important groundwater conduits. Understanding advanced and supported by key findings from Chapters 4 & 5. A revised conceptual summary (Figure 6.1) is presented in this section and described below. Figure 6.1 outlines the above, but also considers the main controls upon GW-fed streams and the processes which influence these controls.

Paleochannels, acting as PFPs, are the dominant conduit for groundwater flow through paraglacial floodplains and streamflow is sustained by continual recharge of the water table across spring, summer, and autumn months (Chapter 3). Development and renewal of PFPs is dependent upon sediment loads exported from upstream by glacial meltwater (Poole *et al.*, 2002). Sediment sustains downstream avulsion and alluviation processes (Orwin and Smart, 2004) that maintain the formation of new PFPs and regeneration of existing channels (Poole *et al.*, 2002). It also suppresses vegetation growth and soil development (Klaar *et al.*, 2015; Lorang and Hauer, 2007) that reduce the efficiency of PFPs as conduits of subsurface flow (Caldwell *et al.*, 2015).

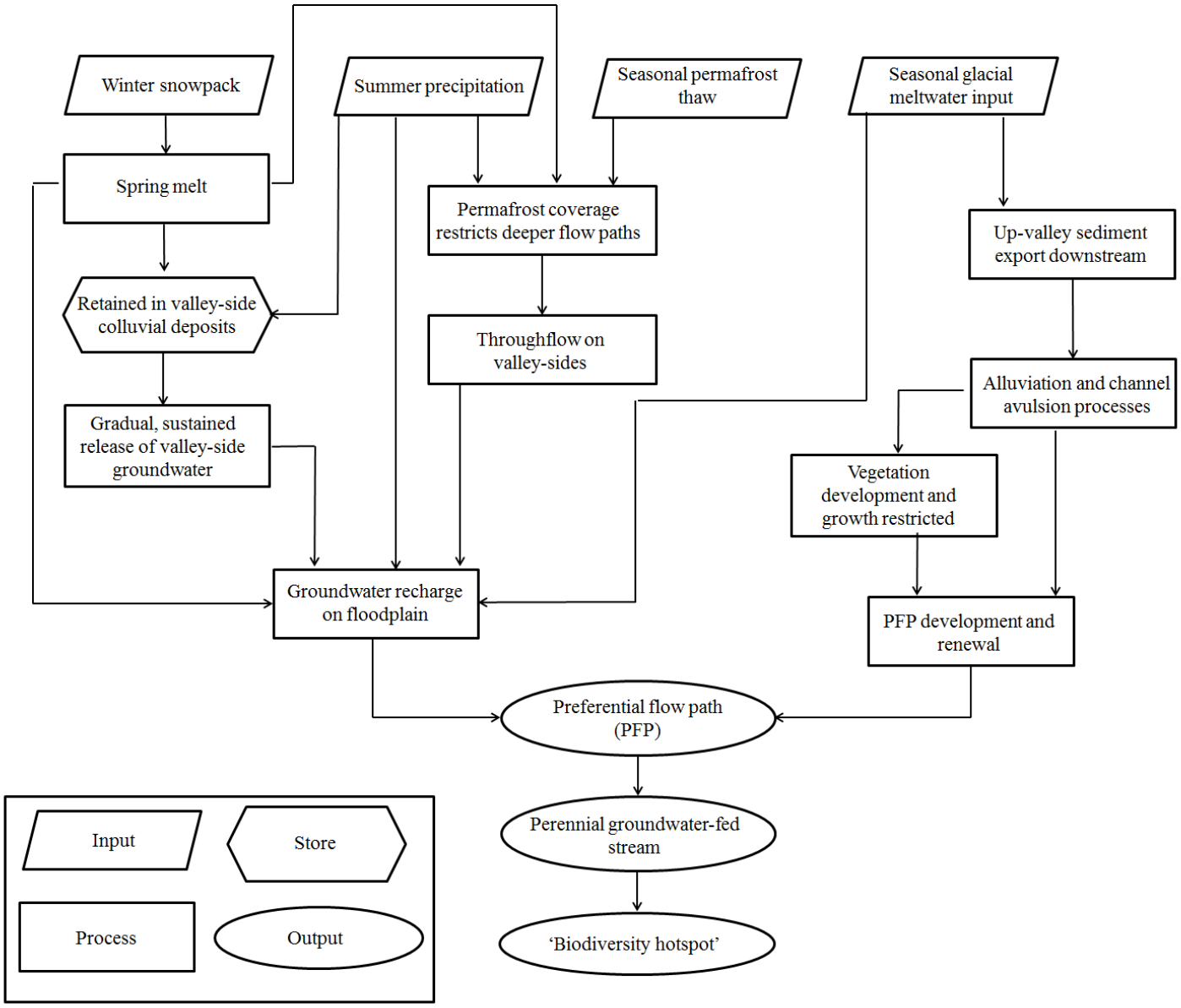

Figure 6.1: Conceptual summary outlining key controls on GW-fed stream presence on paraglacial floodplains. PFPs are the dominant first-order control on their occurrence whose effectiveness to act as channels of flow is dependent upon: (1) continual renewal and development; and (2) recharge of the floodplain water table during summer months. (1) is controlled by up-valley sediment export from glacial meltwaters, which maintains channel avulsion and alluviation, while restricting vegetation growth. Hillslope runoff processes provide an important contribution to (2), particularly colluvial deposits, which retain groundwater on valley sides and provide gradual, sustained flow to the floodplain

Flow from adjacent valley sides (winter snowpack, summer precipitation, and permafrost fluxes) can sustain a large part of GW-fed stream discharge (Chapter 3). These hillslope runoff sources could also provide an important component (alongside glacial meltwaters) of upstream groundwater input to streams (Chapter 3). Furthermore, fractured bedrock, alpine meadows and colluvial deposits on valley sides can all act as important groundwater aquifers (McClymont *et al.*, 2011). In particular colluvial deposits were directly identified as valuable aquifers, influenced by 'old' water (Clow *et al.*, 2003, Liu *et al.*, 2004, Muir *et al.*, 2011, Weekes *et al.*, 2015, Chapter 4). Adjacent valley side flow, and related groundwater stores (e.g. colluvial deposits) are prominent sources of streamflow to GW-fed streams (Chapter 4; Chapter 5), an indication of the pivotal contribution of PFPs to hillslope-floodplain connectivity (Bracken and Croke, 2007; Poole, 2010; Chapter 4; Chapter 5). Spatiotemporal variation in stream physicochemical properties is indicative of the occurrence of multiple, discrete flow pathways (PFPs) (Malard *et al.*, 1999), a further reflection of their role in hydrological connectivity within paraglacial floodplains (Chapter 4, Chapter 5).

The hydrological dynamics of paraglacial catchments are predicted to alter throughout the 21st Century in response to anthropogenic climate change (Barnett *et al.*, 2005). Changes include declining glacial meltwater levels (Huss and Hock, 2015; Zemp *et al.*, 2015) and reduced winter snowpack and earlier spring melt (Nolin, 2012; Stewart, 2009). These changes will lead to an increase in the relative importance of groundwater in paraglacial environments (Hood and Hayashi, 2015; Milner *et al.*, 2009). However, a relative increase in the contribution of groundwater from valley side aquifers (i.e. fracture bedrock, alpine meadow, and colluvial deposits) may not be adequate to sustain perennial flow of GW-fed streams (Levy *et al.*, 2015; Chapter 5). Observations of ephemeral flow in de-glacierised catchments, and during early summer months in glacierised systems (prior to storm events), suggests

relative increases in groundwater contributions from adjacent valley sides (and colluvial deposits) may not be sufficient to sustain perennial GW-fed streamflow (Chapter 5).

In summary PFPs are important first-order controls upon the occurrence of GW-fed streams and are an integral part of hillslope-floodplain connectivity, providing multiple, discrete flow paths through the paraglacial floodplain subsurface. PFP contribution to the hydrological connectivity of the floodplain with adjacent valley sides results in valley side flow, and associated groundwater aquifers (e.g. colluvial deposits), making valuable contributions to GW-fed stream discharge. Declining meltwater flow in paraglacial catchments may though have implications for the long-term stability of GW-fed streams as stable, perennial aquatic environments, with a shift towards ephemeral behaviour.

6.4 Implications for biodiversity hotspots

Climate change will have a number of possible implications for the short- to medium- term (Hydrologic) and long-term (Hydrogeomorphic) controls upon GW-fed streams. An adapted version of Figure 6.1 is presented in **Error! Reference source not found.** which considers the implications of these changes for the stability of GW-fed streams, and which are outlined below.

6.4.1 Shifting hydrological dynamics

Changing hydrological dynamics within paraglacial systems (Deb *et al.*, 2015) is a major concern for biodiversity hotspots (Chapter 5). Declining meltwater fluxes (valley side snowpack and glacial ice) (Barnett *et al.*, 2005; Zemp *et al.*, 2015) and earlier spring melt (Douglas *et al.*, 2013) will undoubtedly lead to a rise in the relative importance of groundwater from colluvial deposits (Hood and Hayashi, 2015; McClymont *et al.*, 2010).

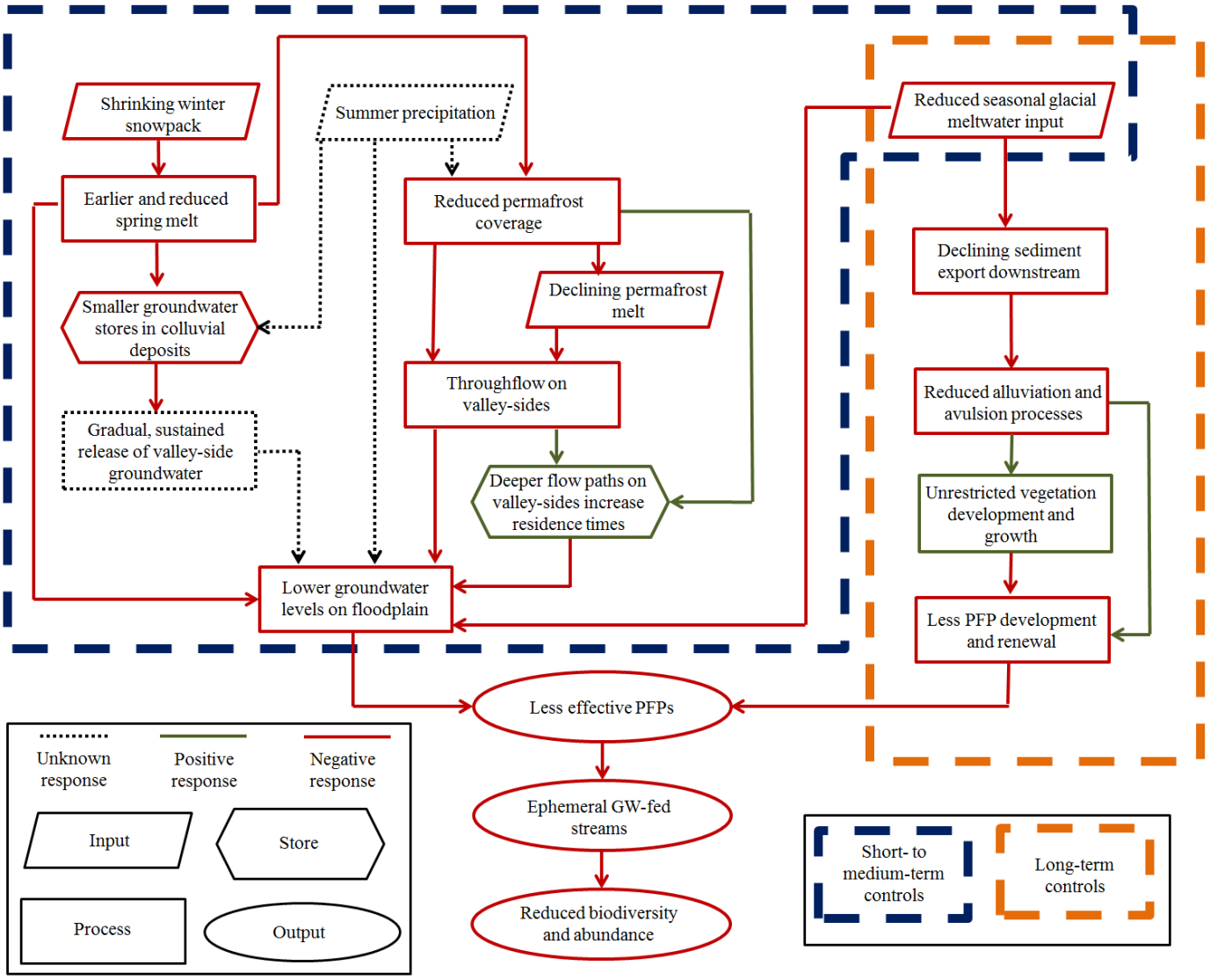

Figure 6.2: Revised conceptual model outlining implications of changes in short to medium-term controls (hydrological dynamics) and long-term controls (hydrogeomorphic processes) upon GW-fed stream occurrence on paraglacial floodplains. Positive, negative, and unknown responses are considered. Positive responses (green) are those which will see an increase in their occurrence in response to changes (e.g. vegetation growth on terraces). Negative responses (red) will see a decline (e.g. smaller snowpack). In the short- to medium-term shrinking winter snowpack, declining permafrost thaw, and subsequent smaller groundwater stores on valley sides may lead to reduced recharge of the floodplain water table. In addition declining permafrost coverage will open up deeper flow paths on valleys-sides which will increase residence times. Long-term consequences of glacial retreat will lead to a decline in up-valley sediment export that will restrict channel avulsion and alluviation processes. Subsequent declines in PFP formation and renewal and increased vegetation growth will have a negative impact on PFP effectiveness and may lead to ephemeral GW-fed streams. Overall, shifts in controls on GW-fed streams may have a detrimental impact on their role as biodiversity hotspots.

Declining permafrost coverage on hillslopes will also open up deeper flow paths, increasing the residence times of throughflow on valley sides (Carey *et al.*, 2013; Douglas *et al.*, 2013).

Summer hydrological dynamics at field sites showed groundwater recharge on terraces was rain-fed or driven (Chapter 5). Particularly given warmer conditions (see section 2.2), and associated increases in glacial meltwater discharge, did not necessarily lead to faster, or greater, recharge of terraces (Chapter 3). Given winter months see a lack of meltwater component and baseflow conditions (Hood and Hayashi, 2015), groundwater recharge of terraces during active months must sustain perennial flow of GW-fed streams during these periods (see section 2.1.1). This is why groundwater levels were lowest in the spring, prior to recharge (Chapter 5). Therefore, if the meltwater component is less significant than previously anticipated (Chapter 3), it should be considered whether declining meltwater components will actually lead to ephemeral GW-fed streamflow. Particularly if there is a trend towards wetter summer months (such as 2014) in paraglacial environments (Stafford *et al.*, 2000).

A declining meltwater component may further increase the relative importance of summer precipitation and subsequently the role of valley-side aquifers (e.g. fractured bedrock, alpine meadow, and colluvial deposits) to retain this flux (McClymont *et al.*, 2011). The potential groundwater storage capacity of colluvial deposits is significant (Clow *et al.*, 2003; Gordon *et al.*, 2015), and water balance work suggests adjacent hillslope area fluxes are sufficiently large to sustain streamflow (Chapter 3). However, despite confidence in the potential for colluvial deposits to act as valuable aquifers, significant uncertainty remains concerning the capability of such surficial deposits to retain groundwater (McClymont *et al.*, 2012; Muir *et al.*, 2011). Mean residence time (MRT) estimates suggest that colluvial deposits do

effectively retain and store water (Chapter 4), which could be essential for GW-fed streams if the relative importance of hillslope runoff to streamflow is to increase.

However, observations of the ephemeral behaviour of GW-fed streams in de-glacierised catchments (Chapter 5) suggests any relative increase in the contribution of groundwater from valley sides may not be sufficient to sustain perennial flow. Furthermore, GW-fed streams that were previously observed as perennial (Crossman *et al.*, 2011) exhibited ephemeral flow patterns in spring months (Chapter 4). This responses in hydrological behaviour occurred after a particularly dry summer (2013; see section 2.2) and may point towards increasingly ephemeral behaviour for GW-fed streams on these paraglacial floodplains, if summer precipitation declines. A declining meltwater component, compounded by reduced summer precipitation input, would have detrimental impacts on the short- to medium-term stability of these important aquatic habitats and their role as biodiversity hotspots (Caldwell *et al.*, 2015; Doering *et al.*, 2007; Levy *et al.*, 2015; Malard *et al.*, 1999; Ward *et al.*, 1999). In addition an associated decline in water table (Levy *et al.*, 2015) would have implications for their capability to support riparian vegetation and provide a critical interlink for the aquatic-terrestrial transition zone (Paetzold *et al.*, 2005; Whited *et al.*, 2007).

6.4.2 Changing geomorphic processes

Further to shifting hydrological dynamics, the recognition of PFPs as being a first-order control upon GW-fed stream occurrence (Chapter 5) raises implications for their long-term stability due to changes in discharge and sediment yields within paraglacial environments (Church and Ryder, 1972; Geilhausen *et al.*, 2013). The effectiveness of PFPs as conduits for flow is reliant upon channel avulsion processes and high sediment yields associated with upstream glacial coverage in paraglacial environments (Church and Ryder, 1972; Gurnell *et*

al., 2000; Poole *et al.*, 2002). Glacial retreat will lead to a long-term decline in sediment yields (Church and Ryder, 1972; Gurnell *et al.*, 2000). In the more immediate term topographic forcing processes, such as channel confinement and incision, will increase (Marren and Toomath, 2014). These processes will be triggered by declining long profile gradients as a consequence of sediment-based ice-marginal over deepening (Marren and Toomath, 2014).

Where deglaciation is still occurring in paraglacial catchments (such as MF Toklat, EF, and Tek), increases in topographic forcing will lead to channelization of flow in the immediate term (Heckmann *et al.*, 2016). This may cause an increase in the formation of new terraces within these catchments in the short-term (Marren and Toomath, 2014), although in the long-term terraces formation will decrease with declining energy in these environments (Gurnell *et al.*, 2000). In addition channelization of flow will restrict the flooding and erosion of existing terraces, leading to a subsequent decline in the renewal of the floodplain landscapes (Arscott *et al.*, 2002). Instead, as the paraglacial environment becomes less dynamic, terraces may become more permanent features on the floodplain and the 'shifting mosaic' of habitats (Van Der Nat *et al.*, 2003; Whited *et al.*, 2007) that is typically observed across paraglacial floodplains will cease to occur.

With restricted renewal of terraces, caused by channelization of flow, existing terraces may become increasingly elevated above the active floodplain (Marren and Toomath, 2014). These terraces (such as those at the MF Toklat, EF, and Tek sites) may subsequently become hydrologically disconnected from the active floodplain and from upstream groundwater recharge (Poole *et al.*, 2006). Such an occurrence would result in GW-fed streams on terraces becoming increasingly dependent upon adjacent valley side water sources for flow, which may not be sufficient to sustain perennial flow (Chapter 5).

Furthermore, sediment supply to terraces would also become restricted (Lorang and Hauer, 2007). Such changes to the upstream sediment and groundwater fluxes to terraces would restrict the development of new PFPs across them (Poole *et al.*, 2002), and might allow for mature vegetation succession development (Caldwell *et al.*, 2015; Lorang and Hauer, 2007). Vegetation development could restrict the effectiveness of existing PFPs to act as conduits of flow (Poole *et al.*, 2002). Long-term declines in PFP formation and effectiveness could compound stresses incurred by GW-fed streams as a consequence of shifting hydrological dynamics. This raises further questions about their continued widespread presence on floodplains (Crossman *et al.*, 2012) and perennial nature (Levy *et al.*, 2015). Such changes may already be observable in de-glacierised catchments, where GW-fed streams are ephemeral, and vegetation succession mature (Chapter 5).

6.5 Future work

This research has highlighted the importance of PFPs and role of adjacent valley side flow in the occurrence of GW-fed streams. It has also raised questions regarding the future stability of these biodiversity hotspots. There is undoubtedly a substantial amount of further research that needs to be considered on these systems. Particularly regarding furthering process-based understanding, transferable at an intra-catchment scale, by considering the following:

- Hydrogeomorphic and physicochemical data from this research strongly support the role of PFPs in GW-fed stream occurrence (Chapter 3-5). Geophysical surveying, such as ground-penetrating radar (GPR), has been successfully applied by others to map subsurface channels (Bayer *et al.*, 2011; Heinz and Aigner, 2003b; McClymont *et al.*, 2011). GPR would assist in mapping hydrological connectivity and improve further our understanding of the role of PFPs in hillslope-floodplain connectivity

- Consideration of the controls on the effectiveness of PFPs as subsurface flow paths should be considered (Poole, 2010). Establishing the potential role of vegetation in reducing hydraulic conductivity (*K*) of PFPs is a priority. In addition improved understanding of the timing and rate of vegetation succession in paraglacial catchments, in response to increased topographic forcing (Marren and Toomath, 2014) and declining sediment yields (Gurnell *et al.*, 2000) should be evaluated
- Groundwater recharge on the terraces has been observed to be rain-fed or driven (Chapter 3-5). If precipitation is a significant component of GW-fed stream discharge, and driver of perennial flow, then greater confidence in the long-term changes in precipitation patterns, currently an area of significant uncertainty, within paraglacial environments is required (Crossman *et al.*, 2013). Increased summer precipitation may reduce the risk of shifts to ephemeral flow, potentially caused by declining meltwater contribution to streams (Levy *et al.*, 2015). In contrast drier conditions may compound the loss of glacial meltwater resulting in ephemeral conditions.
- The implications of declining valley side discontinuous permafrost on biodiversity hotspots have not been considered. It is anticipated that permafrost melt will open up deeper groundwater flow pathways on valley sides (Boucher and Carey, 2010; Douglas *et al.*, 2013). Such changes could influence the hydrologic regimes of GW-fed streams (Carey *et al.*, 2013) and may have further implications for water quality (e.g. increased DOC) (Aiken *et al.*, 2014; Walvoord and Striegl, 2007), which would have a subsequent impact upon aquatic ecology (Chin *et al.*, 2016).

6.6 Final remarks

The research presented in this thesis has contributed significantly to our understanding of the fundamental hydrologic controls upon groundwater-fed surface channels which act as biodiversity hotspots within paraglacial environment. In addition this improved knowledge of their hydrogeomorphic controls and hydrological dynamics raises concerns as to their long-term stability; given anticipated changes in the hydrologic regimes of arctic, sub-arctic, and alpine environments expected as a result of anthropogenic climate change in the 21st Century.

REFERENCES

Addy, S., Soulsby, C., Hartley, A. J. , Tetzlaff, D. 2011. Characterisation of channel reach morphology and associated controls in deglaciated montane catchments in the Cairngorms, Scotland. *Geomorphology* **132**(3–4): 176-186. DOI:http://dx.doi.org/10.1016/j.geomorph.2011.05.007.

Aiken, G. R., Spencer, R. G. M., Striegl, R. G., Schuster, P. F. , Raymond, P. A. 2014. Influences of glacier melt and permafrost thaw on the age of dissolved organic carbon in the Yukon River basin. *Global Biogeochemical Cycles* **28**(5): 525-537. DOI:10.1002/2013GB004764.

Allen, D. M., Whitfield, P. H. , Werner, A. 2010. Groundwater level responses in temperate mountainous terrain: regime classification, and linkages to climate and streamflow. *Hydrological Processes* **24**(23): 3392-3412. DOI:10.1002/hyp.7757.

Anderson, M., Aiken, J., Webb, E. , Mickelson, D. 1999. Sedimentology and hydrogeology of two braided stream deposits. *Sedimentary Geology* **129**(3): 187-199.

Anderson, M. P. 1989. Hydrogeologic facies models to delineate large-scale spatial trends in glacial and glaciofluvial sediments. *Geological Society of America Bulletin* **101**(4): 501-511. DOI:10.1130/0016-7606(1989)101<0501:hfmtdl>2.3.co;2.

Anderson, S. P. 2007. Biogeochemistry of glacial landscape systems Annual Review of Earth and Planetary Sciences. vol 35, 375-399.

Arscott, D. B., Tockner, K., van der Nat, D. , Ward, J. V. 2002. Aquatic habitat dynamics along a braided alpine river ecosystem (Tagliamento River, Northeast Italy). *Ecosystems* **5**(8): 802-814. DOI:10.1007/s10021-002-0192-7.

Arscott, D. B., Tockner, K. , Ward, J. V. 2005. Lateral organization of aquatic invertebrates along the corridor of a braided floodplain river. *Journal of the North American Benthological Society* **24**(4): 934-954. DOI:10.1899/05-037.1.

Ballantyne, C. K. 2002a. A general model of paraglacial landscape response. *The Holocene* **12**(3): 371-376. DOI:10.1191/0959683602hl553fa.

Ballantyne, C. K. 2002b. Paraglacial geomorphology. *Quaternary Science Reviews* **21**(18-19): 1935-2017. DOI:10.1016/s0277-3791(02)00005-7.

Baraer, M., Mark, B. G., McKenzie, J. M., Condom, T., Bury, J., Huh, K.-I., Portocarrero, C., Gómez, J. , Rathay, S. 2012. Glacier recession and water resources in Peru's Cordillera Blanca. *Journal of Glaciology* **58**(207): 134-150. DOI:10.3189/2012JoG11J186.

Baraer, M., McKenzie, J., Mark, B. G., Gordon, R., Bury, J., Condom, T., Gomez, J., Knox, S. , Fortner, S. K. 2015. Contribution of groundwater to the outflow from ungauged glacierized catchments: a multi-site study in the tropical Cordillera Blanca, Peru. *Hydrological Processes* **29**(11): 2561-2581. DOI:10.1002/hyp.10386.

Barnett, T. P., Adam, J. C. , Lettenmaier, D. P. 2005. Potential impacts of a warming climate on water availability in snow-dominated regions. *Nature* **438**(7066): 303-309. DOI:10.1038/nature04141.

Baxter, C., Hauer, F. R. , Woessner, W. W. 2003. Measuring Groundwater–Stream Water Exchange: New Techniques for Installing Minipiezometers and Estimating Hydraulic Conductivity. *Transactions of the American Fisheries Society* **132**(3): 493-502. DOI:10.1577/1548-8659(2003)132<0493:mgwent>2.0.co;2.

Bayer, P., Huggenberger, P., Renard, P. , Comunian, A. 2011. Three-dimensional high resolution fluvio-glacial aquifer analog: Part 1: Field study. *Journal of Hydrology* **405**(1–2): 1-9. DOI:http://dx.doi.org/10.1016/j.jhydrol.2011.03.038.

Benn, D. I. ,Evans, D. J. A. 2010. Glaciers and Glaciation, 2nd edn. Hodder Education, Abingdon, Oxfordshire.

Bennett, M. 2011. Glaciers and Glaciation by Benn, D. I. & Evans, D. J. A. *Boreas* **40**(3): 555-555. DOI:10.1111/j.1502-3885.2011.00212.x.

Blaen, P. J., Hannah, D. M., Brown, L. E. , Milner, A. M. 2014. Water source dynamics of high Arctic river basins. *Hydrological Processes* **28**(10): 3521-3538. DOI:10.1002/hyp.9891.

Blott, S. J. ,Pye, K. 2001. GRADISTAT: a grain size distribution and statistics package for the analysis of unconsolidated sediments. *Earth Surface Processes and Landforms* **26**(11): 1237-1248.

Blume, T. ,van Meerveld, H. J. 2015. From hillslope to stream: methods to investigate subsurface connectivity. *Wiley Interdisciplinary Reviews: Water* **2**(3): 177-198. DOI:10.1002/wat2.1071.

Boucher, J. L. ,Carey, S. K. 2010. Exploring runoff processes using chemical, isotopic and hydrometric data in a discontinuous permafrost catchment. *Hydrology Research* **41**(6): 508-519. DOI:10.2166/nh.2010.146.

Bracken, L. J. ,Croke, J. 2007. The concept of hydrological connectivity and its contribution to understanding runoff-dominated geomorphic systems. *Hydrological Processes* **21**(13): 1749-1763. DOI:10.1002/hyp.6313.

Brown, L. E., Hannah, D. M. , Milner, A. M. 2003. Alpine stream habitat classification: An alternative approach incorporating the role of dynamic water source contributions. *Arctic Antarctic and Alpine Research* **35**(3): 313-322. DOI:10.1657/1523-0430(2003)035[0313:ashcaa]2.0.co;2.

Brown, L. E., Hannah, D. M. , Milner, A. M. 2007. Vulnerability of alpine stream biodiversity to shrinking glaciers and snowpacks. *Global Change Biology* **13**(5): 958-966. DOI:10.1111/j.1365-2486.2007.01341.x.

Brown, L. E., Hannah, D. M., Milner, A. M., Soulsby, C., Hodson, A. J. , Brewer, M. J. 2006. Water source dynamics in a glacierized alpine river basin (Taillon-Gabietous, French Pyrenees). *Water Resources Research* **42**(8). DOI:10.1029/2005wr004268.

Buttle, J. 2006. Mapping first-order controls on streamflow from drainage basins: the T3 template. *Hydrological Processes* **20**(15): 3415-3422. DOI:10.1002/hyp.6519.

Buttle, J. M. 1994. Isotope hydrograph separations and rapid devlivery of pre-event water from drainage basins. *Progress in Physical Geography* **18**(1): 16-41. DOI:10.1177/030913339401800102.

Caballero, Y., Jomelli, V., Chevallier, P. , Ribstein, P. 2002. Hydrological characteristics of slope deposits in high tropical mountains (Cordillera Real, Bolivia). *Catena* **47**(2): 101-116. DOI:10.1016/s0341-8162(01)00179-5.

Cable, J., Ogle, K. , Williams, D. 2011. Contribution of glacier meltwater to streamflow in the Wind River Range, Wyoming, inferred via a Bayesian mixing model applied to isotopic measurements. *Hydrological Processes* **25**(14): 2228-2236. DOI:10.1002/hyp.7982.

Caldwell, S. K., Peipoch, M. , Valett, H. M. 2015. Spatial drivers of ecosystem structure and function in a floodplain riverscape: springbrook nutrient dynamics. *Freshwater Science* **34**(1): 233-244. DOI:10.1086/679300.

Campbell, D. H., Clow, D. W., Ingersoll, G. P., Mast, M. A., Spahr, N. E. , Turk, J. T. 1995. Processes controlling the chemistry of 2 snowmelt-dominated streams in the Rocky Mountains. *Water Resources Research* **31**(11): 2811-2821. DOI:10.1029/95wr02037.

Carey, S. ,Quinton, W. 2005. Evaluating runoff generation during summer using hydrometric, stable isotope and hydrochemical methods in a discontinuous permafrost alpine catchment. *Hydrological Processes* **19**(1): 95-114.

Carey, S. K., Boucher, J. L. , Duarte, C. M. 2013. Inferring groundwater contributions and pathways to streamflow during snowmelt over multiple years in a discontinuous permafrost subarctic environment (Yukon, Canada). *Hydrogeology Journal* **21**(1): 67-77. DOI:10.1007/s10040-012-0920-9.

Carey, S. K. ,Woo, M. K. 2001. Slope runoff processes and flow generation in a subarctic, subalpine catchment. *Journal of Hydrology* **253**(1-4): 110-129. DOI:10.1016/s0022-1694(01)00478-4.

Cauvy-Fraunie, S., Espinosa, R., Andino, P., Jacobsen, D. , Dangles, O. 2015. Invertebrate Metacommunity Structure and Dynamics in an Andean Glacial Stream Network Facing Climate Change. *Plos One* **10**(8). DOI:10.1371/journal.pone.0136793.

Chin, K. S., Lento, J., Culp, J. M., Lacelle, D. , Kokelj, S. V. 2016. Permafrost thaw and intense thermokarst activity decreases abundance of stream benthic macroinvertebrates. *Global Change Biology*: n/a-n/a. DOI:10.1111/gcb.13225.

Church, M. ,Ryder, J. M. 1972. Paraglacial sedimentation - a consideration of fluvial processes conditioned by glaciation. *Geological Society of America Bulletin* **83**(10): 3059-&. DOI:10.1130/0016-7606(1972)83[3059:psacof]2.0.co;2.

Church, M. ,Slaymaker, O. 1989. Disequilibrium of Holocene sediment yield in glaciated British Columbia. *Nature* **337**(6206): 452-454.

Clow, D. W., Schrott, L., Webb, R., Campbell, D. H., Torizzo, A. , Dornblaser, M. 2003. Ground Water Occurrence and Contributions to Streamflow in an Alpine Catchment, Colorado Front Range. *Ground Water* **41**(7): 937-950. DOI:10.1111/j.1745-6584.2003.tb02436.x.

Clow, D. W. ,Sueker, J. K. 2000. Relations between basin characteristics and stream water chemistry in alpine/subalpine basins in Rocky Mountain National Park, Colorado. *Water Resources Research* **36**(1): 49-61. DOI:10.1029/1999wr900294.

Cooper, R. J., Wadham, J. L., Tranter, M., Hodgkins, R. , Peters, N. E. 2002. Groundwater hydrochemistry in the active layer of the proglacial zone, Finsterwalderbreen, Svalbard. *Journal of Hydrology* **269**(3-4): 208-223. DOI:10.1016/s0022-1694(02)00279-2.

Crossman, J., Bradley, C., Boomer, I. , Milner, A. M. 2011. Water Flow Dynamics of Groundwater-Fed Streams and Their Ecological Significance in a Glacierized Catchment. *Arctic, Antarctic, and Alpine Research* **43**(3): 364-379. DOI:10.1657/1938-4246-43.3.364.

Crossman, J., Bradley, C., David, J. N. W. , Milner, A. M. 2012. Use of remote sensing to identify areas of groundwater upwelling on active glacial floodplains: Their frequency, extent and significance on a landscape scale. *Remote Sensing of Environment* **123**: 116-126. DOI:10.1016/j.rse.2012.03.023.

Crossman, J., Futter, M. N. , Whitehead, P. G. 2013. The Significance of Shifts in Precipitation Patterns: Modelling the Impacts of Climate Change and Glacier Retreat on Extreme Flood Events in Denali National Park, Alaska. *Plos One* **8**(9): e74054. DOI:10.1371/journal.pone.0074054.

Death, R. G. ,Winterbourn, M. J. 1995. Diversity Patterns in Stream Benthic Invertebrate Communities: The Influence of Habitat Stability. *Ecology* **76**(5): 1446-1460. DOI:10.2307/1938147.

Deb, D., Butcher, J. , Srinivasan, R. 2015. Projected Hydrologic Changes Under Mid-21st Century Climatic Conditions in a Sub-arctic Watershed. *Water Resources Management* **29**(5): 1467-1487. DOI:10.1007/s11269-014-0887-5.

DENA. 2012. Glacier Monitoring. DENA-FS-064-2012. Denali National Park & Preserve, Denali Park, Alaska.

Devito, K., Creed, I., Gan, T., Mendoza, C., Petrone, R., Silins, U. , Smerdon, B. 2005. A framework for broad-scale classification of hydrologic response units on the Boreal

Plain: is topography the last thing to consider? *Hydrological Processes* **19**(8): 1705-1714. DOI:10.1002/hyp.5881.

DeWalle, D. R. ,Rango., A. 2008. Principles of Snow Hydrology. Cambridge University Press.

Doering, M., Uehlinger, U., Rotach, A., Schlaepfer, D. R. , Tockner, K. 2007. Ecosystem expansion and contraction dynamics along a large Alpine alluvial corridor (Tagliamento River, Northeast Italy). *Earth Surface Processes and Landforms* **32**(11): 1693-1704. DOI:10.1002/esp.1594.

Doering, M., Uehlinger, U. , Tockner, K. 2012. Vertical hydrological exchange, and ecosystem properties and processes at two spatial scales along a floodplain river (Tagliamento, Italy). *Freshwater Science* **32**(1): 12-25. DOI:10.1899/12-013.1.

Domenico, P. A. ,Schwartz, F. W. 1990. Physical and Chemical Hydrogeology. John Wiley & Sons, New York.

Douglas, T. A., Blum, J. D., Guo, L. D., Keller, K. , Gleason, J. D. 2013. Hydrogeochemistry of seasonal flow regimes in the Chena River, a subarctic watershed draining discontinuous permafrost in interior Alaska (USA). *Chemical Geology* **335**: 48-62. DOI:10.1016/j.chemgeo.2012.10.045.

Drexler, J. Z., Snyder, R. L., Spano, D. , Paw U, K. T. 2004. A review of models and micrometeorological methods used to estimate wetland evapotranspiration. *Hydrological Processes* **18**(11): 2071-2101. DOI:10.1002/hyp.1462.

Dunn, S. M. ,Mackay, R. 1995. Spatial variation in evapotranspiration and the influence of land use on catchment hydrology. *Journal of Hydrology* **171**(1–2): 49-73. DOI:http://dx.doi.org/10.1016/0022-1694(95)02733-6.

Embleton-Hamann, C. 2004. Proglacial landforms. In Goudie, A. S. (ed) Encyclopedia of Geomorphology. vol 2. Routledge, London, 810-813.

Eyles, N. ,Kocsis, S. 1988. Sedimentology and clast fabric of subaerial debris flow facies in a glacially-influenced alluvial fan. *Sedimentary Geology* **59**(1): 15-28. DOI:http://dx.doi.org/10.1016/0037-0738(88)90098-X.

Finger, D., Heinrich, G., Gobiet, A. , Bauder, A. 2012. Projections of future water resources and their uncertainty in a glacierized catchment in the Swiss Alps and the subsequent effects on hydropower production during the 21st century. *Water Resources Research* **48**(2): n/a-n/a. DOI:10.1029/2011wr010733.

Finn, D. S., Khamis, K. , Milner, A. M. 2013. Loss of small glaciers will diminish beta diversity in Pyrenean streams at two levels of biological organization. *Global Ecology and Biogeography* **22**(1): 40-51. DOI:10.1111/j.1466-8238.2012.00766.x.

Fishman, M. J. ,Friedman, L. C. 1989. Methods for determination of inorganic substances in water and fluvial sediments Techniques of Water-Resource Investigation. 3rd Edition edn.

Freer, J. I. M., McDonnell, J., Beven, K. J., Brammer, D., Burns, D., Hooper, R. P. , Kendal, C. 1997. Hydrological processes—Letters. Topographic controls on subsurface storm flow at the hillslope scale for two hydrologically distinct small catchmetns. *Hydrological Processes* **11**(9): 1347-1352. DOI:10.1002/(SICI)1099-1085(199707)11:9<1347::AID-HYP592>3.0.CO;2-R.

French, H. M. 2000. Does Lozinski's periglacial realm exist today? A discussion relevant to modern usage of the term ‘periglacial’. *Permafrost and Periglacial Processes* **11**(1): 35-42. DOI:10.1002/(SICI)1099-1530(200001/03)11:1<35::AID-PPP334>3.0.CO;2-6.

Fureder, L., Schutz, C., Wallinger, M. , Burger, R. 2001. Physico-chemistry and aquatic insects of a glacier-fed and a spring-fed alpine stream. *Freshwater Biology* **46**(12): 1673-1690. DOI:10.1046/j.1365-2427.2001.00862.x.

Geilhausen, M., Morche, D., Otto, J. C. , Schrott, L. 2013. Sediment discharge from the proglacial zone of a retreating Alpine glacier. *Zeitschrift Fur Geomorphologie* **57**: 29-53. DOI:10.1127/0372-8854/2012/s-00122.

Genereux, D. 1998. Quantifying uncertainty in tracer-based hydrograph separations. *Water Resources Research* **34**(4): 915-919. DOI:10.1029/98wr00010.

Gleeson, T. ,Paszkowski, D. 2014. Perceptions of scale in hydrology: what do you mean by regional scale? *Hydrological Sciences Journal* **59**(1): 99-107. DOI:10.1080/02626667.2013.797581.

Gordon, R. P., Lautz, L. K., McKenzie, J. M., Mark, B. G., Chavez, D. , Baraer, M. 2015. Sources and pathways of stream generation in tropical proglacial valleys of the Cordillera Blanca, Peru. *Journal of Hydrology* **522**: 628-644. DOI:10.1016/j.jhydrol.2015.01.013.

Goutaland, D., Winiarski, T., Lassabatere, L., Dube, J. S. , Angulo-Jaramillo, R. 2013. Sedimentary and hydraulic characterization of a heterogeneous glaciofluvial deposit: Application to the modeling of unsaturated flow. *Engineering Geology* **166**: 127-139. DOI:10.1016/j.enggeo.2013.09.006.

Gurnell, A. M., Edwards, P. J., Petts, G. E. , Ward, J. V. 2000. A conceptual model for alpine proglacial river channel evolution under changing climatic conditions. *Catena* **38**(3): 223-242. DOI:http://dx.doi.org/10.1016/S0341-8162(99)00069-7.

Harbor, J. ,Warburton, J. 1993. Relative Rates of Glacial and Nonglacial Erosion in Alpine Environments. *Arctic and Alpine Research* **25**(1): 1-7. DOI:10.2307/1551473.

Heckmann, T., McColl, S. , Morche, D. 2016. Retreating ice: research in pro-glacial areas matters. *Earth Surface Processes and Landforms* **41**(2): 271-276. DOI:10.1002/esp.3858.

Heinz, J. ,Aigner, T. 2003a. Hierarchical dynamic stratigraphy in various Quaternary gravel deposits, Rhine glacier area (SW Germany): implications for hydrostratigraphy. *International Journal of Earth Sciences* **92**(6): 923-938. DOI:10.1007/s00531-003-0359-2.

Heinz, J. ,Aigner, T. 2003b. Three-dimensional GPR analysis of various Quaternary gravel-bed braided river deposits (southwestern Germany). *Geological Society, London, Special Publications* **211**(1): 99-110. DOI:10.1144/gsl.sp.2001.211.01.09.

Hodson, A., Porter, P., Lowe, A. , Mumford, P. 2002a. Chemical denudation and silicate weathering in Himalayan glacier basins: Batura Glacier, Pakistan. *Journal of Hydrology* **262**(1–4): 193-208. DOI:http://dx.doi.org/10.1016/S0022-1694(02)00036-7.

Hodson, A., Tranter, M., Gurnell, A., Clark, M. , Hagen, J. O. 2002b. The hydrochemistry of Bayelva, a high Arctic proglacial stream in Svalbard. *Journal of Hydrology* **257**(1–4): 91-114. DOI:http://dx.doi.org/10.1016/S0022-1694(01)00543-1.

Holden, J. ,Burt, T. P. 2002. Piping and pipeflow in a deep peat catchment. *Catena* **48**(3): 163-199. DOI:http://dx.doi.org/10.1016/S0341-8162(01)00189-8.

Hood, J. L. ,Hayashi, M. 2015. Characterization of snowmelt flux and groundwater storage in an alpine headwater basin. *Journal of Hydrology* **521**: 482-497. DOI:10.1016/j.jhydrol.2014.12.041.

Hood, J. L., Roy, J. W. , Hayashi, M. 2006. Importance of groundwater in the water balance of an alpine headwater lake. *Geophysical Research Letters* **33**(13): 5. DOI:10.1029/2006gl026611.

Huss, M. ,Hock, R. 2015. A new model for global glacier change and sea-level rise. *Frontiers in Earth Science* **3**. DOI:10.3389/feart.2015.00054.

Immerzeel, W., van Beek, L. P. H., Konz, M., Shrestha, A. B. , Bierkens, M. F. P. 2012. Hydrological response to climate change in a glacierized catchment in the Himalayas. *Climatic Change* **110**(3-4): 721-736. DOI:10.1007/s10584-011-0143-4.

Immerzeel, W. W., van Beek, L. P. H. , Bierkens, M. F. P. 2010. Climate Change Will Affect the Asian Water Towers. *Science* **328**(5984): 1382-1385. DOI:10.1126/science.1183188.

Jacobsen, D., Milner, A. M., Brown, L. E. , Dangles, O. 2012. Biodiversity under threat in glacier-fed river systems. *Nature Climate Change* **2**(5): 361-364. DOI:10.1038/nclimate1435.

Jencso, K. G., McGlynn, B. L., Gooseff, M. N., Wondzell, S. M., Bencala, K. E. , Marshall, L. A. 2009. Hydrologic connectivity between landscapes and streams: Transferring reach- and plot-scale understanding to the catchment scale. *Water Resources Research* **45**(4): W04428. DOI:10.1029/2008WR007225.

Juen, I., Kaser, G. , Georges, C. 2007. Modelling observed and future runoff from a glacierized tropical catchment (Cordillera Blanca, Perú). *Global and Planetary Change* **59**(1–4): 37-48. DOI:http://dx.doi.org/10.1016/j.gloplacha.2006.11.038.

Kirchner, J. W. 2003. A double paradox in catchment hydrology and geochemistry. *Hydrological Processes* **17**(4): 871-874. DOI:10.1002/hyp.5108.

Klaar, M. J., Kidd, C., Malone, E., Bartlett, R., Pinay, G., Chapin, F. S. , Milner, A. 2015. Vegetation succession in deglaciated landscapes: implications for sediment and landscape stability. *Earth Surface Processes and Landforms* **40**(8): 1088-1100. DOI:10.1002/esp.3691.

Klingbeil, R., Kleineidam, S., Asprion, U., Aigner, T. , Teutsch, G. 1999. Relating lithofacies to hydrofacies: outcrop-based hydrogeological characterisation of Quaternary gravel deposits. *Sedimentary Geology* **129**(3): 299-310.

Knight, J. ,Harrison, S. 2014. Mountain Glacial and Paraglacial Environments under Global Climate Change: Lessons from the Past, Future Directions and Policy Implications. *Geografiska Annaler Series a-Physical Geography* **96**(3): 245-264. DOI:10.1111/geoa.12051.

Langston, G., Bentley, L. R., Hayashi, M., McClymont, A. , Pidlisecky, A. 2011. Internal structure and hydrological functions of an alpine proglacial moraine. *Hydrological Processes* **25**(19): 2967-2982. DOI:10.1002/hyp.8144.

Larned, S. T. 2012. Phreatic groundwater ecosystems: research frontiers for freshwater ecology. *Freshwater Biology* **57**(5): 885-906. DOI:10.1111/j.1365-2427.2012.02769.x.

Lassabatère, L., Angulo-Jaramillo, R., Soria Ugalde, J. M., Cuenca, R., Braud, I. , Haverkamp, R. 2006. Beerkan Estimation of Soil Transfer Parameters through Infiltration Experiments—BEST. *Soil Sci Soc Am J* **70**(2): 521-532. DOI:10.2136/sssaj2005.0026.

Lawrence, D. M. ,Slater, A. G. 2005. A projection of severe near-surface permafrost degradation during the 21st century. *Geophysical Research Letters* **32**(24): n/a-n/a. DOI:10.1029/2005GL025080.

Lencioni, V. ,Spitale, D. 2015. Diversity and distribution of benthic and hyporheic fauna in different stream types on an alpine glacial floodplain. *Hydrobiologia* **751**(1): 73-87. DOI:10.1007/s10750-014-2172-2.

Levy, A., Robinson, Z., Krause, S., Waller, R. , Weatherill, J. 2015. Long-term variability of proglacial groundwater-fed hydrological systems in an area of glacier retreat, Skeiðarársandur, Iceland. *Earth Surface Processes and Landforms*: n/a-n/a. DOI:10.1002/esp.3696.

Liu, F. J., Williams, M. W. , Caine, N. 2004. Source waters and flow paths in an alpine catchment, Colorado Front Range, United States. *Water Resources Research* **40**(9): 16. DOI:10.1029/2004wr003076.

Lorang, M. S. ,Hauer, F. R. 2007. Fluvial geomorphic processes. In Hauer, F. R. & G. A. Lamberti (eds) Methods in stream ecology. Second edn. Academic Press, Burlington, MA, USA, 145-169.

Malard, F., Tockner, K., Dole-Olivier, M. J. , Ward, J. V. 2002. A landscape perspective of surface-subsurface hydrological exchanges in river corridors. *Freshwater Biology* **47**(4): 621-640. DOI:10.1046/j.1365-2427.2002.00906.x.

Malard, F., Tockner, K. , Ward, J. V. 1999. Shifting dominance of subcatchment water sources and flow paths in a glacial floodplain, Vol Roseg, Switzerland. *Arctic Antarctic and Alpine Research* **31**(2): 135-150. DOI:10.2307/1552602.

Malard, F., Tockner, K. , Ward, J. V. 2000. Physico-chemical heterogeneity in a glacial riverscape. *Landscape Ecology* **15**(8): 679-695. DOI:10.1023/a:1008147419478.

Mann, D. H., Groves, P., Reanier, R. E. , Kunz, M. L. 2010. Floodplains, permafrost, cottonwood trees, and peat: What happened the last time climate warmed suddenly in arctic Alaska? *Quaternary Science Reviews* **29**(27–28): 3812-3830. DOI:http://dx.doi.org/10.1016/j.quascirev.2010.09.002.

Marren, P. M. ,Toomath, S. C. 2014. Channel pattern of proglacial rivers: topographic forcing due to glacier retreat. *Earth Surface Processes and Landforms* **39**(7): 943-951. DOI:10.1002/esp.3545.

Mast, M. A., Kendall, C., Campbell, D. H., Clow, D. W. , Back, J. 1995. Determination of hydrologic pathways in an alpine subalpine basin using isotopic and chemical tracers, Loch Vale Watershed, Colorado, USA. *Biogeochemistry of Seasonally Snow-Covered Catchments* (228): 263-270.

Maxey, G. B. 1964. Hydrostratigraphic units. *Journal of Hydrology* **2**(2): 124-129.

McClymont, A. F., Hayashi, M., Bentley, L. R. , Liard, J. 2012. Locating and characterising groundwater storage areas within an alpine watershed using time-lapse gravity, GPR and seismic refraction methods. *Hydrological Processes* **26**(12): 1792-1804. DOI:10.1002/hyp.9316.

McClymont, A. F., Hayashi, M., Bentley, L. R., Muir, D. , Ernst, E. 2010. Groundwater flow and storage within an alpine meadow-talus complex. *Hydrology and Earth System Sciences* **14**(6): 859-872. DOI:10.5194/hess-14-859-2010.

McClymont, A. F., Roy, J. W., Hayashi, M., Bentley, L. R., Maurer, H. , Langston, G. 2011. Investigating groundwater flow paths within proglacial moraine using multiple geophysical methods. *Journal of Hydrology* **399**(1-2): 57-69. DOI:10.1016/j.jhydrol.2010.12.036.

McDonnell, J. J., Bonell, M., Stewart, M. K. , Pearce, A. J. 1990. Deuterium variations in storm rainfall: Implications for stream hydrograph separation. *Water Resources Research* **26**(3): 455-458. DOI:10.1029/WR026i003p00455.

McGuire, K. J., DeWalle, D. R. , Gburek, W. J. 2002. Evaluation of mean residence time in subsurface waters using oxygen-18 fluctuations during drought conditions in the mid-Appalachians. *Journal of Hydrology* **261**(1–4): 132-149. DOI:http://dx.doi.org/10.1016/S0022-1694(02)00006-9.

McGuire, K. J. ,McDonnell, J. J. 2006. A review and evaluation of catchment transit time modeling. *Journal of Hydrology* **330**(3–4): 543-563. DOI:http://dx.doi.org/10.1016/j.jhydrol.2006.04.020.

Miall, A. D. 1978. Lithofacies types and vertical profile models in braided rivers: a summary. In Miall, A. D. (ed) Fluvial Sedimentology. vol 5. Can. Soc. Pet. Geol. Mem., 605-625.

Micheletti, N., Lambiel, C. , Lane, S. N. 2015. Investigating decadal-scale geomorphic dynamics in an alpine mountain setting. *Journal of Geophysical Research-Earth Surface* **120**(10): 2155-2175. DOI:10.1002/2015jf003656.

Miller, R. B., Heeren, D. M., Fox, G. A., Halihan, T., Storm, D. E. , Mittelstet, A. R. 2014. The hydraulic conductivity structure of gravel-dominated vadose zones within alluvial floodplains. *Journal of Hydrology* **513**: 229-240. DOI:10.1016/j.jhydrol.2014.03.046.

Milner, A. M., Brown, L. E. , Hannah, D. M. 2009. Hydroecological response of river systems to shrinking glaciers. *Hydrological Processes* **23**(1): 62-77. DOI:10.1002/hyp.7197.

Milner, A. M., Conn, S. C. , Brown, L. E. 2006. Persistence and stability of macroinvertebrate communities in streams of Denali National Park, Alaska: implications for biological monitoring. *Freshwater Biology* **51**(2): 373-387. DOI:10.1111/j.1365-2427.2005.01488.x.

Milner, A. M. ,Petts, G. E. 1994. Glacial rivers: physical habtat and ecology. *Freshwater Biology* **32**(2): 295-307. DOI:10.1111/j.1365-2427.1994.tb01127.x.

Monteith, J. Evaporation and environment. In: Symposia of the Society for Experimental Biology, 1965. vol 19. p 205.

Moore, R. D., Fleming, S. W., Menounos, B., Wheate, R., Fountain, A., Stahl, K., Holm, K. , Jakob, M. 2009. Glacier change in western North America: influences on hydrology, geomorphic hazards and water quality. *Hydrological Processes* **23**(1): 42-61. DOI:10.1002/hyp.7162.

Mote, P. W., Hamlet, A. F., Clark, M. P. , Lettenmaier, D. P. 2005. Declining mountain snowpack in western North America. *Bulletin of the American Meteorological Society* **86**(1): 39-49. DOI:10.1175/BAMS-86-1-39.

Muhlfeld, C. C., Giersch, J. J., Hauer, F. R., Pederson, G. T., Luikart, G., Peterson, D. P., Downs, C. C. , Fagre, D. B. 2011. Climate change links fate of glaciers and an endemic alpine invertebrate. *Climatic Change* **106**(2): 337-345. DOI:10.1007/s10584-011-0057-1.

Muir, D. L., Hayashi, M. , McClymont, A. F. 2011. Hydrological storage and transmission characteristics of an alpine talus. *Hydrological Processes* **25**(19): 2954-2966. DOI:10.1002/hyp.8060.

Nolin, A. W. 2012. Perspectives on Climate Change, Mountain Hydrology, and Water Resources in the Oregon Cascades, USA. *Mountain Research and Development* **32**: S35-S46. DOI:10.1659/mrd-journal-d-11-00038.s1.

Nowak, A. ,Hodson, A. 2015. On the biogeochemical response of a glacierized High Arctic watershed to climate change: revealing patterns, processes and heterogeneity among micro-catchments. *Hydrological Processes* **29**(6): 1588-1603. DOI:10.1002/hyp.10263.

Oke, T. R. 1987. Boundary layer climates. Methuen, London; New York.

Orwin, J. F. ,Smart, C. C. 2004. The evidence for paraglacial sedimentation and its temporal scale in the deglacierizing basin of Small River Glacier, Canada. *Geomorphology* **58**(1-4): 175-202.

Padilla, A., Rasouli, K. , Déry, S. J. 2015. Impacts of variability and trends in runoff and water temperature on salmon migration in the Fraser River Basin, Canada. *Hydrological Sciences Journal* **60**(3): 523-533. DOI:10.1080/02626667.2014.892602.

Paetzold, A., Schubert, C. , Tockner, K. 2005. Aquatic Terrestrial Linkages Along a Braided-River: Riparian Arthropods Feeding on Aquatic Insects. *Ecosystems* **8**(7): 748-759. DOI:10.1007/s10021-005-0004-y.

Palacky, G. 1988. 3. Resistivity Characteristics of Geologic Targets Electromagnetic Methods in Applied Geophysics. Investigations in Geophysics. Society of Exploration Geophysicists, 52-129.

Pederson, G. T., Betancourt, J. L. , McCabe, G. J. 2013. Regional patterns and proximal causes of the recent snowpack decline in the Rocky Mountains, U.S. *Geophysical Research Letters* **40**(9): 1811-1816. DOI:10.1002/grl.50424.

Petrone, K. C., Jones, J. B., Hinzman, L. D. , Boone, R. D. 2006. Seasonal export of carbon, nitrogen, and major solutes from Alaskan catchments with discontinuous permafrost. *Journal of Geophysical Research: Biogeosciences* **111**(G2): n/a-n/a. DOI:10.1029/2005JG000055.

Podolak, C. J. P. 2013. Predicting the Planform Configuration of the Braided Toklat River, Alaska, With a Suite of Rule-Based Models1. *JAWRA Journal of the American Water Resources Association*: no-no. DOI:10.1111/jawr.12029.

Poole, G. C. 2010. Stream hydrogeomorphology as a physical science basis for advances in stream ecology. *Journal of the North American Benthological Society* **29**(1): 12-25. DOI:10.1899/08-070.1.

Poole, G. C., Stanford, J. A., Frissell, C. A. , Running, S. W. 2002. Three-dimensional mapping of geomorphic controls on flood-plain hydrology and connectivity from aerial photos. *Geomorphology* **48**(4): 329-347. DOI:10.1016/s0169-555x(02)00078-8.

Poole, G. C., Stanford, J. A., Running, S. W. , Frissell, C. A. 2006. Multiscale geomorphic drivers of groundwater flow paths: subsurface hydrologic dynamics and hyporheic

habitat diversity. *Journal of the North American Benthological Society* **25**(2): 288-303. DOI:10.1899/0887-3593(2006)25[288:mgdogf]2.0.co;2.

Quinton, W. L., Bemrose, R. K., Zhang, Y. S. , Carey, S. K. 2009. The influence of spatial variability in snowmelt and active layer thaw on hillslope drainage for an alpine tundra hillslope. *Hydrological Processes* **23**(18): 2628-2639. DOI:10.1002/hyp.7327.

Rahman, K., Etienne, C., Gago-Silva, A., Maringanti, C., Beniston, M. , Lehmann, A. 2014. Streamflow response to regional climate model output in the mountainous watershed: a case study from the Swiss Alps. *Environmental Earth Sciences* **72**(11): 4357-4369. DOI:10.1007/s12665-014-3336-0.

Ratnam, S., Soga, K. , Whittle, R. W. 2001. Revisiting Hvorslev's intake factors using the finite element method Géotechnique. vol 51, 641-645.

Robinson, C. T. ,Doering, M. 2012. Spatial patterns in macroinvertebrate assemblages in surface-flowing waters of a glacially-influenced floodplain. *Aquatic Sciences*. DOI:10.1007/s00027-012-0283-2.

Robinson, Z. P., Fairchild, I. J. , Russell, A. J. 2008. Hydrogeological implications of glacial landscape evolution at Skeioararsandur, SE Iceland. *Geomorphology* **97**(1-2): 218-236. DOI:10.1016/j.geomorph.2007.02.044.

Rodgers, P., Soulsby, C., Waldron, S. , Tetzlaff, D. 2005. Using stable isotope tracers to assess hydrological flow paths, residence times and landscape influences in a nested mesoscale catchment. *Hydrology and Earth System Sciences* **9**(3): 139-155.

Rounds, S. A. 2006. Alkalinity and acid neutralizing capacity (ver. 3.0) US Geological Survey Techniques of Water-Resources Investigations. vol Book 9.

Roy, J. W. ,Hayashi, M. 2009. Multiple, distinct groundwater flow systems of a single moraine-talus feature in an alpine watershed. *Journal of Hydrology* **373**(1-2): 139-150. DOI:10.1016/j.jhydrol.2009.04.018.

Schumm, S. A. ,Rea, D. K. 1995. Sediment yield from disturbed earth systems. *Geology* **23**(5): 391-394. DOI:10.1130/0091-7613(1995)023<0391:syfdes>2.3.co;2.

Silvestri, V., Abou-Samra, G. , Bravo-Jonard, C. 2012. Shape Factors of Cylindrical Piezometers in Uniform Soil. *Ground Water* **50**(2): 279-284. DOI:10.1111/j.1745-6584.2011.00845.x.

Singh, P. ,Bengtsson, L. 2005. Impact of warmer climate on melt and evaporation for the rainfed, snowfed and glacierfed basins in the Himalayan region. *Journal of Hydrology* **300**(1-4): 140-154. DOI:10.1016/j.jhydrol.2004.06.005.

Singhal, B. B. S. ,Gupta, R. P. 2010. Applied Hydrogeology of Fractured Rocks. Springer, Netherlands.

Sklash, M. G. ,Farvolden, R. N. 1979. Role of Groundwater in Storm Runoff. *Journal of Hydrology* **43**(1-4): 45-65. DOI:10.1016/0022-1694(79)90164-1.

Slaymaker, O. 2009. Proglacial, periglacial or paraglacial? *Periglacial and Paraglacial Processes and Environments* **320**: 71-84. DOI:10.1144/sp320.6.

Slaymaker, O. 2011. Criteria to Distinguish Between Periglacial, Proglacial and Paraglacial Environments Quaestiones Geographicae. vol 30, 85.

Snook, D. L. ,Milner, A. M. 2001. The influence of glacial runoff on stream macroinvertebrate communities in the Taillon catchment, French Pyrénées. *Freshwater Biology* **46**(12): 1609-1623. DOI:10.1046/j.1365-2427.2001.00848.x.

Sokal, R. R. ,Rohlf, F. J. 1995. Biometry: the principles and practice of statistics in biological research, 3rd edn. Freeman, New York.

Soulsby, C., Malcolm, I. A., Youngson, A. F., Tetzlaff, D., Gibbins, C. N. , Hannah, D. M. 2005. Groundwater-surface water interactions in upland Scottish rivers: hydrological, hydrochemical and ecological implications. *Scottish Journal of Geology* **41**: 39-49.

Soulsby, C., Malcolm, R., Helliwell, R., Ferrier, R. C. , Jenkins, A. 2000. Isotope hydrology of the Allt a' Mharcaidh catchment, Cairngorms, Scotland: implications for hydrological pathways and residence times. *Hydrological Processes* **14**(4): 747-762. DOI:10.1002/(sici)1099-1085(200003)14:4<747::aid-hyp970>3.0.co;2-0.

Soulsby, C., Rodgers, P. J., Petry, J., Hannah, D. M., Malcolm, I. A. , Dunn, S. M. 2004. Using tracers to upscale flow path understanding in mesoscale mountainous catchments: two examples from Scotland. *Journal of Hydrology* **291**(3-4): 174-196. DOI:10.1016/j.jhydrol.2003.12.042.

Stafford, J. M., Wendler, G. , Curtis, J. 2000. Temperature and precipitation of Alaska: 50 year trend analysis. *Theoretical and Applied Climatology* **67**(1-2): 33-44. DOI:10.1007/s007040070014.

Stanford, J. A. ,Ward, J. V. 1993. An ecosystem perspective of alluvial rivers - connectivity and the hyporheic corridor. *Journal of the North American Benthological Society* **12**(1): 48-60. DOI:10.2307/1467685.

Stephenson, D., Fleming, A., Mickelson, D., Rosenshein, J. , Seaber, P. 1988. Glacial deposits. *Hydrogeology: the geology of North America* **2**.

Stewart, I. T. 2009. Changes in snowpack and snowmelt runoff for key mountain regions. *Hydrological Processes* **23**(1): 78-94. DOI:10.1002/hyp.7128.

Striegl, R. G., Dornblaser, M. M., Aiken, G. R., Wickland, K. P. , Raymond, P. A. 2007. Carbon export and cycling by the Yukon, Tanana, and Porcupine rivers, Alaska, 2001–2005. *Water Resources Research* **43**(2): n/a-n/a. DOI:10.1029/2006WR005201.

Stutter, M. I., Deeks, L. K., Low, D. , Billett, M. F. 2006. Impact of soil and groundwater heterogeneity on surface water chemistry in an upland catchment. *Journal of Hydrology* **318**(1–4): 103-120. DOI:http://dx.doi.org/10.1016/j.jhydrol.2005.06.007.

Sueker, J. K., Ryan, J. N., Kendall, C. , Jarrett, R. D. 2000. Determination of hydrologic pathways during snowmelt for alpine/subalpine basins, Rocky Mountain National Park, Colorado. *Water Resources Research* **36**(1): 63-75.

Surridge, B. W. J., Baird, A. J. , Heathwaite, A. L. 2005. Evaluating the quality of hydraulic conductivity estimates from piezometer slug tests in peat. *Hydrological Processes* **19**(6): 1227-1244. DOI:10.1002/hyp.5653.

Tabacchi, E., Correll, D. L., Hauer, R., Pinay, G., Planty-Tabacchi, A.-M. , Wissmar, R. C. 1998. Development, maintenance and role of riparian vegetation in the river landscape. *Freshwater Biology* **40**(3): 497-516. DOI:10.1046/j.1365-2427.1998.00381.x.

Tague, C. ,Grant, G. E. 2009. Groundwater dynamics mediate low-flow response to global warming in snow-dominated alpine regions. *Water Resources Research* **45**: 12. DOI:10.1029/2008wr007179.

Tekleab, S., Wenninger, J. , Uhlenbrook, S. 2014. Characterisation of stable isotopes to identify residence times and runoff components in two meso-scale catchments in the Abay/Upper Blue Nile basin, Ethiopia. *Hydrology and Earth System Sciences* **18**(6): 2415-2431. DOI:10.5194/hess-18-2415-2014.

Tetzlaff, D. ,Soulsby, C. 2008. Sources of baseflow in larger catchments - Using tracers to develop a holistic understanding of runoff generation. *Journal of Hydrology* **359**(3-4): 287-302. DOI:10.1016/j.jhydrol.2008.07.008.

Thornberry-Ehrlich, T. 2010. Denali National Park and Preserve : geologic resources inventory report. Natural Resource Report NPS/NRPC/GRD/NRR—2010/244. National Park Service, Ft. Collins, Colorado.

Tockner, K., Malard, F., Uehlinger, U. , Ward, J. V. 2002. Nutrients and organic matter in a glacial river-floodplain system (Val Roseg, Switzerland). *Limnology and Oceanography* **47**(1): 266-277.

Tockner, K., Paetzold, A., Karaus, U., Claret, C. , Zettel, J. 2009. Ecology of Braided Rivers Braided Rivers. Blackwell Publishing Ltd., 339-359.

Tranter, M. 2003a. 5.07 - Geochemical Weathering in Glacial and Proglacial Environments. In Turekian, H. D. H. K. (ed) Treatise on Geochemistry. Pergamon, Oxford, 189-205.

Tranter, M. 2003b. Geochemical weathering in glacial and proglacial environments. *Treatise on geochemistry* **5**: 189-205.

Uchida, T., Kosugi, K. i. , Mizuyama, T. 2001. Effects of pipeflow on hydrological process and its relation to landslide: a review of pipeflow studies in forested headwater catchments. *Hydrological Processes* **15**(11): 2151-2174. DOI:10.1002/hyp.281.

Van Der Nat, D., Tockner, K., Edwards, P. J., Ward, J. V. , Gurnell, A. M. 2003. Habitat change in braided flood plains (Tagliamento, NE-Italy). *Freshwater Biology* **48**(10): 1799-1812. DOI:10.1046/j.1365-2427.2003.01126.x.

Vergara, W., Deeb, A., Valencia, A., Bradley, R., Francou, B., Zarzar, A., Grünwaldt, A. , Haeussling, S. 2007. Economic impacts of rapid glacier retreat in the Andes. *Eos, Transactions American Geophysical Union* **88**(25): 261-264. DOI:10.1029/2007EO250001.

Vogt, R. D. ,Muniz, I. P. 1997. Soil and stream water chemistry in a pristine and boggy site in mid-Norway. *Hydrobiologia* **348**: 19-38. DOI:10.1023/a:1003029031653.

Vorosmarty, C. J., McIntyre, P. B., Gessner, M. O., Dudgeon, D., Prusevich, A., Green, P., Glidden, S., Bunn, S. E., Sullivan, C. A., Liermann, C. R. , Davies, P. M. 2010. Global threats to human water security and river biodiversity. *Nature* **467**(7315): 555-561. DOI:http://www.nature.com/nature/journal/v467/n7315/abs/nature09440.html#supplementary-information.

Walvoord, M. A. ,Striegl, R. G. 2007. Increased groundwater to stream discharge from permafrost thawing in the Yukon River basin: Potential impacts on lateral export of carbon and nitrogen. *Geophysical Research Letters* **34**(12): L12402. DOI:10.1029/2007gl030216.

Ward, J. V., Malard, F., Tockner, K. , Uehlinger, U. 1999. Influence of ground water on surface water conditions in a glacial flood plain of the Swiss Alps. *Hydrological Processes* **13**(3): 277-293. DOI:10.1002/(sici)1099-1085(19990228)13:3<277::aid-hyp738>3.0.co;2-n.

Ward, J. V., Tockner, K., Arscott, D. B. , Claret, C. 2002. Riverine landscape diversity. *Freshwater Biology* **47**(4): 517-539. DOI:10.1046/j.1365-2427.2002.00893.x.

Weekes, A. A., Torgersen, C. E., Montgomery, D. R., Woodward, A. , Bolton, S. M. 2015. Hydrologic response to valley-scale structure in alpine headwaters. *Hydrological Processes* **29**(3): 356-372. DOI:10.1002/hyp.10141.

Whited, D. C., Lorang, M. S., Harner, M. J., Hauer, F. R., Kimball, J. S. , Stanford, J. A. 2007. Climate, hydrologic disturbance, and succession: drivers of floodplain pattern. *Ecology* **88**(4): 940-953. DOI:10.1890/05-1149.

Whittaker, R. H. 1960. Vegetation of the Siskiyou Mountains, Oregon and California. *Ecological Monographs* **30**(3): 279-338. DOI:10.2307/1943563.

Williams, M. W., Davinroy, T. , Brooks, P. D. 1997. Organic and inorganic nitrogen pools in talus fields and subtalus water, Green Lakes Valley, Colorado Front Range. *Hydrological Processes* **11**(13): 1747-1760. DOI:10.1002/(sici)1099-1085(19971030)11:13<1747::aid-hyp603>3.0.co;2-b.

Wilson, F. H., Dover, J. H., Bradley, D. C., Weber, R. F., Bundtzen, T. K. , Haeussler, P. J. 1998. Geologic map of central (interior) Alaska US Geological Survey Open-File Report. U.S. Department of the Interior, OF 98-133.

Woodward, G., Perkins, D. M. , Brown, L. E. 2010. Climate change and freshwater ecosystems: impacts across multiple levels of organization. *Philosophical*

Transactions of the Royal Society of London B: Biological Sciences **365**(1549): 2093-2106. DOI:10.1098/rstb.2010.0055.

WRCC., 2014a. Eielson Alaska; Station Daily Time Series. In. http://www.raws.dri.edu.

WRCC., 2014b. Toklat Alaska; Station Daily Time Series. In. http://www.raws.dri.edu.

Yocum, L., Adema, G. , Hults, C., 2006. A baseline study of permafrost in the Toklat Basin, Denali National Park and Preserve, Alaska. Paper presented at the 102nd Annual Meeting of The Cordilleran Section, GSA, 81st Annual Meeting of the Pacific Section, AAPG, and the Western Regional Meeting of the Alaska Section, SPE (8-10 May 2006) Paper No 20-9

Zemp, M., Frey, H., Gärtner-Roer, I., Nussbaumer, S. U., Hoelzle, M., Paul, F., Haeberli, W., Denzinger, F., Ahlstrøm, A. P., Anderson, B., Bajracharya, S., Baroni, C., Braun, L. N., Cáceres, B. E., Casassa, G., Cobos, G., Dávila, L. R., Delgado Granados, H., Demuth, M. N., Espizua, L., Fischer, A., Fujita, K., Gadek, B., Ghazanfar, A., Hagen, J. O., Holmlund, P., Karimi, N., Li, Z., Pelto, M., Pitte, P., Popovnin, V. V., Portocarrero, C. A., Prinz, R., Sangewar, C. V., Severskiy, I., Sigurðsson, O., Soruco, A., Usubaliev, R. , Vincent, C. 2015. Historically unprecedented global glacier decline in the early 21st century. *Journal of Glaciology* **61**(228): 745-762. DOI:10.3189/2015JoG15J017.

APPENDICES

APPENDIX A: HYDRAULIC CONDUCTIVITY DATA FOR UPPER TRANSECT

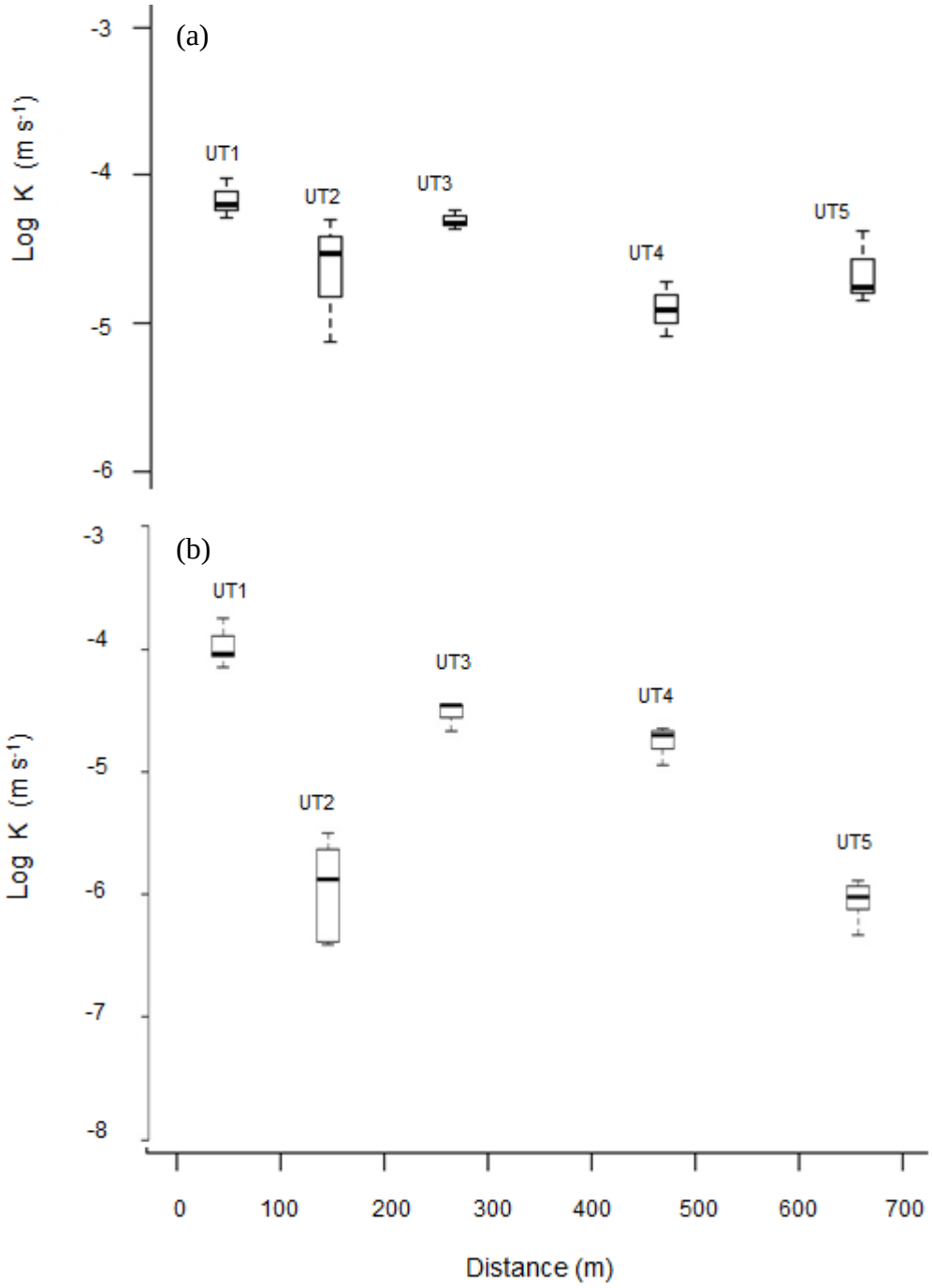

6.6.1 Appendix Ai: Hydraulic conductivity (*K*) measurements at MF Toklat along the upper transect (UT) for; (a) surface *K* ($K_{0.0}$); and (b) *K* at 1.0 m depth ($K_{1.0}$). X-axis indicates distance from the hillslope